Faculty of Science and Engineering

Department of Medical Radiation Sciences

The Optimisation of Routine Paediatric CT Scanning Protocols

Khalid Mohammed Salim Al-Mahrooqi

This thesis is presented for the Degree of
Master of Philosophy
of
Curtin University

November 2015

Declaration

To the best of my knowledge and belief this thesis contains no material previously published by any other person except where due acknowledgment has been made.

This thesis contains no material which has been accepted for the award of any other degree or diploma in any university.

Signature:

Date: 30th November 2015

Acknowledgements

Firstly, I would like to gratefully acknowledge the guidance and support from Prof. Zhonghua Sun and Dr. Curtise Ng, who through their supervision have given me a scientific support and mentoring that inspired my research interests. From day one, they have shown enthusiasm and professionalism that have strengthened and motivated me throughout my research study. As time progressed, both of them greatly invested time and showed a scientific and professional attitude. I sincerely thank them for countless hours of discussion, consultation, support, and advice, which have impacted me profoundly.

Special thanks are given to Mr. Tom Tiang, the MIT CT Supervisor at Princess Margaret Hospital in Western Australia for his tremendous scientific and personal support to my phantom study. I should admit that without his support, I would not have been able to complete the study on time. Further, I wish to acknowledge Mr. Sultan Al Noumani and Mr. Hummod Al Gafri from the Sultan Qaboos University Hospital for their support in my data collection. A special thank is given to Mrs. Melat Habtemariam, the administrative officer of the Department of Medical Radiation Sciences for her ongoing administrative support, which has made my research study progress smoothly and successfully.

Also, I would like to thank the radiology departments in Royal Hospital, Sultan Qaboos University Hospital, Armed Forces Hospital, and Sohar Hospital for allowing me access their data and equipment.

Ultimately, none of this work would have been possible without a blessing from Almighty Allah and my parents. I owe a special debt of gratitude to my wife and kids for their unwavering love and support. Their love and encouragement have guided me during last two years; they were undoubtedly the source of strength and spirit. Lastly, I want to thank my Oman government for the sponsorship and countless support that are given to my family and me during the entire study period at Curtin University.

Abstract

Computed tomography (CT) is an important diagnostic imaging method. However, the radiation risks associated with CT examinations are a major concern, especially in paediatrics because children have highly radiosensitive organs and longer lifetimes in which to manifest the harmful effects of radiation. The aim of this study was to optimise routine paediatric CT scanning protocols in relation to image quality and radiation doses.

The study was performed in three main steps. First, a comprehensive literature review was conducted to identify and discuss factors that influence image quality and radiation dose as well as current paediatric CT dose-saving techniques. Second, a retrospective study was conducted concerning the routine paediatric CT scanning protocols employed in four leading tertiary hospitals in Sultanate of Oman to determine the effects of the identified factors on radiation dose and image quality in clinical (practical) environments. The outcomes of these two steps were used to devise a preliminary optimum routine paediatric CT scanning protocols. Finally, some of the devised protocols were evaluated using a paediatric anthropomorphic phantom, leading to further refinement.

In step one, a comprehensive literature review was conducted to identify and discuss a wide range of factors that affect radiation dosage and image quality in routine paediatric CT examinations. The range of factors includes the following: pitch, over-scanning dose, scan collimation, radiosensitivity, scanogram/scout-view, use of bowtie shaping filters, tube voltage and current, diagnostic reference levels, automatic tube current modulation (ATCM), iterative reconstruction (IR) and patient body size in terms of age, weight and effective diameter.

Further investigation was carried out in step two by a retrospective data analysis that has strengthened our understanding of how paediatric acquisition and reconstruction parameters were normalised in clinical practices. The participating centres were equipped with the latest 64 and 128 multi-detector CT (MDCT) scanners. Step two demonstrated a mix of practices in the centres. All centres used a standard 120 kV for all CT examinations, except for centre D where 80 to 120 kV were applied across all age groups. Significant median differences of tube current time product (mAs)

and volume CT dose indexes ($CTDI_{vol}$) were observed between the centres across age and effective diameter groups for all examinations, with the lowest dose found in centre D ($P< 0.001$) . The findings of low dose techniques in steps one and two led to the development of optimum paediatric CT protocols. The devised chest and abdomen protocols were based on body size in terms of effective diameters which is recommended by International Commission on Radiation Units (ICRU). The tube voltage of 100kV, ATCM and IR techniques dominated all the devised protocols. Also, low kV devised for all post contrast medium protocols taken advantage of the effect of attenuation of iodine at lower tube voltage. Finally, step three validated the devised protocols, and more tests such as lowering tube voltage and tube current with application of IR technique were conducted to manipulate the acquisition parameters for further optimisation. Devised head protocols achieved greater dose reduction up to 76%, yet yielded subjective image quality comparable to the reference protocol. Similarly, chest and abdomen devised protocols demonstrated up to 81% dose reduction, still maintained diagnostic image quality. Moreover, interlinked factors like pitch, ATCM and scan time were further investigated to better understand these factors and reinforce the optimised protocols, with results showing that changing pitch from 0.6 to 1.2 values in Siemens 128-MDCT Flash with ATCM technique increased both $CTDI_{vol}$ and dose length product (DLP) by 6% and 13% respectively, whereas changing pitch from 0.6 to 1.2 in Philips scanner with fixed tube current manifested 6% increase in $CTDI_{vol}$ while 4% decrease in DLP.

In summary, the study results represent one of the first comprehensive paediatric optimisation processes that were systematically approached via three main objectives. It is expected that the devised optimisation paediatric protocols could have profound implications on clinical practices that use 64 MDCT or greater. The study provides a better understanding of the influence of each acquisition reconstruction parameter with regards to image quality and radiation dose. Additional optimisation of paediatric CT practices could be maximised through the introduction of the ICRU effective diameter based on protocols, low tube voltage, an adequate pitch factor and proper adaptation of tube current modulation. Implementation of the iterative reconstruction technique would advocate for the use of the low-dose protocols.

List of publications arising from the thesis

Al Mahrooqi KMS, Ng CKC, Sun Z. 2015.Pediatric Computed Tomography Dose Optimization Strategies: A Literature Review. J Med Imaging Radiat Sci. 46(2): 241-9.

Al Mahrooqi K. 2015. Evaluation of routine paediatric MSCT protocols from a major tertiary hospitals in Oman. J Med Radiat Sci. 62(Suppl 1): 55.

List of conferences

International conferences

Al Mahrooqi K, Sun Z, Ng CKC. 2015. Evaluation of routine paediatric MSCT protocols from major tertiary hospitals in Oman. 2015 NZIMRT-AIR Scientific Meeting 24-26 July, Willington, New Zealand. Oral presentation

National conferences/workshops

Al Mahrooqi KM. 2014. Evaluation of the dose reading in Oman hospitals. A preliminary optimisation of routine paediatric CT protocols. Western Australia CT Users Group Annual Seminar. Oral presentation

Contents

List of tables

List of figures

List of abbreviations

AAPM
American Association of Physicists in Medicine

AIDR
Adaptive iterative dose reduction technique

ALARA
As Low As Reasonably Achievable: principle used in radiation protection relating to doses to people which should always be as low as possible, after all 'reasonable' methods of reduction have been applied.

APSCM
Automatic tube voltage selection with tube current modulation

ASIR
Adaptive statistical iterative reconstruction

ATCM
Automatic tube current modulation

Auto mA
GE modulation technique that enables the longitudinal tube current modulation

BEIR
Biologic Effect of Ionizing Radiation

BMI
Body max index

CNR
Contrast to noise ratio

CT
Computed (or Computerised) Tomography (aka CAT): An imaging technique that uses views of an object from many directions to synthesise a transaxial or cross sectional image.

D-DOM
Dynamic angular dose modulation technique used by Philips Healthcare CT Scanners

DLP
Dose-Length Product: a basic measure of radiation risk calculated by multiplying the CTDI for a scan sequence by the length of coverage in the z-direction (along the patient's length).

CTDI
Computed Tomography Dose Index: a term used in radiation dosimetry that describes the dose from a single rotation of a CT scanner. There are a number of definitions of CTDI commonly used - see the following presentation for more details.

$CTDI_{vol}$

Volume CT dose index

CTDIw

Weighted CT dose index

ED

Emergency departments

FBP

Filtered back projection

FDA

Food and Drug Administration: US body responsible for legislation relating to medical equipment.

FOV

Field Of View (See also SFOV and RFOV): size of an area being imaged.

GE

General Electric

HIS

Hospital Information System. Hospital-wide computer system containing patient details and records.

HU

Hounsfield Unit. The CT scanner display unit. The arbitrary scale is defined by air, which has a CT number of -1000 HU, and water, with a CT number of 0 HU. Named after Sir Godfrey Hounsfield, who developed the first clinical CT scanner.

ICRU

International Commission on Radiation Units and Measurement

IEC

International Electrotechnical Commission

IV

Intravenous contrast material

keV

Kiloelectron-volt

MBIR

Model based iterative reconstruction technique

MDCT

Multi-Detector Computed Tomography (aka MSCT). CT performed with more than one row (or bank) of detectors along the patient's length, capable of producing more than one image simultaneously.

Noise index

Is reference to the standard deviation of CT number within a region of interest in a water phantom of a specific size.

PACS

Picture archiving and communications system. Electronic means to store and distribute medical images (rather than conventional x-ray film).

RIS

Radiology Information System. Radiology department computer system containing patient details and records.

ROI

Region of Interest. A user defined area of an image that can used for purposes such as calculation of pixel statistics.

RSNA

Radiological Society of North America

SAFIRE

Sinogram-affirmed iterative reconstruction is one of the most recently developed iterative reconstruction method used in CT by Siemens manufacture

SD

Standard Deviation. Statistical measure of variation of a series of values around the mean. Used to characterise noise in CT images.

Smart mA

GE modulation technique that enables both longitudinal and angular tube current modulation

SPSS

IBM Statistical Package for Social Sciences

SSD

Surface Shaded Display Method of displaying 3-D volumes achieved by finding 'surfaces' at the boundaries of organs, vessels etc, and displaying them as solid objects.

SSDE

Size specific dose estimation that used to normalise the dose to the specific body size that based on age reference

S-FOV

Scan field of view before the acquisition

Sure Exposure

Longitudinal modulation technique in Toshiba CT scanners

Sure Exposure 3D

Angular and longitudinal modulations technique used by Toshiba CT scanners

VR

Volume Rendered Image. Method for displaying 3-D image data, that assigns colours and degrees of transparency to different CT number ranges. Good for displaying overlapping structure.

Z

Atomic number

Z-DOM

Longitudinal axis (z-axis) dose modulation technique used by Philips Health Care CT scanners.

Chapter 1

Introduction

1.1 Introduction

The development of computed tomography (CT) has revolutionised the role of imaging in medical diagnosis. CT plays an important role in paediatric diagnostic imaging due to its high temporal, spatial and contrast resolution and its wide availability in both routine and emergency situations [1-3]. High temporal resolution creates the opportunity to acquire a large volume of images in short time, which allows scanning small and uncooperative children without the need of sedation. In addition, its superior spatial (when comparing to magnetic resonance imaging) and contrast resolution (in relation to the one of planar x-rays) contributes to better image quality for visualisation of smaller organs with lower fat content of paediatric patients. However, the improved image quality is also associated with the increase of patient dose.

CT undoubtedly provides substantial medical benefits. For example, a multi-centre survey conducted in the United Kingdom (UK) published in 2007 showed that CT utilisation had grown from 5 to 11 percent compared with 10 years before [4]. In 2006, more than 221 million of CT examinations were performed worldwide, 62 million in the United States (US) [5]. In 2011, 85 million of CT scans were performed in the US and 5-11 percent were for children [6]. Although CT examinations contribute to 4–11 percent of all radiological examinations worldwide, CT scans account for 50 to 70 percent of total medical imaging examinations in some countries [7, 8]. Regulatory bodies have established guidelines to encourage appropriate CT utilisation and to protect patients from unnecessary ionisation radiation exposure through the optimisation of CT scan protocols [9-12].

Children are particularly susceptible to radiation risks due to cellular proliferation and their long life spans in which the radiation effects may become manifest [13-16]. The clinical benefits of prescribed examinations must always outweigh the risks [16-18]. After the introduction of multi-detector CT (MDCT), a number of studies and

technical developments on paediatric low-dose protocols were published [19-28] in response to reports about children exposed to more than three times of radiation dose than that of adults due to the use of adult protocols. Since that time, several strategies have been recommended by the literature for the optimisation of paediatric MDCT scanning protocols. Of these strategies, adaptation of scanning parameters based on body weight and tube current modulation techniques have shown a significant reduction in patient dose while still meeting the necessary diagnostic requirements [25, 27, 29-34]. However, recent paediatric CT dose surveys conducted in developed and developing countries have shown remarkable dose variations for the same type of examination and age group [35-39]. International Atomic Energy Agency (IAEA) also indicated that some CT facilities in developing countries still uses adult CT scan parameters for paediatric patients implying a lack of awareness of the issue and protocol optimisation [35,36].

Several developed countries have started to establish platforms for optimisation of paediatric CT practices [4, 40, 41]. However, at this stage, only individual factors for protocol optimisation have been investigated and there is a lack of integrating a range of approaches to maximise the extent of dose savings while still maintaining image quality.

It is important to conduct a study to optimise the paediatric routine CT scanning protocols based on a wide range of factors that influence radiation doses and image quality.

The study aims to optimise paediatric routine CT scanning protocols in relation to image quality and radiation dose. The study objectives are:

- To identify the factors that affect radiation dose and image quality of routine paediatric CT examinations
- To devise optimum routine paediatric CT scanning protocols based on a range of identified factors
- To evaluate the devised protocols in relation to image quality and radiation doses.

1.2 Outline of the thesis

Chapter 2 is a literature review to identify and discuss a wider range of factors that affect radiation dose and image quality of routine paediatric CT examinations. Chapter 3 is about comparison of acquisition parameters and dose of CT examinations collected retrospectively from 4 hospitals in Oman. The outcomes from this retrospective study and Chapter 2 were used to devise the optimum routine paediatric CT scanning protocols. Selected optimised protocols were also evaluated through the use of a paediatric anthropomorphic phantom in Chapter 4. Chapter 5 summarises the significance and implications of this study including the optimised protocols devised. Study limitations and further study directions are also suggested.

1.3 References

1. Blackwell CD, Gorelick M, Holmes JF, Bandyopadhyay S, et al. 2007. Pediatric head trauma: changes in use of computed tomography in emergency departments in the United States over time. Ann Emerg Med. 49(3): 320-4.

2. Thomas KE, Wang B. 2008.Age-specific effective doses for pediatric MSCT examinations at a large children's hospital using DLP conversion coefficients: A simple estimation method. Pediatr Radiol. 38(6): 645-56.

3. Larson DB, Johnson BM, Schnell BM, Goske MJ, et al. 2011. Rising use of CT in child visits to the emergency department in the United States, 1995–2008. Radiology 259(3): 793-801.

4. Shrimpton PC, Hillier MC, Lewis MA, Dunn M. 2006. National survey of doses from CT in the UK: 2003. Br J Radiol. 79(948): 968-80.

5. Dougeni E, Faulkner K, Panayiotakis G. 2012.A review of patient dose and optimisation methods in adult and paediatric CT scanning. Eur J Radiol. 81(4): e665-83.

6. Miglioretti ML, Johnson E, Williams A, Greenlee RT, et al. 2013. Pediatric computed tomography and associated radiation exposure and estimated cancer risk. JAMA pediatrics 167(8): 700-7.

7. Treier R, Aroua A, Verdun FR, Samara E, et al. 2010. Patient doses in CT examinations in Switzerland: Implementation of national diagnostic reference levels. Radiat Prot Dosimetry 142(2-4): 244-54.

8. Deak PD, Smal Y, Kalender WA. 2010. Multisection CT protocols: Sex- and age-specific conversion factors used to determine effective dose from dose-length product. Radiology 257: 158-66.

9. Goske MJ, Applegate KE, Bell C, Boylan J, et al. 2010. Image gently: Providing practical educational tools and advocacy to accelerate radiation protection for children worldwide. Seminars in ultrasound, CT, and MR 31(1): 57-63.

10. Goske MJ, Applegate KE, Boylan J, Butler PF, et al. 2008. The 'Image Gently' campaign: Increasing CT radiation dose awareness through a national education and awareness program. Pediatr Radiol 38(3): 265-9.

11. Strauss KJ, Goske MJ, Kaste SC, Bulas D, et al. 2010. Image gently: Ten steps you can take to optimize image quality and lower CT dose for pediatric patients. Am J Roentgenol. 194(4): 868-73.

12. Boone JM, Strauss KJ, Cody DD, McCollough CH, et al. Size Specific Dose Estimation (SSDE) in Paediatric and Adult Body CT Examination. American Association of Physicists in Medicine (AAPM) Report No. 204, 2011.

13. Seidenbusch MC, Harder D, Regulla DF, Schneider K. 2014.Conversion factors for determining organ doses received by paediatric patients in high-resolution single slice computed tomography with narrow collimation. Zeitschrift fur medizinische Physik. 24(2): 123-137

14. Brisse HJ, Robilliard M, Savignoni A, Pierrat N, et al. 2009. Assessment of organ absorbed doses and estimation of effective doses from pediatric anthropomorphic phantom measurments for multi-detector row CT with and without automatic exposure control. Health Physics 97(4): 303-14.

15. Mathews JD, Forsythe AV, Brady Z, Butler MW, et al. 2013.Cancer risk in 680,000 people exposed to computed tomography scans in childhood or adolescence: data link age study of 11 million Australians. BMJ 346: f2360.

16. Pearce MS, Salotti JA, Little MP, McHugh K, et al. 2012.Radiation exposure from CT scans in childhood and subsequent risk of leukaemia and brain tumours: a retrospective cohort study. The Lancet 380(9840): 499-505.

17. Brenner DJ, Doll R, Goodhead DT, Hall EJ, et al. 2003. Cancer risks attributable to low doses of ionizing radiation: assessing what we really know. Proceedings of the National Academy of Sciences of the United States of America 100(24): 13761-6.

18. Brenner DJ, Hall J. 2007. Computed tomography — An increasing source of radiation exposure. The New Eng J of Med 357: 2277-84.

19. Morton RP, Reynolds RM, Ramakrishna R, Levitt MR, et al. 2013.Low-dose head computed tomography in children: A single institutional experience in pediatric radiation risk reduction. J Neurosurg Pediatr.12(4): 406-10.

20. Arch ME, Frush DP. 2008. Pediatric body MDCT: A 5-year follow-up survey of scanning parameters used by pediatric radiologists. Am J Roentgenol.191(2): 611-7.

21. Brisse HJ, Brenot J, Pierrat N, Gaboriaud G, Savignoni A, et al. 2009.The relevance of image quality indices for dose optimization in abdominal multi-detector row CT in children: Experimental assessment with pediatric phantoms. Phys Med Biol. 54: 1871–1892.

22. Brady Z, Ramanauskas F, Cain TM, Johnston PN. 2012. Assessment of paediatric CT dose indicators for the purpose of optimisation. Br J Radiol. 85:1488-98.

23. Chapman T, Swanson JO, Phillips GS, Parisi MT, et al. 2013. Pediatric chest CT radiation dose reduction: Protocol refinement based on noise injection for pulmonary nodule detection accuracy. Clin Imaging 37(2): 334-41.

24. Cheng PM, Vachon LA, Duddalwar VA. 2013. Automated pediatric abdominal effective diameter measurements versus age-predicted body size for normalization of CT dose. J Digit Imaging 26(6): 1151-5.

25. Dong F, Davros W, Pozzuto J, Reid J. 2012.Optimization of kilovoltage and tube current-exposure time product based on abdominal circumference: An oval phantom study for pediatric abdominal CT. Am J Roentgenol.199(3): 670-6.

26. Feng ST, Law MW, Huang B, Ng S, et al. 2010. Radiation dose and cancer risk from pediatric CT examinations on 64-slice CT: A phantom study. Eu J Radiol.76(2): e19-23.

27. Frush DP, Soden B, Frush KS, Lowry C. 2002. Improved pediatric multidetector body CT using a size-based color-coded format. Am J Roentgenol. 178(3): 721-6.

28. Huda W, Vance A. 2007. Patient radiation doses from adult and pediatric CT. Am J Roentgenol.188(2): 540-6.

29. Reid J, Gamberoni J, Dong F, Davros W. 2010. Optimization of kVp and mAs for pediatric low-dose simulated abdominal CT: Is it best to base parameter selection on object circumference? Am J Roentgenol.195(4):1015-20.

30. Hopkins KL, Pettersson DR, Koudelka CW, Spinning K, et al. 2013. Size-appropriate radiation doses in pediatric body CT: A study of regional community adoption in the United States. Pediatr Radiol. 43(9): 1128-35.

31. Kim JH, Kim MJ, Kim HY, Lee MJ. 2014.Radiation dose reduction and image quality in pediatric abdominal CT with kVp and mAs modulation and an iterative reconstruction technique. Clini Imaging 38(5):710-4.

32. Solomon JB, Li X, Samei E. 2013.Relating noise to image quality indicators in CT examinations with tube current modulation. Am J Roentgenol. 200(3): 592-600.

33. Cheng PM. 2013.Automated estimation of abdominal effective diameter for body size normalization of CT dose. J Digit Imaging 26(3): 406-11.

34. Singh S, Kalra MK, Moore MA, Shailam R, et al. 2009. Dose reduction and compliance with pediatric CT protocols adapted to patient size, clinical indication, and number of prior studies. Radiology 252(1): 200-8.

35. Muhogora WE, Ahmed NA, Alsuwaidi JS, Beganovic A, et al. 2010. Paediatric CT examinations in 19 developing countries: Frequency and radiation dose. Rad Protec Dosimetry 140(1): 49-58.

36. Vassileva J, Rehani MM, Applegate K, Ahmed NA, et al. 2013. IAEA survey of paediatric computed tomography practice in 40 countries in Asia, Europe, Latin America and Africa: Procedures and protocols. Eur Radiol. 23(3): 623-31.

37. Fukushima Y, Tsushima Y, Takei H, Taketomi-Takahashi A, et al. 2012. Diagnostic reference level of computed tomography (CT) in Japan. Rad Protec Dosimetry 151(1): 51-7.

38. Yakoumakis E, Karlatira M, Gialousis G, Dimitriadis A, et al. 2009. Effective dose variation in pediatric computed tomogarphy: Dose reference levels in Greece. Health Physics 97(6): 595-603.

39. Santos J, Foley S, Paulo G, McEntee MF, et al. 2014.The establishment of computed tomography diagnostic reference levels in Portugal. Radio Protc Dosimetry 158(3): 307-17.

40. Jarvinen H, Merimaa K, Seuri R, Tyrvainen E, et al. 2011.Patient doses in paediatric CT: Feasibility of setting diagnostic reference levels. Radiat Protc Dosimetry 147(1-2): 142-6.

41. Roch P, Aubert B. 2013. French diagnostic reference levels in diagnostic radiology, computed tomography and nuclear medicine: 2004-2008 review. Radiat Protc Dosimetry 154(1): 52-75.

Chapter 2

Literature Review of Factors Affecting Radiation Dose and Image Quality of Routine Paediatric CT Examinations

2.1 Introduction

Optimisation of paediatric routine CT scan protocols requires an ongoing rigorous process since advances in technology continually change the design and capabilities of CT scanners, even from the same manufacturers. Also, the nature of small body with lack of visceral fat and a wide range of children body size needed to be considered due to changes in the interaction and absorption of radiation [1]. Although CT technology has recently yielded high quality images performed at progressively lower doses, the common practice of applying CT protocols from the existing scanner model to the newer one cannot take full advantage of the new technologies [3, 4]. This is especially true when an institution has multiple CT scanner models developed by the same or different manufacturers. Development of optimum paediatric CT protocols requires a solid understanding of technical aspects of CT such as scanning parameters, image reconstruction applications, radiation dose saving techniques and the intravenous (IV) contrast material administration.

This chapter reviews the current literature related to CT dose optimisation and identifies the factors affecting the radiation dose and image quality of routine paediatric CT examinations for devising the optimised protocols in Chapter 3. The main factors include patient body size and radiosensitivity, scanning parameters and new dose saving techniques. Finally, this chapter ensures that approached methods used are in line with current practices of paediatric CT imaging in grounded research work.

2.2 Patient body size (age, weight and diameter)

Children differ from adults in several aspects. One of the main differences between children and adults is the body mass and proportion. Also, a great variation of body sizes exists between newborn and 15 years old children and even between the same age patients there could be notable differences. The body weight of children varies

from several kg up to 100 kg. Other physiological differences include variations of calcium and protein matrix in bone, cartilage, muscles and fat [6]. The selection of appropriate CT protocols for paediatric patients is challenging.

The paediatric CT protocols based on age categories have been considered not appropriate due to the variation of body size of patients with the same age [5, 7-10]. Also, several recent studies have shown a significant prevalence of overweight and obesity among children globally. The prevalence of overweight and obesity among preschool children rose between 1990 and 2010, not only in the developed countries but also in the developing ones [11-14]. Recent studies have shown that approximately one-third of children and adolescents are either overweight or obese, a tripling over the past few decades [14, 15]. Furthermore, Muthuri et al. [16] in their systematic review concluded that globally the weighted average of obesity was higher in the girls than boys and higher in those with higher socioeconomic status. Thus, the estimated protocols based on age category may underestimate or overestimate the body size, which affect both the radiation dose and image quality.

For more than a decade, emergency departments (ED) in many institutions determine the appropriate drug dosage and equipment size based on body weight of paediatric patients. For example, Broselow-Luten paediatric colour-coded system has helped to substantially reduce the drug administration error rate in the emergency department [17]. Colour-coded CT formatting that equipped in some MDCT is an extension of a clinical colour-coded system. This method organised paediatric CT protocols into body categories based on weight. It is believed that this system provides a simple and preferable method of scanning that result in close adherence to CT protocols, minimising variations that can lead to additional radiation dose to infants and children [18]. In 2001, General Electric (GE) became, the first CT manufacturer to introduce pre-loaded colour coded paediatric protocols based on the child's weight classification [19] (Table 2.1). Despite the fact that this system is in routine use since 2002, many paediatric facilities still operate by default protocols that are based on child's age [20-24].

Patient age may provide a way to adjust CT scanning parameters in children but does not address dose normalisation in small sized adults [25]. Recently, many studies emphasise that scanning parameters in children must be designed based on their weight or body diameter rather than age [5, 7-10, 26]. Although, as part of the

assessment and management in most of the paediatric clinics and ED, weight, height and body max index (BMI) are collected for each patient, radiologists and technologists are unlikely to consider them for adapting the routine scanning protocols unless contrast material administration is required.

Table 2.1 Automatic exposure colour coded control guidelines for paediatric chest and abdomen scans based on a GE MDCT scanner [19].

				Noise Index	
Colour Code	Weight (kg)	Height, (cm)	Age	Chest	Abdomen and pelvis
Pink	5.5-7.4	60–67	2.5–5.5 m	9.5	6.5
Red	7.5–9.4	67–75	5.5–11.5 m	10.0	0 7.5
Purple	9.5–11.4	75–85	11.5–22 m	10.5	8.5
Yellow	11.5–14.4	85–97	22 m–3 y, 2 m	11	9.5
White	14.5–18.4	97–109	3y, 2 m–5y, 2 m	12	10.5
Blue	18.5–23.4	109–121	5y, 2 m–7y, 4 m	13	11.5
Orange	23.5–29.4	121–133	7y, 4 m–9y, 2 m	14	12.5
Green	29.5–36.4	133–147	9y, 2 m–13y, 6 m	15	13.5
Black	36.5–55	>147	>13 y, 6 m	16	14

kg: kilogram, cm: centimetre, y: year, m: month, Noise index: is reference to the standard deviation of CT number within a region of interest in a water phantom of a specific size

The most available and valuable technique to adjust tube current in regards to the patient's size is automatic tube current modulation (ATCM), which automatically adapts the radiation dose to the size of children while maintaining desired image quality [7]. This technique allows tube current to be decreased automatically for regions with lower x-ray attenuation, while maintaining an acceptable level of image noise and improving radiation dose efficiency [27, 28]. Furthermore, manufacturers have introduced new software that automatically selects both the tube voltage (value 70, 80, 90, 100, 120 or 140kV) and tube current on the basis of patient attenuation measured from the CT (scout image) and the user specified CT study task [29-32]. However, these techniques should be used with care in children, due to the fact that appropriate weight-age-body region reference settings is still lacking in many scientific literature as well as to what extent the CT protocols already have been

optimised [5, 33]. Further discussion on this area will be covered in details in the sections of tube voltage and tube current.

In 2011, the American Association of Physicists in Medicine (AAPM) advanced this idea by recommending a method of adjusting CT dose index values based on the effective diameter of the patient [34, 35]. This method is derived from the International Commission on Radiation Units and Measurement (ICRU) report 74 of paediatric body size parameters [36]. However, this method has demonstrated a wide variation in the patient size with respect to age [37, 38]. Pearce [29] illustrated in his study that the estimation of effective diameter method extrapolated from ICRU report is a poor predictor. They found most of the patients below the age of 6 had abdominal effective diameter less than predicted by ICRU curve, while ages 6 to 12 patients demonstrated a broad range of effective diameter above the ICRU curve. The results of this study support the need for the combination of the average patient's size (weight, height and body diameter) rather than age category when taking a step to optimise the paediatric protocols.

Weight or body size related to the age category of children is one of the core elements that influences to all technical parameters that is applied to optimise the paediatric CT protocols. The Alliance Image campaign, the organisation of leading medical societies and regulatory groups, explicitly states that "children are not just smaller adults; their bodies are different and require a different approach to imaging". Furthermore, several studies have recommended that paediatric CT protocols should be defined by patient size taking into account their high radiosensitivity and longer lifetime [39, 40].

2.3 Patient radiosensitivity

A large portion of the exposure from diagnostic procedures comes from CT imaging [41-43]. The use of CT has become more frequent in paediatric radiology [44-46]. This is particularly a concern for children as they are more susceptible to radiation-induced carcinogenesis as well as have a long life span for cancer to develop [39, 47-49]. Several models based on data from the Life Span Study of Japanese atomic bomb survivors have been applied to estimate the risk of radiation induced cancer by CT [39].

This technique has been criticised due to the differences in the sources of radiation and the population exposed [40, 50, 51]. Some investigators claim that no risks are associated with low radiation dose as there are no direct studies of cancer risk in patients who had undergone CT scan [52]. However, the availability of new and more extensive data have strengthened the Biologic Effects of Ionizing Radiation (BEIR) Report VII Linear-no-threshold model – "the risk of cancer proceeds a linear fashion at lower doses without a threshold and the smallest dose has the potential to cause a small increase in risk to human" [39, 40, 53]. This has led to increasing number of studies concerned with the organ doses administrated in paediatric CT examinations [29, 54, 55].

Organ doses are higher in children, and consequently effective dose per energy imparted increases as a body size decrease for all type of CT examination [43, 55-62]. Factors that needed be considered in paediatric CT protocols are the body size and their high radiosensitivity [29, 60-62].

Direct epidemiologic proof has been given for a heightened risk for the neoplastic disease after CT examination in the age under 22 years [29, 40, 54, 64]. CT radiation dose and cancer risks decrease exponentially with increasing patient chest diameter, and it is further decreased exponentially with increased patient age [65]. Higher organ doses in younger children result in conversion coefficients for neonates being five folds higher for the head and three folds higher for the body than those for 15 years old [65].

The risks of CT scan vary according to scan type, with consistently high risks for chest and abdomen CT [67]. The chest and abdomen contain more radiosensitive organs than the head, and the trunk coefficients are greater (4-7 fold) than those for the head at all ages [68]. Furthermore, the projected risks are higher in females than in males for scans that exposed the chest because of the increased likelihood of breast and lung cancer [67, 69]. A study conducted by Pearce [29] in the United Kingdom (UK), found that children who receive active bone marrow dose from CT of 30 mGy or higher were at 3.2 times greater likelihood of getting leukaemia and that children who receive a brain doses of 50 mGy or higher were at 2.8 times greater risk of brain tumour. Similarly, Miglioretti [51] stated that solid cancer risks were higher in girls than boys, and tended to be highest for both chest and abdomen scans. Breast, thyroid, and lung cancers and cases of leukaemia accounting for 68%

of female, whereas cases of brain, lung, and colon cancers and cases of leukaemia account for 51% of future cancer in boys. Distribution doses to the brain, red bone marrow, lungs, breast thyroid and colon wall by age group and anatomic region is illustrated in Table 2.2.

In a recent retrospective cohort study [54] of 11 million children in Australia who underwent CT scan from the period 1985 to 2005 emphasise the direct association between paediatric CT and increased risk of cancer in brain, digestive organs, skin, soft tissue, female genital organs, urinary tract and thyroid. Also, the result of this study shows the incident risk ratio of solid cancer is higher in the female compared to the men [70]. This is similar to the observation on young adults below 22 years exposed to CT scan in the UK study [71].

Table 2.2 Distributions of doses to the brain, red bone marrow, lungs, breast thyroid and colon wall by age group and anatomic region [51].

	Head scan			Abdomen/Pelvis scan			Chest scan			Spine scan		
	Solid cancer			Solid cancer			Solid cancer			Solid cancer		
Age	Girls	Boys	Leuk	Girls	Boys	Leuk	Girls	Boys	Leuk	Girls	Boys	Leuk
	Lifetime Attribution Risks of Cancer per 10,000 CT Scans											
<5y	17.5	7.4	1.9	33.9	14.8	0.8	28.4	8.4	0.6	37.5	5.3	0.7
5-9y	1.6	2.4	0.9	25.8	13.7	0.7	30.5	9.2	0.5	26.2	7.9	0.4
10-14y	1.1	2.1	0.5	27.2	13.1	1.0	20.9	6.1	0.4	12.5	08.6	0.5
	No. of CT Scans Leading to 1 case of cancer (Rounded by the Nearest 10)											
<5y	570	1350	5250	300	670	12170	350	1190	17470	270	1890	14630
5-9y	6130	4150	11660	390	730	14470	330	1080	20570	380	1260	26940
10-14y	9020	4660	21160	370	760	10380	480	1650	25430	800	1170	22020

y: year, leuk: leukaemia

Eventually, current radiation safety philosophy is based on the assumption that any radiation dose at any magnitude can induce cancer. Therefore, it is crucial to design

paediatric CT protocols that address the organ dose that correspond to body size due to the fact that the organ sensitivity is linear to the body size as well as the tissue type. For example, it is important to consider the female group aged between 8-16 years when developing the chest protocols as the breast in this period develops rapidly with glandular tissues, which makes them more susceptible to radiation [72].

2.4 Scanning parameters and other technical considerations

Advances in MDCT have promoted and extended the clinical use of CT scanners, resulting in both the introduction of new scanning protocols and more frequent CT scans [73]. The following subsections cover a range of scanning parameters and other technical considerations that could be optimised for safer examinations without compromising the image quality.

2.4.1 Tube voltage (kV)

The tube voltage determines the quality and to some extent the quantity of the incident x-rays photons [73]. It is an important scanning parameter that should be optimised in CT practices particularly for young patients [8, 9, 75]. Variation in tube voltage causes substantial changes in CT dose as well as image noise and contrast [6]. Table 2.3 illustrates an example of how the relative absorbed dose varies with kV for one particular scanner model in the standard CTDI phantoms. The CTDI metric indicated the influence of the kV to the tube output. Nowadays, MDCT scanners are equipped with four or five discrete kV setting, ranged between 70 and 140 kV for different diagnostic tasks and body sizes [1].

Table 2.3 Absorbed dose of different tube voltage settings [1].

Tube voltage (kV)	Relative CTDIw*
80	0.4
100	0.7
120	1.0
140	1.4

*From CTDIw data for GE LightSpeed VCT in 16 and 32 cm diameter PMMA phantoms. CTDIw: weighted CT dose index

The relationship between dose and tube voltage is not linear, but it is approximately related to the square of the kV. As a general rule of thumb, the x-ray tube voltage changes according to the square of the ratio between the new and reference kV [74]. Thus, at constant tube current (mA) and tube rotation (s) decreasing kV from 120 to 80 decreases radiation dose in air from 58.8 to 21.9 mGy [76].

Studies revealed that using lower tube voltage highly depends on patient size and diagnostic task, where up to 50% of dose reduction can be achieved [1, 77-80]. For paediatric CT head, the use of 80 kV instead of 120 kV along with reduced mAs results in decreased dose up to three times without significantly affecting the image quality [81, 82]. Similarly, reduced kV for paediatric CT head resulted in decreased the $CTDI_{vol}$ by 31% without significantly affecting the contrast to noise ratio (CNR) [82].

For the CT chest, the manipulation of kV resulted in a reduction of $CTDI_{vol}$ by 23% with lower CNR compared to that of the CT brain [82]. Furthermore, a substantial reduction in radiation dose can be realised by combining tube current modulation (TCM) and low tube voltage (80 / 90 kV instead of 100 / 120 kV) [68]. Reduced kV and the use of TCM have reduced paediatric chest CT dose to well below 1 millisievert [65]. In addition, Huda et al [82] found that the effective dose can be up to 30 times higher when radiosensitive organs such as breast are within the primary beam and it increases about 25% when the tube voltage is changed from 90 to 120kV.

There is an overall agreement in many phantom and clinical studies that lowering of tube voltage from 100-80 kV reduces radiation dose and improves image contrast, particularly in young patients [2, 32, 84]. Recent phantom studies suggest that the tube voltage in CT examinations for regions with high intrinsic contrast such as chest, bones and CT angiography could be even lowered to approximately 60 kV [5].

Differential absorption of x-rays for the image formation is greatly influenced by the photoelectric effect. The photoelectric effect is the process where the absorbed x-ray photons interact with inner shell electrons of the atom. This process is inversely proportional to the third power of kV $(1/E)^3$ and directly proportional to the third power of the atomic number (Z^3) [1]. Thus, in the situation of contrast enhancement CT, contrast material such as intravenous iodine is administrated to improve contrast

sensitivity to abnormal vasculature or clot within blood vessels. Iodine within contrast media has *Z* of 53, which has a *k*-absorption edge of 33.2 keV [85]. On other hand, the tube voltage value 120 kV beam has an average energy range of 30-60 keV while 80 kV beam has an average of 24-40 keV [76]. Therefore, the increased enhancement of iodine on CT images obtained at a lower kV is fundamental due to the increased linear attenuation coefficient of iodine [86]. Schindera [76] and Macari [86] showed that increased iodine attenuation at lower tube voltage provides more iodine signal and improves the conspicuity of hyper- or hypo-vascular structures (Figure 2.1). Furthermore, increased enhancement at lower doses is an ideal synergy for contrast enhancement CT examinations. In patients who are small enough, it may be used to improve image quality and reduce radiation exposure [3]. Hence, low voltage significantly improves CNR; lowers the radiation dose; and reduces the amount of contrast material needed. This ultimately results in a reduction of the potential risks of contrast-induced nephropathy [88].

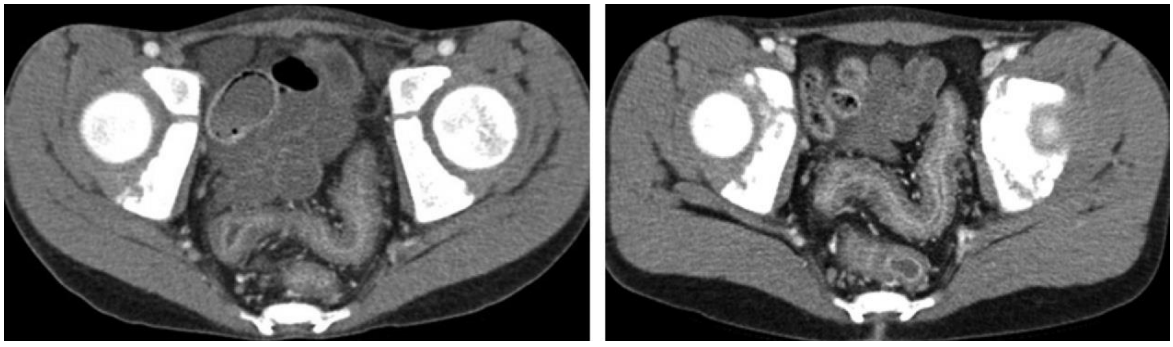

Figure 2.1 Improved contrast enhancement at a lower tube voltage in an 11-year-old boy. Two CT examinations were performed in a 4-month interval, one at 120 kV with a $CTDI_{vol}$ of 5.18 mGy (a) and the other at 100 kV with a $CTDI_{vol}$ of 3.98 mGy (b), following a 50-second delay after contrast material injection. The 100 kV image shows improved contrast enhancement and visualisation of mural stratification [2]

Automatic tube voltage selection with tube current modulation (APSCM) is a newly developed software that automatically adjusts the kV and mAs by measuring attenuation of the patient based on 'scout image' and tasks a specific mAs value that further determine the appropriate kV that range between 80 and 140 kV [3, 31, 32, 89]. The advantage is that it directly detects patient attenuation and adjusts the CT technique to maintain the dose and image quality. In most paediatric patients, tube voltage changed to 70, 80, or 100 kV, resulted in an estimated dose reduction up to

27% compared with the standard 120 kV [32]. Despite the increase in effective mAs, dose reduction would still be substantial while maintaining the CNR at low kV [32]. In daily practice, application of APSCM in paediatric contrast studies and coronary CTA is found to be a feasible method to reduce radiation exposure while maintaining diagnostic image quality [32, 89]. However, the implementation of APSCM is not entirely independent, and CT technologist has to select the reference kV and effective mAs first based on a reference patient size and expected image quality (Figure 2.2). Also, the user must select a contrast strength setting on the basis of contrast iodine or non-contrast iodine studies. For instance, Siemens CARE kV software provides 1-12 strength setting, where 1 refers to the non-contrast study and 12 for highest iodine contrast gain at lower kV [90]. Therefore, the implementation of this tool requires a rigorous process that is based on clinical task and how accurately the paediatric protocols are optimised.

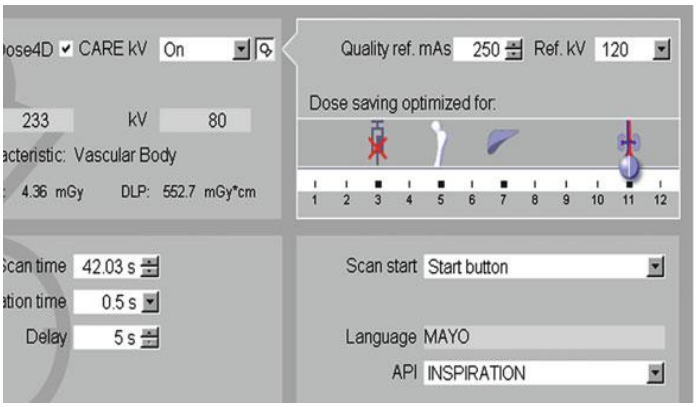

Figure 2.2 Example of using automatic software to select the optimal tube voltage and to prescribe the dose-reduced technique (CARE kV, Siemens Healthcare). The reference technique was at 120 kV and 250 quality reference mAs. The slider bar position, which corresponds to a strength setting, was at 11. 80 kV was identified as the optimal tube voltage [1]

There is an absolute agreement in many scientific studies regarding the influence of kV on both radiation dose and image quality particularly with the contrast enhanced studies. However, the scanner related parameters, such as scanner geometry, beam filtration, detector design and efficiency sometimes negatively influence the image quality with lower tube voltage. Also, there is a lack in the literature of low kV for non-contrast studies because soft tissue contrast is not highly dependent on the tube voltage. Tube voltage affects both the beam energy and intensity, thus the relationship between kV, dose, and image quality is much more complex than the relationship between tube current and dose.

2.4.2 mA and mAs

mA reduction is the most frequently used method for reducing the radiation dose in diagnostic imaging procedures. The product of mA and exposure time (*s*) controls the number of x-ray photons produced during the scan. There is a linear relationship between mAs and dose. For example, radiation dose for a 200 mAs with $CTDI_{vol}$ of 20 mGy can be lowered 50% by decreasing the tube current to 100 mAs (if all other parameters are kept constant). However, increasing the mAs is directly proportional to the radiation dose and inversely proportional to the quantum mottle in the image noise [6, 91, 92]. Quantum mottle is a principal contributor to image noise. Image noise refers to the random nature by which x-rays interact with image receptor and is increased with decreasing number of x-ray photons. Lowering mAs decreases the radiation dose with an increase in image noise (a major drawback) but as long as the images with diagnostic quality this increase in noise can be accepted [6]. The tube current should be adjusted in response to the patient's physical dimensions and the specific imaging task. The larger the patient, the more mAs required to prevent an unacceptable increase of quantum mottle. However, as mAs vary in range depending on the kV setting and the children body varies in size, body weight alone may under or overestimate the dose requirements, because their body diameter may be larger or lower even for identical weight [5].

Based on the aforementioned, several body size specific paediatric CT protocols have been suggested [8-10, 23, 93]. McCollough [94] mentioned that for CT imaging of the head, approximately 2 to 2.5 factor is appropriate in the reduction of the mAs from an adult to a newborn. Also, for CT imaging of the body, a reduction in mAs of a factor of 4 to 5 from adult techniques is acceptable for infants [5]. Although several studies in phantoms have shown that the mAs can be halved for each 3.5 – 4 cm reduction in body diameter, in clinical practice 4-6 cm reduction is used due to the image noise issue that resulted from a lack of visceral fatty tissue in small children [5, 95, 96]. Numerous investigators have shown that mAs should be adjusted as a function of patient size in relation to the overall attenuation of the anatomy of interest [5, 22, 28, 95, 97, 98]. The exception is for imaging of the head, wherein attenuation is relatively well defined by age because the primary attenuation comes from the skull and the process of bone formation in the skull is age dependent [98].

Scanning time is one of the major factors that affect image quality in the paediatric population. Most modern MDCT scanners apply tube rotation time of 0.28-0.5 s resulting in shorter examination times, which has led to expanding the application of paediatric studies [100]. This benefit reduces the need for sedation and allows the imaging of less cooperative children, making the use of CT in paediatric more feasible and is now commonly practiced for evaluation of broad pathologies in brain, thorax and abdomen [43]. However, shorter rotation time may result in increased image noise due to the reduction in the number of profiles that used in image reconstruction [5]. Thus, a rotation time of 0.5s is the best option when considering the image quality.

One has to be crucial when comparing the mAs that given in different manufacturer or scan mode. It is important to note that mAs is indicative of relative radiation exposure of a particular tube on a given type of CT scanner, at given kV. It does not indicate the absolute output when the scanner is made by a different manufacturer or when other kV settings are used [99]. Therefore, for the purpose of comparing radiation dose, mAs should be scaled to a value on each scanner that gives equivalent image quality in terms of spatial resolution, contrast resolution and noise rather than a fixed mAs value [101].

2.4.3 Automatic tube current modulation

Automatic tube current modulation is one of the widely available and the important function to adjust CT technique based on patient size while maintaining both image quality and the radiation dose. It refers to a technique that enable dynamic automatic adjustment of the tube current in the *x, y* plane (angular modulation), along the *z*-axis (*z*-axis modulation), or both to the size and attenuation of the body part being scanned [6]. As a result, image quality can be improved due to a constant noise level in all slices and radiation dose can be reduced [102, 103]. In longitudinal or *z*-axis ATCM, the tube current is varied along the *z*-axis of the patient, with higher mAs used in areas with more tissues to penetrate such as shoulders and pelvis (Figure 2.3), and lower mAs are used in regions of relatively little-attenuating tissues, such as lungs.

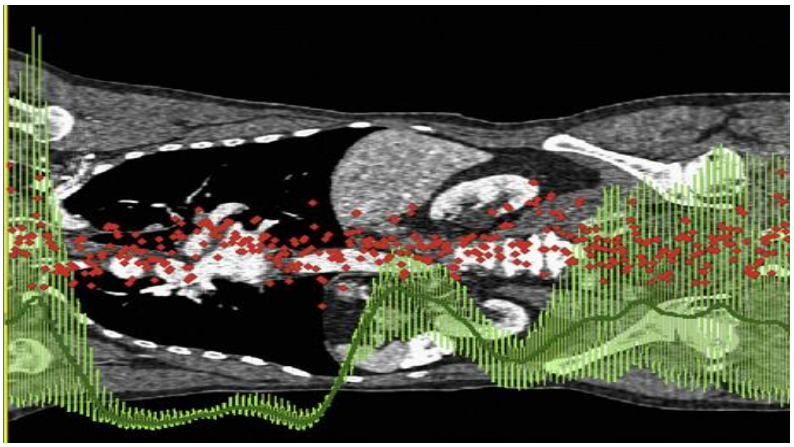

Figure 2.3 Dose modulation for chest, abdomen and pelvis. The tube current is highest at the shoulder, abdominal and pelvis area

The modulation technique and setting used differ considerably depending on manufacturers (Table 2.4). The "CARE Dose 4D" (Siemens Medical Solutions, Forchheim, Germany) uses the concept of quality reference effective mAs (QRM) a tube current x rotation time/pitch. The user is to reference effective mAs for the entire study based on a specific predefined image quality based on patient weights 80 kg and 20 kg for adult and paediatric respectively. New scanners use a single reference patient, weighing 70-80 kg that can be used for both adult and paediatric protocols [104]. The Dose Right (Phillips Medical System, Cleveland, OH, USA) require the user to introduce reference image from prior studies into a database that will be used as reference image quality for the new examination. On other hand, the Auto mA technique (GE Healthcare, Waukesha, WI, USA) uses the noise index (NI), defined as the noise level in the centre of a water phantom using a reference scan method with the selected kV, 200 mA, selected slice thickness and a standard reconstruction kernel. Finally, Sure Exposure software (Toshiba, Medical System, Otawara-Chi, Japan) is comparable with GE System. The primary parameter of this system is the standard deviation (SD), reflecting the noise in all positions along the Z-axis of the patient acquired in a circular water phantom comparable to the size of the patient [1, 5, 99].

Table 2.4 Automatic tube current modulation techniques presently available from different CT scanner manufacturers [104, 105]

AEC Technique	x-y Axis Angular	z-Axis Longitudinal	x-y-z Combined	Selected Parameter
Siemens	CARE Dose	ZEC	CARE Dose 4D	Reference mAs
Philips	D-DOM	Z-DOM	—	mAs per slice
GE	Smart mA	Auto mA	Auto mA 3D	Noise index, minimum and
Toshiba	—	SureExposure	SureExposure3D	Standard deviation of HU

AEC: automatic exposure control, *x-y*: angular modulation, *x-y-z*: angular modulation along the patient during the CT acquisition, CARE Dose: tube current modulations in the *x*,*y* and *z* direction, D-DOM: dynamic angular dose modulation, Z-DOM: z-axis dose modulation, GE: General electric, Smart mA: enables both longitudinal and angular tube current modulation, Auto mA: enables the longitudinal tube current modulation, Sure Exposure: longitudinal modulation in Toshiba, Sure Exposure 3D: both angular and longitudinal modulations, Noise Index*:* The technique parameter entered by the user to determine the desired noise level, HU: Hounsfield unit

Solomon [27] have shown that on comparing Smart mA (GE Healthcare) and CARE Dose 4D (Siemens Healthcare) tube current modulation, Smart mA produces images with the same noise levels irrespective of patient size or shape, whereas CARE Dose 4D maintains constant diagnostic image quality across patient sizes. The detailed implementations of the ATCM vary among the vendors, which initially require the user to select a desired measure of image quality as starting quality.

In departments where dose optimisation has implemented, this technological innovation has added dose savings up to 70% while maintaining adequate diagnostic image quality [5, 9, 68]. Previous study shows that ATCM resulted in 50% of dose reduction for breast in CT chest scans compared to a constant tube current scans [106]. Likewise, Duan et al. [107] suggested that organ-based tube current modulation is a useful method to reduce the dose to the anterior patient surface without affecting image quality or total dose delivered over 360°.

When designing and optimising CT protocols, it is required to balance the need for acceptable image quality with the mandate to keep radiation exposure as low as reasonably achievable. This is especially important for clinical tasks, such as paediatric brain and lung nodule detection that are particularly sensitive to image quality [27, 108]. ATCM makes it possible to design protocols that will produce images of similar quality for patients of different shapes and size [6, 8, 92, 109].

However, its implementation requires caution because different manufacturers apply ATCM differently and use different quality reference indicator. Also, it depends on how accurately quality reference index are chosen to produce images with the desired noise level in paediatric patients. Furthermore, an appropriate body size region reference setting is still lacking in scientific literature as well as to what extent the CT protocols are already optimised [5, 110, 111]. Moreover, $CTDI_{vol}$ changes over the scan length and can be higher at different sections in the scan range when applying the ATCM technique. Thus, estimation of the organ based effective dose with use of these averages may not be accurate [1, 88]. According to Brisse [58], automatic exposure control (AEC) in paediatric anthropomorphic resulted in substantial dose reduction for thyroid, lungs, oesophagus, and breasts in the range of 6% to 39%. However, it also led to higher organ doses for salivary glands, urinary bladder and ovaries as high attenuation from the skull base and pelvic bones increases the mAs with the longitudinal AEC. Therefore, the desired image quality for ATCM must be selected carefully, as higher quality can lead to higher radiation exposure. Also, CT technologist must be aware of the influence of pitch and scan time to the current modulation particularly in scanners that report the tube current in terms of the effective mAs such as Siemens and Philips.

2.4.4 Iterative reconstruction (IR)

As previously mentioned, excessive low dose acquisitions can cause images with lots of artefacts and quantum mottle. To overcome this issue, CT manufacturers have recently developed the iterative reconstruction (IR) algorithm as an image reconstruction technique.

The IR uses multiple iterative algorithms which results in longer time but can substantially reduce the image noise from the same raw data through complex modelling of detector response and of the statistical behaviour of measurement [112]. This technique was initially used in the first generation of CT when relatively small volume of data was dealt with. As CT technology evolved, enormous data were acquired for the single study and the IR technique was not used due to limitation in data analysis capacity of the computers in these days. Thus, for more than four decades, the reconstruction technique was predominated with filtered back projection (FBP) algorithm that uses only a single reconstruction on several

fundamental assumptions about scanner geometry as a compromise between reconstruction speed and image noise. Recently, IR techniques have re-emerged due to the exponential growth of computer technology and the ongoing effort to lower the CT dose while maintaining the diagnostic value. This innovative reconstruction technique allows dose reduction without loss of image quality compared to existing FBP.

The four major CT manufacturers have recently developed their IR products as summarised in Table 2.5. GE Healthcare introduced model-based IR called VEO, ASIR. On the other hand, Siemens presented sinogram affirmed IR (SAFIRE), a reconstruction method that works in both raw data and image space. Philips introduced their IR, iDose at Radiological Society of North America (RSNA) 2009, which aims at producing a noise appearance with respect to structure and spectrum similar to FBP results. This software recently upgraded to iDose^4. Toshiba introduced their adaptive iterative dose reduction (AIDR) software in the USA in 2010 [113].

In terms of image quality, performance of different IR products particularly in routine paediatric CT examinations is a current controversial topic among radiologist since they are scanner- specific and also depend on many other system parameters that have a remarkable influence on the reconstruction performance such as low kV technique.

Table 2.5 List of statistical reconstruction software products of major vendors of clinical CT systems and the year of introduction [6]

Acronym	Meaning	Vendor
ASIR	Adaptive statistical iterative reconstruction	GE 2008
VEO (MBIR)	Product name used the statistical model based iterative reconstruction method	GE 2009
IRIS	Image reconstruction in image space	Siemens 2009
SAFIRE	Sinogram affirmed iterative reconstruction	Siemens 2010
iDose^4	(product name)	Philips 2009
AIDR	Adaptive iterative dose reduction	Toshiba 2010

SAFIRE is one of the most recently developed IR method that uses the raw data for the model-based forward projection and comparison to improve signal to noise ratio and to reduce artefacts [114]. In SAFIRE, five different strengths of iteration are used to reduce noise, and the image noise reduced as the strength of the iteration increased. The user can adjust the image noise reduction by adjusting the strength of the iteration. According to Kalra [109] this IR technique can provide diagnostically acceptable abdominal CT images in most patients at 50% to 75% reduced radiation doses compared with the FBP-based image reconstruction used with most clinical CT equipment. However, the optimal SAFIRE strength for paediatric studies are quite complicated compared to the adult in daily practice. So, it is important to determine the acceptable and optimal strength of SAFIRE for use with low dose CT in clinical practice [115]. However, despite that the higher iteration yield more noise reduction, higher iteration strength in paediatric chest may have inferior visibility of small anatomic structures as well as major pixelated blocky appearance of images which is unpleasant to the radiologist and may lead to misdiagnosing [116, 117].

Since 2009, several studies on adaptive statistic IR (ASIR) demonstrated dose reductions from 18% up to 65% depending on diagnostic and patient requirements, and a possible dose reduction of 36% was estimated for paediatric cardiac CT examinations [117, 118]. Vorona et al. [119] proved that the use of 40% ASIR with a 38% decrease in mAs lowered the radiation dose in paediatric abdominal CT examination by an average of 33% while maintaining diagnostically acceptable images. Mieville et al. [117] concluded in their study that using the mode-based IR VEO (GE Healthcare, Milwaukee, EI) that depends on the clinical objective for small structures and cases involving paediatric follow-up, very high dose reduction (exceeding 90%) might be achievable, although a long reconstruction time is still required. Similarly, Lee [120] revealed that low-dose protocol with 50% ASIR was proven to deliver significant radiation dose decrease in paediatric chest CT, providing 60.3% and 56.2%, reductions in, DLP, and effective dose, respectively, compared with the routine dose studies with FBP without significantly affecting image quality.

The performance of these IRs depend on the dose level used to form the image and the accuracy of the noise model, which requires further investigation and more widely applied tests before routine application in the field. Although, higher iteration

settings are associated with the much lower noise compared with the FBP technique, an exaggerated selection of their strength in paediatric may have inferior visibility of small anatomic structures [113, 120-124]. Also, the individual preferences of practicing radiologists in their visual familiarity with traditional FBP must be taken into account when considering this technique, as some radiologist described IR images as "plastic" or "fogy" in appearance [101, 123]. Furthermore, the current computer processing hardware is still slow to enable near real-time display of images during the scanning. There is approximately five-second delay between the initiation of scan and the display of IR images [122, 123]. For the appropriate use of this technique, radiologist must establish in collaboration with CT technologist a standard protocol based on particular pathology sensitivity, age and body size in relation to the iteration strength as well as selection of the proper choice of reconstruction kernel [119, 125].

2.4.5 Diagnostic reference levels (DRLs)

Diagnostic reference levels (DRLs) expressed in terms of volume CT dose index ($CTDI_{vol}$, mGy), dose length product (DLP, mGy-cm) and effective dose (*E,* mSv) for each examination. Current CT scanners provide $CTDI_{vol}$ and DLP doses information for each prescribed scan series.

The $CTDI_{vol}$ is the average absorbed dose in the phantom with 16 or 32 cm diameter. It is a function of kV, mAs, bundle filtering, collimation and pitch ($CTDI_{vol}$ = CT weighted (CTDIw)/ pitch). CTDIw represents the measurement dose in both central and peripheral of phantom. The $CTDI_{vol}$ displayed on the scanner console before the initiation of scan allows the operator to confirm the proper acquisition output protocols and are recorded as part of the dose reading at the end of the examination.

DLP is the product of the $CTDI_{vol}$ and scan length ($DLP=CTDI_{vol}$ x Scan Length) [83, 94, 126-128]. In more detail, DLP reflects the total energy absorbed attributable to the complete scan acquisition. Thus, an abdomen CT might have the same $CTDI_{vol}$ as an abdomen and pelvis CT exam, but the latter exam would have a greater DLP that is directly proportional to the *z*- axis of the scan volume.

As mentioned above, dose readings are derived either from 16 or 32 cm CTDI phantom. The 16 cm CTDI phantom is intended to present the approximate size of

an adult head or paediatric abdomen, whereas the 32 cm CTDI phantom is for an adult abdomen. Hence, various studies consider the 16-cm phantom a closer approximation to paediatric chest and abdomen size than the 32-cm phantom, and therefore recommend the use of the smaller phantom for paediatric body CT dosimetry [7, 57, 127, 128]. Despite this recommendation, the application of these phantom sizes to various CT examinations are unclear among manufacturers. According to MacDougall et al. [102], Siemens calculates $CTDI_{vol}$ using the 32-cm phantom for all body protocols and the 16-cm for all head protocols for both adult and paediatric, whereas GE (GE Healthcare Technologies, Waukesha, Wisconsin) uses the 32-cm phantom only for adult body protocols and the 16-cm phantom for paediatric body and all head protocols. As a result, CT dose to a small patient (i.e., a patient with an average diameter less than 32 cm) may be underestimated. In particular, without adjusting dose data for body size, excessive radiation dose in small patients may be difficult to detect in a large dose database [35]. Professional organisations such as AAPM and International Commission on Radiological Protection (ICRP) have recommended the phantom size for the $CTDI_{vol}$ and DLP calculations to be displayed on the final dose screen, yet this has not become a feature of the current scanners [93, 129].

The effective dose is used to assess the stochastic effect of radiation exposure such as the probability of induction of cancer and genetic problem. The effective dose depends on the type of radiation, radiosensitivity of organs and absorbed dose [59]. In CT scan, effective dose is commonly estimated by using the DLP displayed on the console multiplying with age and region specific conversion coefficients (Table 2.6) (E/DLP), which are considered independent of CT scanner type and manufacturer [67, 81]. However, most of the displayed dose reading for paediatric CT trunk referred to the 32 cm phantom. Thus, the use of DLP data may substantially underestimate the effective dose to children undergoing body examinations. Shrimpton [66] and Wong et al. [75] have found that this can be compensated by multiplying paediatric body DLP values that are based on 32cm phantom by a factor of two before applying the age-appropriate conversion coefficient. It must be clear that this dose should not be intended for retrospective use for estimation of doses to individuals, it can be used here as an optimisation tool

that allow comparison with similar procedures undertaken at different institution [5, 34, 102, 129].

Table 2.6 Effective dose per dose-length product (DLP) over various body regions and (standard) patient ages [102]

Region	**Effective dose per DLP(mSv(mGycm)$^{-1}$) by age**				
	Neonate	**I year old**	**5 years old**	**10 years old**	**Adult**
Head & Neck	0.013	0.0085	0.0057	0.0042	0.0031
Head	0.011	0.0067	0.0040	0.0032	0.0021
Neck	0.017	0.012	0.011	0.0079	0.0059
Chest	0.039	0.026	0.018	0.013	0.014
Abdomen & pelvis	0.049	0.039	0.020	0.015	0.015
Trunk	0.044	0.028	0.019	0.014	0.015

DLP: dose length product

The use of DRLs has been proposed as an optimisation tool by ICRP [68]. According to Kritsaneepaiboon et al. [21], the details and implementation of this dose reading are the tasks for the regional, national, and local official bodies. There are several studies that established, presented and proposed national DRLs in the adult population. However, there are only few studies which presented DRLs for the paediatric population based on age or body size [21, 23, 33, 69, 97, 130, 131]. The recommended age-based national DRLs for paediatric CT was published in UK in 2006 [71], followed by national DRLs survey in German in 2007 [33] and Switzerland study [97] in 2008. On the other hand, weight –based dose readings were published in Australia in 2010 [23], in Finland in 2011 [130] and in Thailand in 2012 [21], which revealed the discrepancies between the age and weight groups. For example, when comparing the UK study based on age and the Australian study based on weight for helical chest examinations, there is 66% difference of DRLs values for the 0-10 kg group (equivalent to 1 year) when comparing to the 1-year age group of UK survey. Also, the Australian study shows 59% reduction on DRLs for the 11-25 kg group as (equivalent to 5 years) compare to the UK survey. When comparing age-based DRLs to weight-based DRLs, the age-based DRLs for the younger children frequently demonstrated higher dose levels, while the older

children's age-based DRLs were lower than weight-based DRLs [23]. Some radiation protection experts may argue in regards to the comparison given due to the scanners specific involved in each study.

It is quite difficult to define what a standard size child is, or even to set a standard size in age category particularly with the wide age range and problems relating to obesity in modern society [23]. Nevertheless, several studies concern the paediatric radiation doses have widely acknowledged that CT scanning should be performed using weight-based protocols. Further, the AAPM Task Group 204 described a method for adjusting $CTDI_{vol}$ values based on the effective diameter of the patient, where effective diameter defined as the diameter of the circle whose area is the same as the patient cross section [98]. This task was aimed to address the problem of dose normalisation using data from both physical phantoms and Monte Carlo-based measurement. However, extracting the effective diameter manually in a clinical environment is not feasible. Nonetheless, few studies had initiated effort to obtain the patient diameter automatically [8-10].

Despite the vast controversial of how the DRLs approached, it is clear that both $CTDI_{vol}$ and DLP are very useful tools that are allowing direct comparison of the estimated radiation dose among scanners of different manufacturers. For example, $CTDI_{vol}$ provides a consistent and reproducible quantitative measure in quantifying the radiation output of a CT scanner [5], and therefore provides a very useful way to compare the doses delivered by various scan protocols or to achieve a specific level of image quality for a particular size patient [75, 126]. Hence, these dose values can be used as guidelines for the optimisation of paediatric CT protocols by prescribing the right dose for a particular patient size based on weight and diagnostic task [99, 126]. However, neither $CTDI_{vol}$ nor DLP should be used to estimate effective dose or potential cancer risk for any individual patient [97, 126, 132]. In addition, $CTDI_{vol}$ must not be used as an indicator dose when automatic dose modulation applied, because it either corresponds to the maximum value of the *z*- axis modulation or the mean of the maximum values of the AP and lateral direction of the ATCM [5].

2.4.6 Scanogram or scout- view

The first step in CT image formation is the scout-view that determines the pre-acquisition parameters such as ATCM, kV, APSCM, and scan range. There are four factors that must be considered before the scout-view take place: scout view length, patient position and centring, tube position, kV and mAs settings.

The length of the scout-view should be as short as possible to include precisely the required region of interest. For example, a chest CT scout-view must cover the area of chest without unnecessarily including the neck and abdomen. However, users must exercise caution in selecting the area of scout-view when applying the ATCM because some CT scanners use the scout-view data for tube current mapping to achieve the required image quality.

Optimum patient positioning and centring in the gantry are necessary for any CT study and it is important for technological innovative dose reduction functions such as pre-patient beam collimation, beam shaping filters and ATCM to be operated appropriately [91, 92]. Phantom and clinical studies have shown that improper positioning of the patient in the gantry iso-centre can adversely affect specific image quality with the ATCM [104, 133, 134]. This compromise in image quality may be due to the use of bow-tie filters in CT scanners. Thus, use of lower dose ATCM technique in paediatric patients who are off-centred to the gantry can lead to a disproportionate increase in image noise as well as the surface and peripheral radiation dose [92]. Lai et al. [134] have suggested that organ based -ATCM may increase the dose to the eyes by 18% and double the superficial dose to the breast in the off-centre patient.

In a study conducted by Sorantin et al. [108] with paediatric phantom shows that two-thirds of scout view dose can be saved by just placing the tube below the CT couch, which is possible in new CT machine. A posterior-anterior projection of scout image in the supine patient significantly reduces doses to radiosensitive organs, such as male gonads, thyroid, breast and the lens of the eye [136]. Furthermore, a default setting of kV and mA for scout-view can add unnecessary radiation dose in the small paediatric patient. These fixed settings can account for adding more than 50% dose in a single chest CT examination [108]. Further, adjusting scout-view of 80 kV from the default 120 kV and changing the tube position from 180˚ to 0˚, radiation

exposure could be reduced to less than exposure of a chest radiograph [137]. Unfortunately, the scout view dose is neglected by many CT technicians during their daily practice, particularly in paediatric patients. For example, in CT chest, usually neck and large part of the abdomen are exposed unnecessarily as well as in abdomen examination large area of chest are included during the scout view.

2.4.7 Pitch and scan collimation

The pitch, scan collimation and gantry rotation factors are interlinked to each other as well as to detector configuration used in CT scanner. Pitch is related to scan collimation and tube rotation and influences both image quality and radiation dose [6, 126]. In a single detector CT (SDCT) scanner, the pitch is defined as the ratio of the table index per x-ray tube rotation to the slice width or collimation. Advanced MDCT technology introduced some confusion regarding the definition of pitch, as some manufacturers use different definitions of pitch that is related to the table travel per tube rotation to the width of individual data channels. Thus, as the number of data channels increased, the two definitions of pitch lead to further confusion [1, 6].

It was until International Electrotechnical Commission (IEC) reissued their safety standard and specifically addressed the definition of the pitch to the original definition (table travel normalised to the total beam collimation) as the only accepted definition of pitch in both SDCT and MDCT scanners [6]. Nevertheless, the concept of pitch and its related radiation dose and image quality is quite different between the SDCT and the advanced MDCT. For example, with SDCT scanners, pitch greater than 1-1.5 reduces the radiation dose by a third and doubling the pitch halves the radiation dose if other parameters are not changed [42]. On the other hand, using higher pitch does not result in dose saving, which is an important practical consideration with MDCT scanners relying on adaptive axial interpolation and the effective mAs concept [1]. For some MDCT scanners such as Toshiba and GE, tube current is automatically increased where the pitch increase to maintain the CNR [6, 98]. Also, increasing the pitch may significantly increase the negative dose effect of over scanning particularly with MDCT scanner that utilised less than 32 channels and decreased in spatial resolution [137]**.** Nevertheless, the use of the lower pitch values provides image quality at the same patient dose whether manual or automatic tube current modulation technique being used [138].

In fact, the pitch has less effect on image quality of MDCT scanner than SDCT scanner. Nevertheless, in situations such as imaging of liver metastases or pancreas lesions that required thinner collimation, an increased pitch may lead to misdiagnosis due to the degradation of the section sensitivity profile [6].

Image noise is proportional to the square root of the number of x-rays to image formation [3], so as the number of x-rays scales with slice thickness. Image noise is proportional to the square root of the slice thickness if all other parameters are unchanged during image acquisition and reconstruction [1, 5, 96]. As a result, 2-mm thick image slices, if reconstructed from the same raw data and with the same reconstruction algorithm, may contain twice as much noise compare to the 4-mm thick image. Beside the image noise, the thinner slice also has the negative influence on the over-beaming effect resulting in an increase in radiation dose that will be discussed later [6].

Paediatric imaging required thinner collimation during acquisition especially along the z-axis to maximise image spatial resolution. However, this increases the image noise due to the collimation factor and the effect of the x-ray absorption in small children body size that lack visceral and fatty tissue. Nevertheless, less noise can be tolerated in paediatric imaging than in adolescent and adult. According to Nievelstein et al. [5] the choice of collimation depends on the clinical question and the size of the patient and should balance the necessary z-axis resolution noise and low radiation level. In addition, CT post processing reconstruction software provides wide range of tools that can be utilised to minimise the image noise. One of the preferable methods used while interpreting the image is the “scan thin-view thick” method.

Thus, it is crucial that the user must be aware of the concept of scanner that is used to avoid pitch misuse and scan collimation in relation to the radiation dose. Usually, thinner slice or high pitch burden radiation dose to the patient is used due to the required high tube current to compensate the image noise. This is quite remarkable in paediatric subjects where image noise is inherited due to the physiological variations of calcium and protein matrix in bone, cartilage and fat of children body.

2.4.8 Over-scanning and over beaming

Over-scanning is a reconstruction algorithm that is partly associated with the need to scan a slightly large volume than the planned volume to get sufficient data interpolated for reconstruction of the beginning and the end slice [5, 138]. Usually, there is an additional half rotation at both start and end of the intended scan length, which may increase the dose up to 20% for head and neck studies and may be up to 35% for chest and abdomen examination [62]. The over-scanning length increases with increasing beam width and pitch. According to Dougeni [140], length range about 5 to 7 cm was reported for chest and abdomen–pelvis scans; however, this drops to about 3 cm for smaller beam widths. In addition, Sorantin et al. [107] mentioned that MDCT scanner for a collimation of 64x0.6 mm, the length of over-scanning is approximately 2 cm at the start and end of the scan range for a pitch of 1 and increases with higher pitch value. For instance, Fujii et al. [62] reported additional scan range of up to 25% for adult chest CT (1.375 and 1.015 pitch factor) and up to 47% for paediatric chest CT examinations (pitch factor 1.406) [141]. Similarly, Kalra [6] shows that with a larger beam width such as 64 x 0.625 mm (40 mm) compared to 32 x 0.625 mm (20 mm), there was more over-scanning with the larger effective collimation when smaller area was scanned as in infant's chest. However, this problem has been minimised by the state of art MDCT scanners that are equipped with adaptive pre-patient collimators capable of blocking most of the unnecessary radiation at the beginning and end of the scan range [108]. Yet, this is applicable on scanner operated with more than 64 multi-slices, and caution must be taken in scanners without adaptive collimators.

Over-beaming is the excess dose per rotation as the consequences of focal spot penumbra falls outside the active detector area that not used for imaging purposes [137, 141]. This is quite remarkable with MDCT scanners as more than one active detector channel is used. Thus, the reconstruction algorithm requires a homogenous illumination of all detectors. As a result, penumbra must either totally or partially be excluded from detection with widening the beam bundle by opening up the pre-collimation. So the detector is 'over-beamed', and a certain portion of the radiation that exposes the patient remains unused Figure 2.4. The focal spot size, the ratio distance between collimator and detectors, and the distance between the focal spot and detector determine the penumbra size [5, 136]. In modern CT scanners the

penumbra measures between 1 and 1.5 mm on both side of the collimated bundle. Therefore, the dose increasing effect of over-beaming decreases with increasing number of detectors and slice collimation, which is minor in MDCT scanners with 32 slices or more [5].

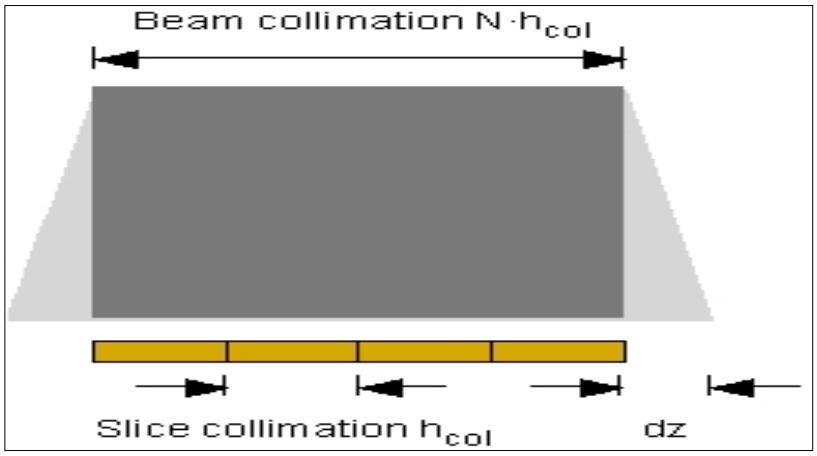

Figure 2.4 Shows over-beaming. The X-ray bundle consists of the umbra (black) and penumbra (grey), caused by the diverging bundle. In MDCT the penumbra is excluded from detection by the detector array in order to achieve a uniform illumination of the detectors (overbeaming) [5].

2.4.9 Bowtie shaping filters

The main purpose of bowtie filters is to compensate for variation in the patient's body thickness, and to ensure rays passing through the patient are hardened similarly. Its name given for its bowtie-like shape, which is usually a piece of material (aluminium), placed between the X-ray source and an object to be imaged. This beam shaping filters ensure the uniform distribution of photon flux attenuated with various body thickness along the detectors that helps to improve image quality and overall radiation dose rate delivered to the patient [141, 143].

Most CT scanners provide the various select size of the bowtie filter such as large, medium and small based on the type of examination and the scan field of view (FOV) [102]. According to Nievelstein et al. [5], the scan FOV must be tailored as much as possible to the size of the body region of interest. Likewise, Lobo and Antunes [144] emphasised that, in paediatric CT examination, the FOV should be as

small as possible to increase spatial resolution and avoid oversampling. Furthermore, this filters function best when the patient is centred at the gantry iso-centre. However, with off centring of the patient, less X-ray photons pass through the patient's thicker centre part, causing increasing noise in the centre of the image, while more X-ray photons pass through the peripheral portion of the body cross section, resulting in increasing radiation dose [6]. This rise in image noise may get worse especially when patients scanned with low dose or ATCM technique.

Li et al. [133] on their study of the "automatic patient centring for MDCT: effect on radiation dose" shown that almost 95% of patients undergoing chest or abdominal CT were off-centred in the gantry. Consequently, off centring increased the peripheral and surface by 12-18% and 4-49%, respectively, at off-centre distance 3-6 cm [6]. Moreover, Boone et al. [98] mentioned that as the entrance dose to the skin of the patient is a part a function of the distance of the skin from the focal spot of the scanner, positioning the patient's body in the middle of the gantry reduces the radiation dose to the patient. Thus, the operator must be aware of how the bowtie shaping flitters are designed regarding the paediatric patient along their wide body size, the consequences of off centring and improper selecting of FOV.

2.5 Conclusion

In this chapter, it is evident that the principal aim of optimisation of paediatric protocols is to adjust imaging parameters and utilise protective measures to obtain diagnostic images with lowest possible radiation dose while maintaining image quality.

Variation of children body size complicates the optimisation process. Current CT practices rely on the children's age and weight that do not always normalise the actual body size to the acquisition parameters.

Paediatric CT practices must consider the higher dose risk in children due to their longer life expectancy, which allows more time for any harmful effects of radiation to manifest. Also, the average risks among the children vary; it is higher in infants and young children compared to older children. Furthermore, some developing organs and tissues in the young female such as breasts are more sensitive to

radiation. Therefore, optimisation of paediatric CT must address the variation in body size and ongoing evolution in CT technology.

In all circumstances, optimisation of protection is not about minimising radiation dose, but balancing the detriments and benefits. This is particularly important in the paediatric population, where an optimisation requires an ongoing process of manipulating a broad range of parameter settings to address the wide range in children size. Also, besides the body size, there are many other differences in maturation such as a low calcium and protein matrix in the bone, more cartilage, less muscle and fat.

It is clear that it is impossible to have a global reference paediatric protocols that precisely provide same scan parameters due to varying paediatrics' physiological pattern, ongoing evolution in CT technology, different scan manufacturers, different scanner mode, different radiation dose techniques as well as different clinical diagnostic task. This makes comparison among scanners difficult and exchange of protocols almost impossible even with same manufacturer. Nevertheless, recently published studies show a significant reduction in radiation dose by optimising paediatric CT protocols based on the body size rather than the manufactured default protocols based on age categories. Also, CT manufacturers have introduced new software or techniques that maintain the balance between the reduction on radiation dose and the diagnostic acceptability such as MDCT, organ dose tube current modulation, automatic tube voltage as well as the iteration reconstruction technique. Special consideration should be given to the availability of qualified medical imaging physicists who are able to verify the protocols that are designed by the manufacturer. Furthermore, radiologists and CT technologists must understand the advance in technology and its clinical application and be aware of the factors that affect image quality and radiation dose to patients undergoing CT examinations.

2.6 References

1. Tack D, Kalra Mk, Gevenois PA. Radiation Dose from Multidetector CT. 2nd ed. New York: Springer Heidelberg; 2012.

2. Yu LF, Bruesewitz MR, Thomas KB, Fletcher JG, et al. 2011. Optimal tube potential for radiation dose reduction in pediatric CT: Principles, clinical implementations, and pitfalls. Radiographics 31(3): 835-48.

3. Sodickson A. 2012.Strategies for reducing radiation exposure in multi-detector row CT. Radiol Clin N Am. 50: 1-14.

4. Sodickson A. 2013.Strategies for reducing radiation exposure from multidetector computed tomography in the acute care setting. Cana Assoc Radiol J. 64(2): 119-29.

5. Nievelstein RA, van Dam IM, van der Molen AJ. 2010. Multidetector CT in children: Current concepts and dose reduction strategies. Pediatr Radiol. 40(8): 1324-44.

6. Kalra MK, Saini S, Rubin GD. MDCT from Protocols to Practice. Verlag Italia: Springer; 2008.

7. Singh S, Kalra MK, Moore MA, Shailam R, et al. 2009. Dose reduction and compliance with pediatric CT protocols adapted to patient size, clinical indication, and number of prior studies. Radiology. 252(1): 200-8.

8. Dong F, Davros W, Pozzuto J, Reid J. 2012.Optimization of kilovoltage and tube current-exposure time product based on abdominal circumference: An oval phantom study for pediatric abdominal CT. Am J Roentgenol. 199(3): 670-6.

9. Reid J, Gamberoni J, Dong F, Davros W. 2010. Optimization of kVp and mAs for pediatric low-dose simulated abdominal CT: Is it best to base parameter selection on object circumference? Am J Roentgenol.195(4): 1015-20.

10. Hopkins KL, Pettersson DR, Koudelka CW, Spinning K, et al. 2013. Size-appropriate radiation doses in pediatric body CT: A study of regional community adoption in the United States. Pediatr Radiol. 43(9): 1128-35.

11. Griffiths C, Gately P, Marchant PR, Cooke CB. 2013. A five year longitudinal study investigating the prevalence of childhood obesity: Comparison of BMI and waist circumference. Public Health 127(12): 1090-6.

12. Lyu Y, Ouyang F, Ye XY, Zhang J, Lee SK, et al. 2013.Trends in overweight and obesity among rural preschool children in southeast China from 1998 to 2005. Public Health. 127(12): 1082-9.

13. Miqueleiz E, Lostao L, Ortega P, Santos JM, Astasio P, et al. 2014. Trends in the prevalence of childhood overweight and obesity according to socioeconomic status: Spain, 1987-2007. Eur J Clin Nutrition. 68(2): 209-14.

14. Economos CD, Bakun PJ, Herzog JB, Dolan PR, Lynskey VM, et al. 2014. Children's perceptions of weight, obesity, nutrition, physical activity and related health and socio-behavioural factors. Public Health Nutrition 17(1): 170-8.

15. Flegal KM, Carroll MD, Kit BK, Ogden CL. 2012. Prevalence of obesity and trends in the distribution of body mass index among US adults, 1999-2010. JAMA 307(5): 491-7.

16. Muthuri SK, Francis CE, Wachira LJ, Leblanc AG, et al. 2014. Evidence of an overweight/obesity transition among school-aged children and youth in Sub-Saharan Africa: A systematic review. PloS One 9(3): e92846.

17. Luten RC, Wears RL, Broselow J, Zaritsky A, et al. 1992. Length-based endotracheal tube and emergency equipment in pediatrics. Ann Emerg Med. 21(8): 900-4.

18. Frush DP, Soden B, Frush KS, Lowry C. 2002. Improved pediatric multidetector body CT using a size-based color-coded format. Am J Roentgenol. 178(3): 721-6.

19. Color-coded CT protocols help reduce pediatric radiation dose. 2009. http://www.auntminnie.com/index.aspx?sec=ser&sub=def&pag=dis&ItemID=8604. (Accessed on 27 Mar 2014).

20. Santos J, Foley S, Paulo G, McEntee MF, et al. 2014. The establishment of computed tomography diagnostic reference levels in Portugal. Radiat Prot Dosimetry. 158(3): 307-17.

21. Kritsaneepaiboon S, Trinavarat P, Visrutaratna P. 2012. Survey of pediatric MDCT radiation dose from university hospitals in Thailand: A preliminary for national dose survey. Acta Radiologica. 53(7): 820-6.

22. Arch ME, Frush DP. 2008. Pediatric body MDCT: A 5-year follow-up survey of scanning parameters used by pediatric radiologists. Am J Roentgenol. 191(2): 611-7.

23. Watson DJ, Coakley KS. 2010. Paediatric CT reference doses based on weight and CT dosimetry phantom size: local experience using a 64-slice CT scanner. Pediatr Radiol. 40(5): 693-703.

24. Vassileva J, Rehani MM, Applegate K, Ahmed NA, et al. 2013. IAEA survey of paediatric computed tomography practice in 40 countries in Asia, Europe, Latin America and Africa: Procedures and protocols. Eur Radiol. 23(3): 623-31.

25. Cheng PM, Vachon LA, Duddalwar VA. 2013. Automated pediatric abdominal effective diameter measurements versus age-predicted body size for normalization of CT dose. J Digit Imaging. 26(6): 1151-5.

26. Goo HW. 2012. CT radiation dose optimization and estimation: An update for radiologists. Korean J Radiol. 13(1): 1-11.

27. Solomon JB, Li X, Samei E. 2013. Relating noise to image quality indicators in CT examinations with tube current modulation. Am J Roentgenol. 200(3): 592-600.

28. Sookpeng S, Martin CJ, Gentle DJ, LopezGonzalez MR. 2014. Relationships between patient size, dose and image noise under automatic tube current modulation systems. J Radiol Protec. 34(1): 103-23.

29. Pearce MS, Salotti JA, Little MP, McHugh K, et al. 2012. Radiation exposure from CT scans in childhood and subsequent risk of leukaemia and brain tumours: A retrospective cohort study. The Lancet. 380(9840): 499-505.

30. Eller A, Wuest W, Scharf M, Brand M, et al. 2013. Attenuation-based automatic kilovolt (kV)-selection in computed tomography of the chest: Effects on radiation exposure and image quality. Eur J Radiol. 82(12): 2386-91.

31. Park YJ, Kim YJ, Lee JW, Kim HY, et al. 2012. Automatic tube potential selection with tube current modulation (APSCM) in coronary CT angiography: Comparison of image quality and radiation dose with conventional body mass index-based protocol. J Cardiov CT. 6(3): 184-90.

32. Siegel MJ, Hildebolt C, Bradley D. 2013. Effects of automated kilovoltage selection technology on contrast-enhanced pediatric CT and CT angiography. Radiology 268(2): 538-47.

33. Galanski M, Nagel H, Stamm G. Paediatric CT Exposure Practice in the Federal Republic of Germany: Results of a Nationwide Survey in 2005–2006. Hannover: Medizinische Hochschule; 2007.

34. Brink JA, Morin RL. 2012. Size-specific dose estimation for CT: How should it be used and what does it mean? Radiology. 265(3): 666–8.

35. Cheng PM. 2013. Automated estimation of abdominal effective diameter for body size normalization of CT dose. J Digit Imaging. 26(3): 406-11.

36. Zoetelief J, Dance DR, Drexler G, Ja¨rvinen H, Paretzke HG, Allisy P. 2005. Patient dosimetry for x rays used in medical imaging. J ICRU 5(2): iv-vi.

37. Brady SL, Kaufman RA. 2012. Investigation of American Association of Physicists in Medicine Report 204 size-specific dose estimates for pediatric CT implementation. Radiology. 265(3): 832-40.

38. Kleinman PL, Strauss KJ, Zurakowski D, Buckley KS, et al. 2010. Patient size measured on CT images as a function of age at a tertiary care children's hospital. Am J Roentgenol. 194(6): 1611-19.

39. Brenner DJ, Doll R, Goodhead DT, Hall EJ, et al. 2003. Cancer risks attributable to low doses of ionizing radiation: assessing what we really know. Proceedings of the National Academy of Sciences of the United States of America. 100(24): 13761-6.

40. Linet MS, Kim KP, Rajaraman P. 2009. Children's exposure to diagnostic medical radiation and cancer risk: epidemiologic and dosimetric considerations. Pediatr Radio. 39: S4-26.

41. Krille L, Zeeb H, Jahnen A, Mildenberger P,et al. 2012. Computed tomographies and cancer risk in children: A literature overview of CT practices, risk estimations and an epidemiologic cohort study proposal. Radiat Environ Biophys. 51(2): 103-111.

42. Paterson A, Frush DP. 2007. Dose reduction in paediatric MDCT: General principles. Clin Radiol. 62(6): 507-17.

43. Feng ST, Law MW, Huang B, Ng S, et al. 2010. Radiation dose and cancer risk from pediatric CT examinations on 64-slice CT: A phantom study. Eur J Radiol. 76(2): e19-23.

44. Seeram E. 2014. Computed tomography dose optimization. Radio Techno. 85(6): 665-675.

45. Krille L, Hammer GP, Merzenich H, Zeeb H. 2010. Systematic review on physician's knowledge about radiation doses and radiation risks of computed tomography. Eur J Radiol. 76(1): 36-41.

46. Larson DB, Johnson BM, Schnell BM, Goske MJ, et al. 2011. Rising use of CT in child visits to the emergency department in the United States, 1995–2008. Radiology. 259(3): 793-801.

47. Larson DB, Johnson LW, Schnell BM, et al. 2011. National trends in CT use in the emergency department: 1995-2007. Radiology. 258(1): 164-1973.

48. Rodgerson C. 2014. ALARA and paediatric imaging in radiation therapy: A survey of Canadian paediatric imaging practice. Radiography 20(3): 183-188.

49. Matthews K, Brennan PC, McEntee MF. 2014. An evaluation of paediatric projection radiography in Ireland. Radiography. 20(3): 189-194.

50. Chodick G, Ronckers CM, Shalev V, Ron E. 2007. Excess lifetime cancer mortality risk attributable to radiation exposure from computed tomography examinations in children. Isr Med Assoc J. 9(8): 584-7.

51. Miglioretti DL, Johnson E, Williams A, Greenlee RT, Weinmann S, Solberg LI, et al. 2013. The use of computed tomography in pediatrics and the associated radiation exposure and estimated cancer risk. JAMA Pediatrics. 167(8): 700-7.

52. Tubiana M, Feinendegen LE, Yang C, Kaminski JM. 2009. The linear no-threshold relationship is inconsistent with radiation biologic and experimental data. Radiology. 251(1): 13-22.

53. Kleinerman RA. 2006. Cancer risks following diagnostic and therapeutic radiation exposure in children. Pediatr Radiol. 36(2): 121-5.

54. Akhlaghi P, Hakimabad HM, Motavalli LR. 2013. An overview of exposure parameters, dose measurements and strategies for dose reduction in pediatric CT examinations. Radio Prot Dosmetry. 49(1): 9-15.

55. Mathews JD, Forsythe AV, Brady Z, Butler MW, Goergen SK, Byrnes GB, et al. 2013. Cancer risk in 680,000 people exposed to computed tomography scans in childhood or adolescence: Data linkage study of 11 million Australians. BMJ 346: f2360.

56. Huda W, Gkanatsios N. 1997. Effective dose and energy imparted in diagnostic radiology. Med Phys. 24(8): 1311-6.

57. Thomas KE, Wang B. 2008. Age-specific effective doses for pediatric MSCT examinations at a large children's hospital using DLP conversion coefficients: A simple estimation method. Pediatr Radiol. 38(6): 645-56.

58. Brisse HJ, Robilliard M, Savignoni A, Pierrat N, Gaboriaud G, De Rycke Y, et al. 2009. Assessement of organ absorbed doses and estimation of effective doses from pediatric anthropomorphic phantom measurments for multi-detctor row CT with and without automatic exposure control. Health Physics. 97(4): 303-14.

59. Christner JA, Kofler JM, McCollough CH. 2010. Estimating effective dose for CT using dose-length product compared with using organ doses: Consequences of adopting International Commission on Radiological Protection publication 103 or dual-energy scanning. Am J Roentgenol. 194(4): 881-9.

60. Seidenbusch MC, Regulla D, Schneider K. 2010. Radiation exposure of children in pediatric radiology part 7: Conversion factors for reconstruction of organ dose during thoracoabdominal babygrams. Rofo 182(5): 415-21.

61. Fujii K, Aoyama T, Koyama S, Kawaura C. 2007. Comparative evaluation of organ and effective doses for paediatric patients with those for adults in chest and abdominal CT examinations. Br J Radiol. 80(956): 657-67.

62. Fujii K, Aoyama T, Yamauchi-Kawaura C, Koyama S, et al. 2009. Radiation dose evaluation in 64-slice CT examinations with adult and paediatric anthropomorphic phantoms. Br J Radiol. 82(984): 1010-8.

63. Huda W, Vance A. 2007. Patient radiation doses from adult and pediatric CT. Am J Roentgenol. 188(2): 540-6.

64. Seidenbusch MC, Harder D, Regulla DF, Schneider K. 2014. Conversion factors for determining organ doses received by paediatric patients in high-resolution single slice computed tomography with narrow collimation. Zeitschrift fur medizinische Physik. 24(2): 123-137.

65. Westra SJ, Li X, Gulati K, Singh S, et al. 2013. Entrance skin dosimetry and size-specific dose estimate from pediatric chest CTA. J Cardiovasc Comput Tomogr. 8(2): 97-107.

66. Shrimpton PC. Assessment of patient dose in CT. NRPB-PE/1/2004. United Kingdom: National Radiological Protection Board (NRPB), 2004.

67. Gonzalez AB, Mahesh M, Kim KP, Bhargavan M, et al. 2009. Projected cancer risks from computed tomographic scans performed in the United States in 2007. Arch Intern Med. 169(22): 2071-7.

68. Dougeni E, Faulkner K, Panayiotakis G. 2012. A review of patient dose and optimisation methods in adult and paediatric CT scanning. Eur J Radiol. 81(4): e665-83.

69. Doody MM, Lonstein JE, Stovall M, Hacker DG, et al. 2000. Breast cancer mortality after diagnostic radiography findings from the U.S. scoliosis cohort study. Spine 25(16): 2052-63.

70. McFadden S, Hughes C, D'Helft CI, McGee A, et al. 2013. The establishment of local diagnostic reference levels for paediatric interventional cardiology. Radiography. 19(4): 295-301.

71. Shrimpton PC, Hillier MC, Lewis MA, Dunn M. 2006. National survey of doses from CT in the UK: 2003. Br J Radiol. 79(948): 968-80.

72. Mathieu KB, Turner AC, Khatonabadi M, McNitt-Gray MF,et al. 2013. Varying kVp as a means of reducing CT breast dose to pediatric patients. Phys Med Bio. 58(13): 4455-69.

73. Hansen J, Jurik AG. 2009.Analysis of current practice of CT examinations. Acta Oncologica. 48(2): 295-301.

74. Bushong SC. Radiographic Imaging and Radiologic Science for Technologists, 9 ed. St. Louis, MO: Mosby, Inc., 2008.

75. Wong ST, Yiu G, Poon YM, Yuen MK, et al. 2012. Reducing radiation exposure from computed tomography of the brain in children-Report of a practical approach. Child Nerv Syst. 28(5): 681-9.

76. Mayo J, Thakur Y. 2013. Pulmonary CT angiography as first-line imaging for PE: Image quality and radiation dose considerations. Am J Roentgenol. 200(3): 522-8.

77. Schindera ST, Nelson RC, Mukundan S, Paulson EK, et al. 2008. Hypervascular liver tumors: Low tube voltage, high tube current multi-detector row CT for enhanced detection-Phantom study. Radiology. 246(1):125-32.

78. Waaijer A, Prokop M, Velthuis BK, Bakker CJG, et al. 2007. Circle of Willis at CT angiography: Dose reduction and image quality-reducing tube voltage and increasing tube current settings. Radiology. 242(3): 832-9.

79. Kalender WA, Deak P, Kellermeier M, van Straten M, Vollmar SV. 2009. Application- and patient size-dependent optimization of x-ray spectra for CT. Med Phys. 36(3): 993-1007.

80. Frush DP. 2008. Pediatric abdominal CT angiography. Pediat Radio. 38(2): 259-66.

81. Staniszewska MA, Obrzut M, Rybka K. 2005.Phantom studies for possible dose reduction in CT head procedures. Radiat Prot Dosimetry. 114(1–3): 326–31.

82. Santos J, Batista MD, Foley S, Paulo G, McEntee MF, Rainford L. 2014. Paediatric CT optimisation utilising Catphan(R) 600 and age-specific anthropomorphic phantoms. Radiat Prot Dosimetry. 162(4): 586-96.

83. Huda W, Ogden KM, Khorasani MR. 2008. Converting dose-length product to effective dose at CT. Radiology. 248(3): 995-1003.

84. Nakaura T, Awai K, Oda S, Funama Y, et al. 2011. Low-kilovoltage, high-tube-current MDCT of liver in thin adults: Pilot study evaluating radiation dose, image quality, and display settings. Am J Roentgenol. 196(6): 1332-8.

85. Mahesh M. MDCT Physics: The Basic Technology, Image Quality and Radiation Dose. Philadelphia: Lippincott Williams & Wilkins, 2009.

86. National Institute of Standards and Technology. Tables of X-ray Mass Attenuation Coefficients and Mass Energy-absorption Coefficients. 2009. http://www.nist.gov/pml/data/xraycoef/ (Accessed on 13 Dec 2014)

87. Macari M, Spieler B, Kim D, Graser A, et al. 2010. Dual-source dual-energy MDCT of pancreatic adenocarcinoma: Initial observations with data generated at 80 kVp and at simulated weighted-average 120 kVp. Am J Roentgenol.194: 27-32.

88. Papadakis AE, Perisinakis K, Raissaki M, Damilakis J. 2013. Effect of x-ray tube parameters and iodine concentration on image quality and radiation dose in cerebral pediatric and adult CT angiography: A phantom study. Invest Radiol. 48(4): 192-9.

89. Schindera ST, Winklehner A, Alkadhi H, Goetti R, et al. 2013. Effect of automatic tube voltage selection on image quality and radiation dose in abdominal CT angiography of various body sizes: A phantom study. Clin Radiol. 68(2): 79-86.

90. Siegel MJ, Hildebolt C, Bradley D. 2013. Effects of automated kilovoltage selection technology on contrast-enhanced pediatric CT and CT angiography. Radiology 268(2): 538-47.

91. Kalra MK, Maher MM, Saini S. 2004. What is the optimum position of arms for acquiring scout images for whole-body CT with automatic tube current modulation? Am J Roentgenol. 181: 596-7.

92. Kalra MK, Toth TL. Patient Centering in MDCT: Dose Effects, 2nd ed. Berlin Heidelberg: Springer-Verlag, 2011.

93. Brady S, Kaufman R. 2012. Investigation of American Association of Physicists in Medicine Report 204 size-specific dose estimates for pediatric CT implementation. Radiology. 265: 832-40.

94. McCollough CH, Bruesewitz MR, Kofler JM. 2006. CT dose reduction and dose management tools: Overview of available options. Radiographics 26(6): 503-12.

95. Frush DP. MDCT in children: Scan techniques and contrast issues. In: Kalra MK, Sanjay S, Rubin GD (eds) Multidetector CT: From Protocols to Practice. Heidelberg: Springer Verlag, 2008.

96. McCollough CH, Primak AN, Braun N, Kofler J, Yu L, Christner J. 2009. Strategies for reducing radiation dose in CT. Radiologic Clin N Am. 47(1): 27-40.

97. Verdun FR, Gutierrez D, Vader JP, Aroua A, et al. 2008. CT radiation dose in children: a survey to establish age-based diagnostic reference levels in Switzerland. Eur Radiol.18(9): 1980-6.

98. Boone JM, Strauss KJ, Cody DD, McCollough CH, et al. Size Specific Dose Estimation (SSDE) in Paediatric and Adult Body CT Examination. American Association of Physicists in Medicine (AAPM) Report No. 204, 2011.

99. McCollough CH, Primak AN, Braun N, Kofler J, Yu L, Christner J. 2009. Strategies for reducing radiation dose in CT. Radiol Clin N Am. 47: 27-40.

100. Macdougall RD, Strauss KJ, Lee EY. 2013. Managing radiation dose from thoracic multidetector computed tomography in pediatric patients: Background, current issues, and recommendations. Radiol Clin of N Am. 51(4): 743-60.

101. McCollough C, Cody D, Edyvean S, Geise R, et al. The Measurement, Reporting, and Management of Radiation Dose in CT. Report of AAPM Task Group

23: CT Dosimetry.Diagnostic Imaging Council CT Committee. American Association of Physicists in Medicine, 2008.

102. MacDougall RD, Strauss KJ, Lee EY. 2013. Managing radiation dose from thoracic multidetector computed tomography in pediatric patients: Background, current issues, and recommendations. Radiol Clin of N Am. 51(4): 743-60.

103. Kusk RT. 2014. Incorrectly placed gonad shields: Effect on CT automatic exposure correction from four different scanners. Radiography. 20(3): 241-245.

104. Soderberg M, Gunnarsson M. 2010. Automatic exposure control in computed tomography-An evaluation of systems from different manufacturers. Acta radiologica. 51(6): 625-34.

105. Singh S, Kalra MK, Ali Khawaja RD, Padole A, et al. 2014. Radiation dose optimization and thoracic computed tomography. Radiol Clin N Am. 52(1): 1-15.

106. Angel E, Yaghmai N, Jude CM, DeMarco JJ, et al. 2009. Dose to radiosensitive organs during routine chest CT: Effects of tube current modulation. Am J Roentgenol. 193(5): 1340-5.

107. Duan X, Wang J, Christner JA, Leng S, et al. 2011. Dose reduction to anterior surfaces with organ-based tube-current modulation: Evaluation of performance in a phantom study. Am J Roentgenol.197(3): 689-95.

108. Sorantin E, Weissensteiner S, Hasenburger G, Riccabona M. 2013. CT in children-Dose protection and general considerations when planning a CT in a child. Eur J Radiol. 82(7): 1043-9.

109. Kalra MK, Woisetschla M, Dahlstro N, Singh S, et al. 2012.Radiation dose reduction with sinogram affirmed iterative reconstruction technique for abdominal computed tomography. J Comput Assist Tomogr. 36(3): 339-46.

110. Darge K, Jaramillo D, Siegel MJ. 2008.Whole-body MRI in children: Current status and future applications. Eur J Radiol. 68(2): 289-98.

111. Galanski M, Nagel H, Stamm G. Paediatric CT Exposure Practice in the Federal Republic of Germany: Results of a Nationwide Survey in 2005–2006. Hannover: Medizinische Hochschule; 2007.

112. Clarke R, Lewis EF. 2015. Feasibility of using iterative reconstruction to reduce radiation dose for computed tomography pulmonary angiograms. J Med Imaging Radiat Sci. 46(1): 50-56.

113. Beister M, Kolditz D, Kalender WA. 2012. Iterative reconstruction methods in X-ray CT. Physica Medica. 28(2): 94-108.

114. Froemming AT, Kawashima A, Takahashi N, Hartman RP, et al. 2013. Individualized kV selection and tube current reduction in excretory phase computed tomography urography: Potential for radiation dose reduction and the contribution of iterative reconstruction to image quality. J Comput Assist Tomogr. 37(4): 551-9.

115. Hwang HJ, Seo JB, Lee HJ, Lee SM, Kim EY, Oh SY, et al. 2013. Low-dose chest computed tomography with sinogram-affirmed iterative reconstruction, iterative reconstruction in image space, and filtered back projection: studies on image quality. J Comput Assist Tomogr. 37(4): 610-7.

116. Smith EA, Dillman JR, Goodsitt MM, Christodoulou EG, Keshavarzi N, Strouse PJ. 2014. Model-based iterative reconstruction: effect on patient radiation dose and image quality in pediatric body CT. Radiology. 270(2): 526-34.

117. Mieville FA, Berteloot L, Grandjean A, Ayestaran P, et al. 2013. Model-based iterative reconstruction in pediatric chest CT: Assessment of image quality in a prospective study of children with cystic fibrosis. Pediatr Radiol. 43(5): 558-67.

118. Juri H, Matsuki M, Inada Y, Tsuboyama T, et al. 2013. Low-dose computed tomographic urography using adaptive iterative dose reduction 3-dimensional: Comparison with routine-dose computed tomography with filtered back projection. J Comput Assist Tomogr. 37(3): 426-31.

119. Vorona GA, Ceschin RC, Clayton BL, Sutcavage T, et al. 2011. Reducing abdominal CT radiation dose with the adaptive statistical iterative reconstruction technique in children: A feasibility study. Pediat Radiol. 41(9): 1174-82.

120. Lee Y, Jin KN, Lee NK. 2012. Low-dose computed tomography of the chest using iterative reconstruction versus filtered back projection: comparison of image quality. J Comput Assist Tomogr. 36(5): 512-7.

121. Hwang HJ, Seo JB, Lee HJ, Lee SM, et al. 2013. Low-dose chest computed tomography with sinogram-affirmed iterative reconstruction, iterative reconstruction in image space, and filtered back projection: studies on image quality. J Comput Assist Tomogr. 37(4): 610-7.

122. Lee SH, Kim MJ, Yoon CS, Lee MJ. 2012.Radiation dose reduction with the adaptive statistical iterative reconstruction (ASIR) technique for chest CT in children: An intra-individual comparison. Eur J Radiol. 81(9): e938-43.

123. Prakash P, Kalra MK, Digumarthy SR, Hsieh J, Pien H, Singh S, et al. 2010. Radiation dose reduction with chest computed tomography using adaptive statistical iterative reconstruction technique: Initial experience. J Comput Assist Tomogr. 34(1): 558–67.

124. Liu L. 2014. Model-based iterative reconstruction: A promising algorithm for today's computed tomography imaging. J Med Imaging Radiat Sci. 45(2): 131-136.

125. Suzuki S, Nishiyama Y, Kuwahara S, Hikosaka S, Monma K, Odagiri H. 2013. Adaptive statistical iterative reconstruction algorithm for measurement of vascular diameter on computed tomographic angiography in vitro. J Comput Assist Tomogr. 37(2): 311-6.

126. Theocharopoulos N, Damilakis J, Perisinakis K, Tzedakis A et al. 2006. Estimation of effective doses to adult and pediatric patients from multislice computed tomography: A method based on energy imparted. Med Phys. 33(10): 3846-56.

127. McCollough CH, Leng S, Yu L, Cody DD, et al. 2011. CT dose index and patient dose: They are not the same thing. Radiology. 259(2): 311–6.

128. Tootell A, Szczepura K, Hogg P. 2014. An overview of measuring and modelling dose and risk from ionising radiation for medical exposures. Radiography. 20(2): 323-332.

129. Brady Z, Ramanauskasr F, Cain M, Franzcrf. 2012. Assessment of paediatric CT dose indicators for the purpose of optimisation. Br J Radiol. 85: 1488-98.

130. Jarvinen H, Merimaa K, Seuri R, Tyrvainen E, Perhomaa M, Savikurki-Heikkila P, et al. 2011. Patient doses in paediatric CT: Feasibility of setting diagnostic reference levels. Radiat Prot Dosimetry. 147(1-2): 142-6.

131. Yakoumakis E, Karlatira M, Gialousis G, Dimitriadis A, et al. 2009. Effective dose variation in pediatric computed tomography: dose reference levels in Greece. Health Phys. 97(6): 595-603.

132. Galanski M, Nagel H, Stamm G. Paediatric CT Exposure Practice in the Federal Republic of Germany: Results of a Nationwide Survey in 2005–2006. Hannover: Medizinische Hochschule; 2007.

133. Li J, Udayasankar UK, Toth TL, Seamans J et al. 2007. Automatic patient centering for MDCT: Effect on radiation dose. Am J Roentgenol. 188(2): 547-52.

134. Gaspoz F, Monnin P, Petter D, Ple J, et al. 2015. Precision and accuracy of measurements on CT scout view. J Med Imaging Radiat Sci. 46(3): 309-316.

135. Lai NK, Chen TR, Tyan YS, Tsai HY. 2013. Off-centre effect on dose reduction to anterior surfaces with organ-based tube-current modulation. Radiation Measurements. 59:155-9.

136. Strauss KJ, Goske MJ, Kaste SC, Bulas D, Frush DP, et al. 2010. Image gently: Ten steps you can take to optimize image quality and lower CT dose for pediatric patients. Am J Roentgenol. 194(4): 868-73.

137. O'Daniel JC, Stevens DM, Cody DD. 2005. Reducing radiation exposure from survey CT scans. Am J Roentgenol. 185: 509-15.

138. Schilham A, van der Molen AJ, Prokop M, de Jong HW. 2010. Overranging at multisection CT: An underestimated source of excess radiation exposure. Radiographics. 30(4): 1057-67.

139. Ranallo FN, Szczykutowicz T. 2015. The correct selection of pitch for optimal CT scanning: Avoiding common misconceptions. J Am Coll Radiol. 12(4): 423-4.

140. Dougeni E, Faulkner K, Panayiotakis G. 2012. A review of patient dose and optimisation methods in adult and paediatric CT scanning. Eur J Radiol. 81(4): 665-83.

141. Tsalafoutas IA. 2011. The impact of overscan on patient dose with first generation multislice CT scanners. Physica medica. 27(2): 69-74.

142. van der Molen AJ, Geleijns J. 2007. Overranging in multisection CT: quantification and relative contribution to dose-Comparison of four 16-section CT scanners. Radiology. 242(1): 208-16.

143. Liu F, Wang G, Cong W, Hsieh SS, Pelc NJ. 2013. Dynamic bowtie for fan-beam CT. J Xray Sci Technol. 21(4): 579-90.

144. Lobo L, Antunes D. 2013.Chest CT in infants and children. Eur J Radiol. 82 (7): 1108-17.

Chapter 3

Paediatric routine CT scanning protocols: a retrospective study of four main hospitals in Oman

3.1 Introduction

Relevant literature was reviewed extensively in Chapter 2, in order to identify factors that affect both radiation dose and image quality of routine paediatric CT examinations. The present chapter, assesses the protocols of paediatric routine CT scanning, based on analysis of data from four main tertiary hospitals, in the Sultanate of Oman. The information on protocols and dose readings, gathered across the four hospitals, was evaluated on a comparative basis. The outcomes of this retrospective study, and findings from the literature review, were then used to devise optimum routine paediatric CT scanning protocols.

3.2. Materials and methods

3.2.1 Retrieval of data from medical records

The selected four main tertiary hospitals in Oman, were approached for obtaining medical records of routine paediatric CT scans, performed during the two-year period between 2012 and 2014. The selected patients belonged to the age group 0-16 years, and included those who were referred for routine CT scans, as a part of routine head, chest and abdomen scans. Patients referred for CT angiography or trauma examination, were excluded from the retrospective study. All the obtained images were considered as diagnostic, because they were retrieved from Picture Archiving and Communication System (PACS) with, post-scan diagnostic reports. Ethical approval was provided by the Curtin Human Ethics Research Committee, and also individual ethics committees from each hospital.

A total of 1,574 paediatric CT scans, collected from these four clinical centres, were assessed for the following: acquisition parameters, patient age group, body size in

terms of effective diameter and volume CT dose index (CTDI $_{vol}$). In particular, age wise characterisation of the patients, was done as follows: <2 years, 2-5 years, 6-10 years and 11-16 years.

3.2.2 Type of MDCT scanners

Four CT scanners were involved in this study including SOMATOM Definition Flash, Siemens Healthcare, Germany (128-MDCT scanner), SOMATOM Definition AS, Siemens Healthcare, Germany (64-MDCT scanner) and two iDose4 Care Brilliance, Phillips Healthcare, Netherlands (64-MDCT scanners). All four scanners underwent regular quality assurance by the vendors and medical physicists of each hospital.

3.2.3 CT dose quantity

The extracted $CTDI_{vol}$ values for head examinations, were based on the 16 cm phantom, whereas chest and abdomen examinations, were based on the 32 cm phantom, as reported by manufacturers. Literatures on diagnostic reference levels (DRLs) [1-4] show that for patients less than 10 years of age, a multiplication factor of 2 was applied to the displayed chest and abdomen $CTDI_{vol}$ values that were based on the 32 cm phantom, in order to convert the same, into a form suitable for comparison with published $CTDI_{vol}$ values that based on the 16cm phantom. This point is extremely important, because a smaller body size (of child patients) absorbs a greater dose than a larger body, using the same acquisition parameters [4-6].

Dose values between different centres were compared using median values and dose range [3, 7]. Additionally, the 3rd quartiles of the collected $CTDI_{vol}$ values were compared with the national DRLs from different countries, in line with the accepted practice of DRL studies [1, 2, 4, 8-11].

3.2.4 Normalisation of acquisition parameters and dose readings to body size

Literature and influential organisations, stipulate effective diameter as an accurate surrogate tool for body size CT optimisation, to tailor the paediatric CT acquisition parameters, across the age range spectrum of children. Recent studies have employed a size-specific dose estimation (SSDE), developed by the American Association of Physicists in Medicine (AAPM), for normalisation of dose values to body size [12-14].

In the present study, the effective diameter was taken from records of chest and abdomen images, in corroboration with patient size, as recommended by the International Commission on Radiation Units (ICRU) data [15].This method, however, demonstrated wide disparity in patient size with respect to age [12, 16, 17]. Body size was computed from the effective diameter as the function of the square root of the product of the anterior-posterior (AP) and lateral dimensions of the axial CT image. This method was recommended by existing literature on radiation dose studies [12, 13, 18, 19]. With a view to increase the sample size, the effective diameter was measured at the level of second lumbar vertebra, for both chest and abdomen scans. The value thus obtained, was used to assess the extracted acquisition parameters in conjunction with $CTDI_{vol}$.

3.2.5 Data analysis

Analysis of data was done with the help of descriptive statistics. Median, first and third quartiles, interquartile range and percentage of frequency, were calculated using IBM Statistical Package for Social Sciences (SPSS) Version 22, in line with the accepted norms of dose surveys [3, 7]. Categorical variables were presented as frequencies or percentages. Variation between median acquisition parameters and dose readings among different age groups across the four centres, was demonstrated by application of the Kruskal-Wallis test [16, 20]. Significant difference was indicated by p values <0.05.

3.3 Results

Table 3.1 shows the characteristics of participating centres along with the corresponding CT scanners used in the study. As evident from the table, the only CT scanner equipped with an iterative reconstruction technique, belonged to centre D.

Table 3.2 lists patients' characteristics. A total of 1574 paediatric scans comprising head, chest and abdomen examinations, were obtained from the selected four centres in the Sultanate of Oman. Of them, head CT scans (608/1574), abdominal CT scans (560/1574) and chest CT scans (459/1574), represented 38%, 36% and 26% respectively. Fifty-seven percent (897/1574) constituted scans from males, while 43% (677/1574) were from females.

Tables 3.3 - 3.6 display the percentage, median and range of scanning parameters and $CTDI_{vol}$ values for routine head, chest and abdomen examinations. Figures 3.1-3.10 illustrate the median, 1st and 3rd quartile, and interquartile range of the tube current, $CTDI_{vol}$ and effective diameter of chest and abdomen examinations. The 3rd quartile values for the $CTDI_{vol}$ of the collected samples, were compared with the DRLs of different countries in Table 3.7.

Table 3.1 Characteristics of CT scanner used

Centre	Manufacturer	Mode	Algorithm reconstruction
A	Philips HealthCare	64 MDCT	FBP
B	Philips HealthCare	64 MDCT	FBP
C	Siemens HealthCare	64 MDCT 4Ddose SOMATOM	FBP
D	Siemens HealthCare	Dual Source 128 MDCT Flush SOMATOM	FBP/IR

Key - MDCT: multi-detector CT; FBP: filtered back projection; IR: iterative reconstruction

Table 3.2 Patients' characteristics for head, chest and abdomen examinations

Characteristics	No. Of patients	Overall percentage (%)	Gender percentage (%)	
Age in years			**M**	**F**
Head examination				
<2	135	9	5	4
2-5	143	9	5	4
6-10	130	8	5	3
11-16	200	13	8	3
Subtotal	608	40	23	17
Chest examination				
<2	104	8	5	3
2-5	107	5	3	2
6-10	99	6	3	3
11-16	152	7	4	3
Subtotal	459	26	15	11
Abdomen examination				
<2	81	4	2	2
2-5	83	6	3	3
6-10	120	8	5	3
11-16	276	18	9	9
Subtotal	560	36	19	17
Centres				
A	391	25	14	9
B	326	21	12	10
C	455	29	15	10
D	458	29	16	14
TOTAL	1574	100	57	43

Key - M: male, F:Female

Table 3.3 Summary of percentage, median and range values of acquisition parameters and dose reading for head, chest and abdomen CT examinations

Age	Parameters	Head	Chest	Abdomen
<2y	Effective diameter (cm)		12 (8-19)	12 (8-19)
	kV 120kV/100kV/80kV*	120 (80-120) 76% , 20%, 4%	120 (80-120) 54% , 13%, 33%	100 (80-120) 25%, 56%, 19%
	EffectivemAs	144 (125-200)	97 (34-250)	106 (21-250)
	Slice Thick (mm)	2 (1-3)	2 (1-3)	2 (1-5)
	Pitch	0.7 (0.6-1)	0.9 (0.64-3)	0.8 (0.6-1.4)
	Time (Sec)	0.7 (0.5-1)	0.5 (0.3-0.5)	0.3 (0.3-0.64)
	TCM**	57%	47%	67%
	Axial scan mode***	23%	0%	0%
	$CTDI_{vol}$ (mGy)	25 (12-51)	4 (1-16)	4 (1-16)
……				...
2-5y	Effective diameter (cm)		15 (10-18)	
	kV 120kV/100kV/80kV*	120(80-120) 81%, 14%, 5%	100 (80-120) 43%, 53%, 4%	100 (80-120) 41%, 56%, 3%
	EffectivemAs	200 (142-250)	103 (45-196)	120 (45-196)
	Slice Thick (mm)	2 (1-5)	2 (1-3)	2 (1-5)
	Pitch	0.68 (0.6-0.8)	3 (0.6-3)	0.9 (0.6-1.4)
	Time (Sec)	0.5 (0.50.1)	0.3 (0.3-0.50)	0.3 (0.3-0.1)
	TCM**	31%	60%	62%
	Axial scan mode***	31%	0%	0%
	$CTDI_{vol}$ (mGy)	38 (13-61)	4 (1-15)	4 (2 -13)
……				...
6-10y	Effective diameter (cm)		15 (12-22)	15 (12-22)
	kV 120kV/100kV/80kV*	120 (100-120) 79% , 20%, 1%	120 (100-120) 52%, 48%	120 (80-120) 55% , 42%, 3%
	EffectivemAs	222 (163-350)	116 (27-300)	124 (27-211)
	Slice Thick (mm)	2.5 (1-3)	2 (1-3)	2 (1-5)
	Pitch	0.7 (0.6-0.8)	3 (0.6-3)	0.9 (0.6-1.4)
	Time (Sec)	0.9 (0.5-1.3)	0.3 (0.3-0.7)	0.3 (0.3-0.6)
	TCM**	47%	61%	60%
	Axial scan mode***	31%	2%	0%
	$CTDI_{vol}$ (mGy)	50 (13-61)	4 (3-16)	5 (2-21)
……				...
11-16y	Effective diameter (cm)		21 (15-29)	21 (15-29)
	kV 120kV/100kV/80kV*	120 (100-120) 94%, 6%	120 (100-120) 79% , 21%	120 (100-120) 91% - 9%
	Effective mAs	255 (233-400)	126 (45-304)	140 (39-470)
	Slice Thick (mm)	2 (1-3)	2 (1-3)	3 (1-5)
	Pitch	0.7 (0.6-0.8)	0.89 (0.6-3)	1.1 (0.6-1.4)
	Time (Sec)	1 (0.5-1.3)	0.5(0.3-1)	0.3 (0.3-1)
	TCM**	28%	45%	26%
	Axial scan mode***	14%	2%	0%
	$CTDI_{vol}$ (mGy)	51 (15- 59)	7 (3-20)	8 (3-20)

Key -- kV: tube voltage; eff-mAs: effective tube current time product; TCM: tube current modulation; $CTDI_{vol}$: volume CT dose index; DLP: dose length product; NA: not available; 32 cm& 16 cm: reference CTDI phantom size

*percentages of cases employed with tube voltages 80kV -120 kV

**percentages of cases employed TCM

***percentages of cases employed axial scan mode

Note: $CTDI_{vol}$ values for head examinations are based on the 16 cm reference phantom while the $CTDI_{vol}$ for chest and abdomen examinations are based on the 32 cm phantom.

3.3.1 Head CT scans

Table 3.3 and Figure 3.1 shade light on the wide variation observed in acquisition parameters, corresponding to $CTDI_{vol}$ in all anatomical areas, across the complete spectrum of age range. Overall, the median tube voltage of 120 kV (76% – 94%) dominated the head CT scan protocols, across all age groups in three centres (A – C), whereas the median tube voltage of 100 kV (6% - 21%), was used only by centre D, which employed a range between 80 – 120 kV (Table 3.4).

The median $CTDI_{vol}$ for the age group <2 years, was significantly lower than that of the 2 – 5 years age group (p<=0.00), whereas there was no significant difference between the age groups of 2 - 5 years and 6 – 10 years (p<=0.097). Figure 3.1 shows wide inter-quartile range of mAs and $CTDI_{vol}$ for all age groups; extensive variation can be seen particularly in the age groups of 6 – 10 years and 11 – 16 years.

Table 3.4 and Figure 3.2 (a) depict variations in the median mAs for all age groups across all the centres. The median mAs used in the centres C and D were found to be significantly lower (p=<0.002 - 0.00) than that of centres A and B for all age groups. Furthermore, a wide variation in interquartile range was observed, and the age groups of 5 – 6 years, and 11 – 16 years in both centres A and B, showed significant high median mAs.

Marked variation was also noted among the $CTDI_{vol}$ values for all age groups, irrespective of the centre Table 3.4 and Fig 3.2 (b). Centre B exhibited wide interquartile range for both the following age groups <2 years and 2-5 years. The median dose value was higher for the age groups 6-10 years and 11-16 years, indicating the application of adult protocols in paediatric CT scan procedures. The median $CTDI_{vol}$ was significantly different among the four centres, and centres C and D demonstrated significantly lower median dose values (p< =0.00), with 36% and 44% dose reduction, respectively. Overall, data analysis from centre D showed a significant fall in median $CTDI_{vol}$ and represented a narrow quartile range for all age groups.

With respect to the remaining acquisition parameters, Table 3.4 demonstrates 72-96% application of the axial scan mode in most protocols used in centre C, whereas 90-100% helical mode was used by the other centres. Both centres C and D applied 72% - 100% TCM for all age groups. With regard to the pitch factor, all centres used

a narrow pitch median value ranging between 0.64 and 0.8. Similarly, scan time also ranged between 0.5 and 1 second. Detector collimation or slice thickness varied between 2-3 mm. Besides the dataset used for routine head CT, a 2 mm median value slice thickness was observed in all age groups and centres.

Table 3.4 Percentages, median, range of acquisition parameters, and radiation doses (head CT examinations)

Age	Parameters	Centre A	Centre B	Centre C	Centre D
	kV	120	120	120	100 (80-100)
	eff-mAs	200 (140-200)	250 (200-400)	112 (100-120)	142 (136-168)
	Thickness (mm)	2.5 (2-2.5)	2.5	2.5 (1.2-3)	3
	Pitch	0.64	0.64	Axial	0.8
	Time Sec	0.86 (0.78-1)	0.71 (0.5-1)	1	1
<2y	TCM*	0%	0%	90%	95%.
	Axial can mode**	3%	0%	70%	0%
	$CTDI_{vol}$ 32cm(mGy)	25 (17-25)	25 (25 -51)	16 (14-17)	14 (13-15)
	kV	120	120	120	100 (80-120)
	eff-mAs	300 (250-400)	250 (250-400)	141 (129-190)	151 (140-194)
	Thickness (mm)	2.3 (2-3)	2.5	2.4 (1-5)	3
	Pitch	0.64	0.64	Axial	0.8
	Time Sec	0.96 (0.5-1)	0.75 (0.5-1)	1	1
	TCM*	0%	0%	72%	100%
2-5y	Axial scan bode**	5%	2%	92%	2%
	$CTDI_{vol}$ 32cm (mGy)	45 (32-51)	35 (32-51)	20 (19-28)	14 (13-17)
	kV	120	120	120	100 (100-120)
	eff-mAs	280 (250-400)	400 (250-400)	190 (153-210)	166 (145-192)
	Thickness (mm)	2 (2-3)	2.5	2 (1 -3)	3
	Pitch	0.64	0.64	Axial	0.8
	Time Sec	0.97 (0.5-1.3)	0.94 (0.5-1)	1	1
6-10y	TCM*	0%	0%	72%	96%
	Axial scan mode**	6%	0%	95%	0%
	$CTDI_{vol}$ 32cm (mGy)	44 (32-51)	51 (50-51)	27 (22-29)	14 (13-17)
	kV	120	120	120	100 (100-120)
	eff-mAs	400 (0)	400 (0)	244 (190-259)	228 (221-246)
	Thickness (mm)	2	2.5	2.4 (1.2-3)	3
	Pitch	0.64	0.64	Axial	0.8
	Time Sec	1.2 (1-1)	1 (0.5-1)	1	1
11-16y	TCM*	0%	0%	89%	90%
	Axial scan mode**	5%	0%	96%	2%
	$CTDI_{vol}$ 32cm (mGy)	51 (50-51)	51 (51-51)	36 (29-38)	21 (20-22)

Key -- kV: tube voltage; effective tube current time product; (s): second; TCM: tube current modulation; $CTDI_{vol}$: volume CT dose index; DLP: dose length product; NA: not available

*percentages of cases employed TCM

**percentages of cases employed axial scan mode

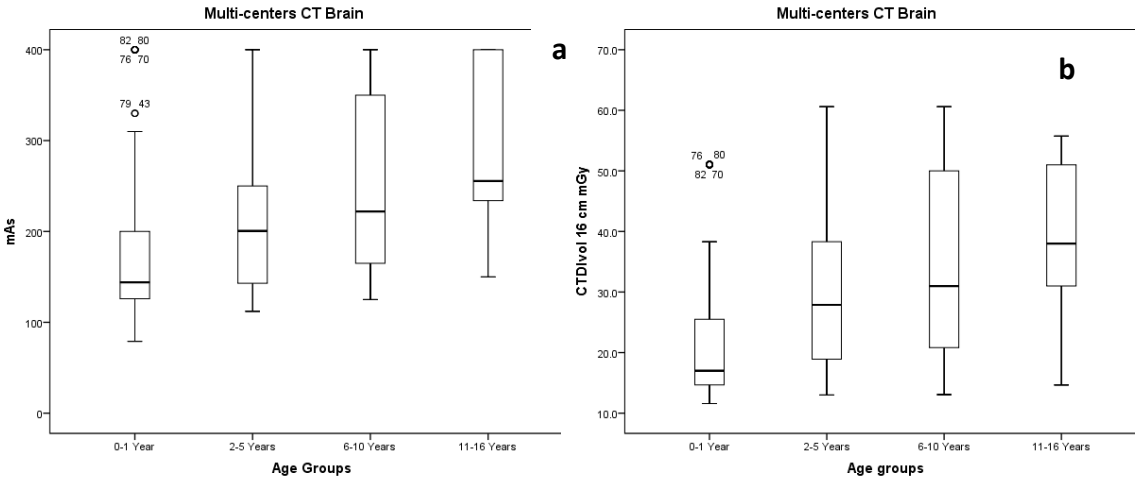

Figure 3.1 Overall distribution of (a) mAs, and (b) corresponding $CTDI_{vol}$ for head CT age group (box plots define 1st–3rd quartiles ; line in box indicates median; Star: mean; outer boundaries non-outlier range, which includes observed values that fall within the inter-quartile range "IQR" ± 1.5×IQR; circles outliers)

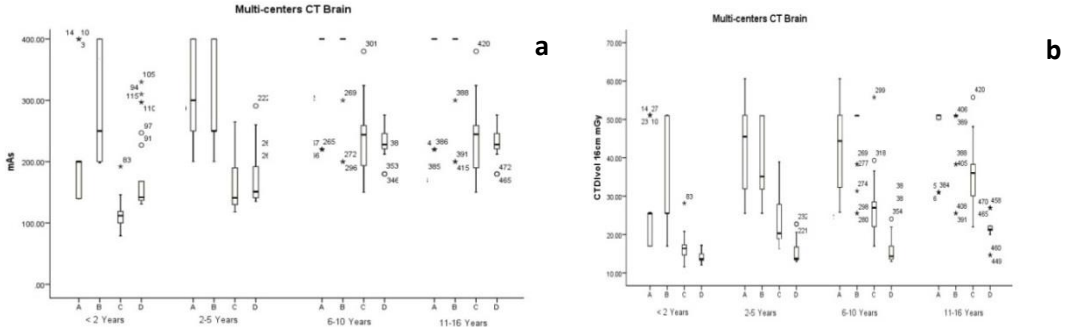

Figure 3.2 Multi-centre box plots distribution of (a) mAs, and (b) corresponding $CTDI_{vol}$ for head CT by group

3.3.2 Chest CT scans

Chest CT scans formed the smallest proportion of the total number of scans (26% or 459/1574). The percentage and magnitude of tube voltage used was as follows: 43%-79% for 120 kV; 11%-52% for 100 kV, and 4%-33% for 80 kV (Table 3.3). Table 3.5 shows that a standard 120 kV value was applied across all age groups in three centres, whereas the fourth centre – Centre D – applied a median tube voltage of 100 kV.

Figure 3.3 (a) shows no significant difference in the median mAs among the age groups below 11 years, in both centres A and B (p = 0.449-0.530), whereas the inter-quartile mAs varied for all age groups. On the other hand, the $CTDI_{vol}$ interquartile did not show significant discrepancy for age groups below 11 years, whereas extensive variation was noticed for the 11-16 years age group Fig. 3.3(b).

Figure 3.4 (a) shows very high values of mAs and $CTDI_{vol}$ in the effective diameter groups, <14cm and 15-18cm. Figure 3.4 (b) indicates a wide interquartile variation of $CTDI_{vol}$ in the 19-23 cm and 24-28 cm groups.

Figure 3.5 illustrates variation in median mAs and $CTDI_{vol}$ across all age groups. Centre D showed a significantly lower dose for age groups below 10 years, with respect to the overall median $CTDI_{vol}$ (p<=0.000). In contrast, centre A demonstrated a significantly higher dose with overall median (p<=0.000), for the age groups below 10 years. Moreover, the interquartile varied extensively in the age group of 6-10 years. Interestingly, centre D showed substantial interquartile variation in both mAs and $CTDI_{vol}$ for the 11-16 years age group, with mAs varying from100 to 300 and 6-13 mGy Fig 3.5. Nevertheless, centre D exhibited significantly lower median $CTDI_{vol}$ for age groups below 11 years.

Most of the centres used the helical scanning mode for the remaining chest acquisition parameters .The pitch factor ranged between 0.64 and 3.0 (Table 3.3), and scan time between 0.3 to 1 second. Centre D used a high pitch of 3, and short exposure time of 0.28 seconds for all chest examinations. Scan collimation or slice thickness varied between 1-5 mm.

Table 3.5 Median and range values of acquisition parameters, body size and radiation doses of CT chest examinations and percentage for TCM

Age	Parameters	Centre (A)	Centre (B)	Centre (C)	Centre (D)
	Effective diameter (cm)	12 (8-16)	NA	12 (8-15)	12 (8-16)
	kV	120 (80-120)		120 (100-120)	100 (80-120)
	EffectivemAs	80 (45-250)		45 (45-100)	109 (34-234)
	Slice Thick (mm)	2		2.9 (1-5)	2 (1-2)
<2y	Pitch	0.86		1.4	3
	Time (Sec)	0.75		0.5	0.28
	TCM*	0%	0%	23%	70%
	$CTDI_{vol}$ 32cm (mGy)	5 (3-16)		4 (2-7)	4 (2-6)
	$CTDI_{vol}$16cm (mGy)	13 (7-32)		8 (4-14)	7 (3 -12)
……					
	Effective diameter (cm)	14 (12-17)		15 (13-17)	15 (10-18)
	kV	120 (80-120)	120	120 (80-120)	100 (80-120)
	effectivemAs	80 (50-103)	64 (44-200)	45 (45-200)	120 (92-200)
	Slice Thick (mm)	2.2 (2-3)	3	3.6 (1-5)	2 (1-2)
2-5y	Pitch	0.86	1.17	1.4	3
	Time (Sec)	0.6	0.5	0.5	0.28
	TCM*	0%	0%	34%	92%
	$CTDI_{vol}$32cm (mGy)	5 (1-7)	4 (2.9-13)	4 (3-15)	4 (3-6)
	$CTDI_{vol}$16cm (mGy)	10 (2-13)	8 (6-26)	8 (7-30)	8 (6-12)
……					
	Effective diameter (cm)	17 (15-21)		13 (12-22)	17 (13-22)
	kV	120 (100-120)	120	120 (100-120)	100 (80-120)
	EffectivemAs	45 (30-250)	79 (49-82)	45 (45-300)	127 (98-168)
6-10y	Slice Thick (mm)	2.4 (1.5-3)	3	2.5 (1-5)	2 (1-2)
	Pitch	0.86	1.17	1.4	3
	Time (Sec)	0.6	0.5	0.5	0.28
	TCM*	0%	0%	12%	96%
	$CTDI_{vol}$ 32cm (mGy)	9 (3-16)	5 (3 -9)	5 (3.4-14.5)	4 (3.2-8)
	$CTDI_{vol}$ 16cm (mGy)	17 (7-32)	10 (6 -17)	10 (7-29)	9 (6-16)
……					
	Effective diameter (cm)	21 (15-26)		21 (17-29)	19 (17-26)
	kV	120 (100-120)	120	120	100 (100-120)
	Effective mAs	118 (45-250)	150 (53-324)	125 (45-300)	147 (102-304)
11-16y	Slice Thick (mm)	2.8 (2-3)	3	2.5 (1.5-5)	2 (1-2)
	Pitch	0.86 (0.86-0.89)	1.17	1.4	3
	Time (Sec)	0.6 (0.6-1.1)	0.5	0.5	0.28
	TCM*	0%	0%	71%	91%
	$CTDI_{vol}$ 32cm (mGy)	8 (3-16)	10 (3-21)	10 (3-21)	6 (4-20)

Key -- kV: tube voltage; eff-mAs: effective tube current time product; TCM: tube current modulation; $CTDI_{vol}$: volume CT dose index; DLP: dose length product; NA: not available; 32 cm & 16 cm: reference CTDI phantom size
*percentages of cases employed TCM

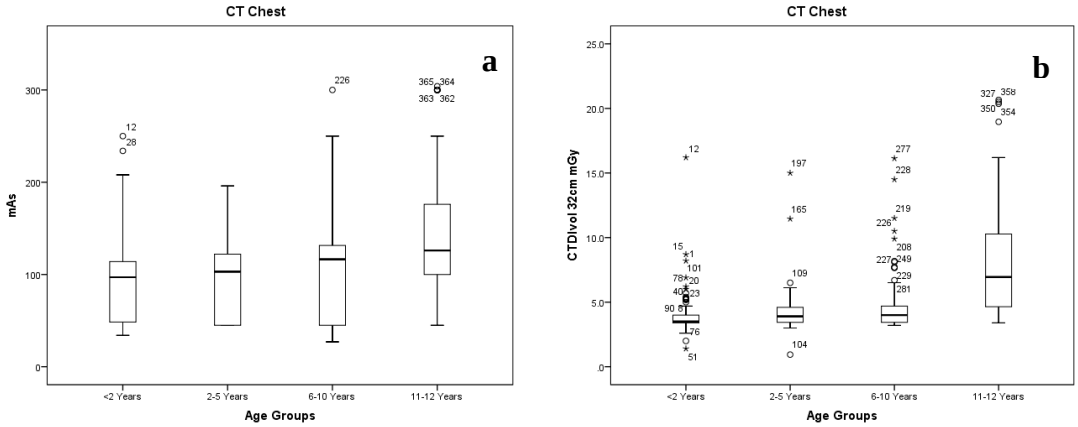

Figure 3.3 Box and whisker plots showing variation in the overall chest mAs and $CTDI_{vol}$ corresponding to the age groups

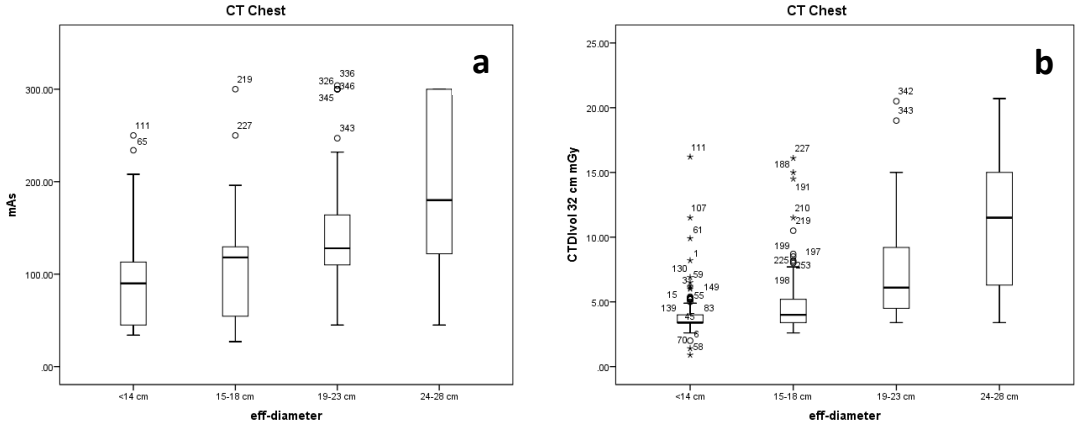

Figure 3.4 Box and whisker plots showing variation in the overall chest mAs and CTD_{Ivol} corresponding to body size

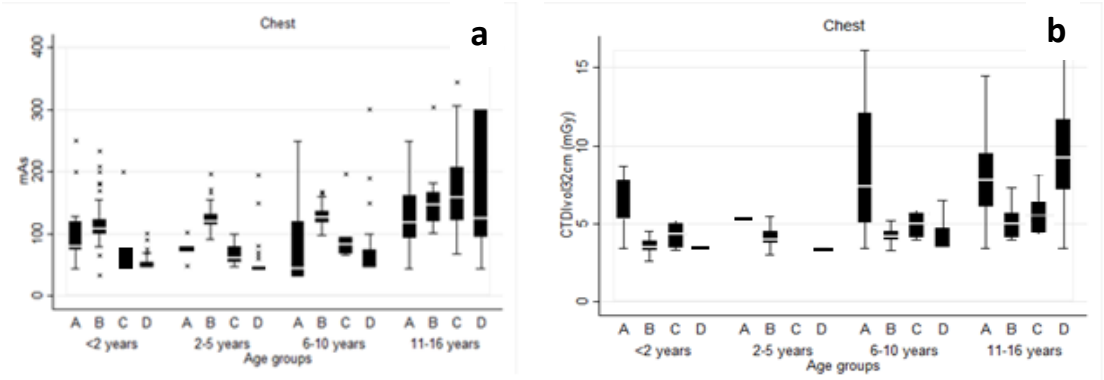

Figure 3.5 Box and whisker plots showing variation in the multi-centres chest mAs and $CTDI_{vol}$ corresponding to body size

3.3.3 Abdomen CT scans

Data analysis for abdomen CT scans revealed a pattern similar to that of the data from chest CT scans. Median values of 120 kV and 100 kV were applied across all age groups in centres A and B, and centres C and D respectively Table 3.6. There was no difference in the median mAs and $CTDI_{vol}$ for the age groups 2-5 years and 6-10 years (p= 0.052-0.219). Similarly, notable variation was evident in the interquartile range, but there was no significant difference in median mAs and kV (p=0.17) for patients above 10 years Fig 3.6.

With respect to the effective diameter, the median mAs and $CTDI_{vol}$ differed significantly (p = 0.035-0.000) across size groups Fig 3.7. Maximum variation of interquartile range was observed in the groups of 19-23 cm, 24-29 cm, and >30 cm.

In almost all the centres, a majority of the remaining abdomen acquisition parameters used the helical scan mode. Pitch factor ranged between 0.64 and 1.4 (Table 3.3), and scan time between 0.3 to 1 second. Centre D used a time period of 0.28 seconds for all examinations. Scan detector collimation or slice thickness ranged between 1-5 mm.

3.3.4 Dose readings corresponding to effective diameter

Figures 3.9 and 3.10 reveal a wide interquartile range for chest and abdomen $CTDI_{vol}$ within the same effective diameter, particularly for the group above 17 cm. For example, interquartile $CTDI_{vol}$ values showed high variation within 23 cm effective diameter, between 5 and 14 mGy Figs. 3.9, 3.10. Extreme outlier values of similar diameters were also observed. Figure 3.11 compares the current dataset of effective diameter, with the ICRU age function effective diameter. The dataset of patients below 10 years had effective diameters substantially lower than those obtained from the ICRU, whereas patients between 10-16 years demonstrated a wide range both above and below the ICRU curve.

Table 3.6 Median values and range of acquisition parameters, body size and radiation dose of CT abdomen examinations

Age	Parameters	Centre A	Centre B	Centre C	Centre D
	Effec diameter (cm)	13 (11-14)	NA	13 (9-17)	12 (8-16)
	kV	120 (80-120)	120	100 (100-120)	100 (80-120)
<2y	Effective mAs	80 (40-250)	53 (47-200)	109 (28-155)	109 (34-200)
	Slice Thick (mm)	2	3	2.9 (1-5)	2 (1-2)
	Pitch	0.86	NA	1.4	3
	Time (Sec)	0.75	0.5	0.5	0.28
	TCM*	0%	0%	100%	83%
	$CTDI_{vol}$32cm (mGy)	7 (2-17)	5 (3-13)	4 (2-6)	4 (2-7)
	$CTDI_{vol}$ 16cm (mGy)	13 (4-33)	11 (6-20)	9 (4-12)	7 (3-13)
	Effect diameter (cm)	14 (13-17)	NA	15.5 (11-19)	15 (11-18)
	kV	120 (80-120)	120	100 (100-120)	100 (80-120)
2-5y	Effective mAs	80 (60-150)	53 (44-56)	124 (45-190)	120 (54-196)
	Slice Thick (mm)	2.2 (2-3)	3	3.6 (4)	2 (1-2)
	Pitch	0.86	1.17	1.4	3
	Time (Sec)	0.58 (0.56-0.64)	0.5	0.5	0.28
	TCM*	0%	0%	78%	100%
	$CTDI_{vol}$ 32cm (mGy)	6 (4-10)	3 (3-13)	5 (3 -13)	4.3 (2-8)
	$CTDI_{vol}$ 16cm (mGy)	12 (8-20)	7 (5.7-7.2)	11 (7 -26)	8.5 (4-16)
	Effect diameter (cm)	17 (14-23)	NA	17 (14-29)	17 (13-22)
	kV	120 (80-120)	120	120 (100-120)	100 (80-120)
6-10y	Effective mAs	90 (40-167)	67 (49-131)	142 (34-211)	125 (70-180)
	Slice Thick (mm)	2.4 (1.5-3)	3	2.5 (1-5)	2 (1-2)
	Pitch	0.86	1.17	1.4	3
	Time (Sec)	0.59 (0.56-0.64)	0.5	0.5	0.28
	TCM*	0%	0%	82%	85%
	$CTDI_{vol}$ 32cm (mGy)	6 (2-10.5)	5 (3-9)	7 (2 -14)	5 (2-8)
	$CTDI_{vol}$ 16cm (mGy)	12 (4-21)	10 (6-17)	13 (5-29)	9 (4-16)
	Effect diameter (cm)	21 (13-33)		20 (14-33)	19 (15-32)
	kV	120 (80-120)	120	120 (100-120)	100 (100-120)
11-16y	Effective mAs	150 (41-470)	150 (53-324)	118 (39-420)	130 (102-350)
	Slice Thick (mm)	2.8 (2-3)	3	2.5 (1.5-5)	2 (1-2)
	Pitch	0.86 (0.86-0.89)	1.17	1.4	3
	Time (Sec)	0.7 (0.6-1.1)	0.5	0.5	0.28
	TCM*	0%	0%	75%	79%
	$CTDI_{vol}$ 32cm (mGy)	9 (3-20)	10 (3.4-21)	8 (3-14)	6 (4-20)

Key - y: year, kV: tube voltage; eff-mAs: effective tube current time product; TCM: tube current modulation; $CTDI_{vol}$: volume CT dose index; DLP: dose length product; NA: not available; 32 cm & 16 cm: reference CTDI phantom size
*percentages of cases employed TCM

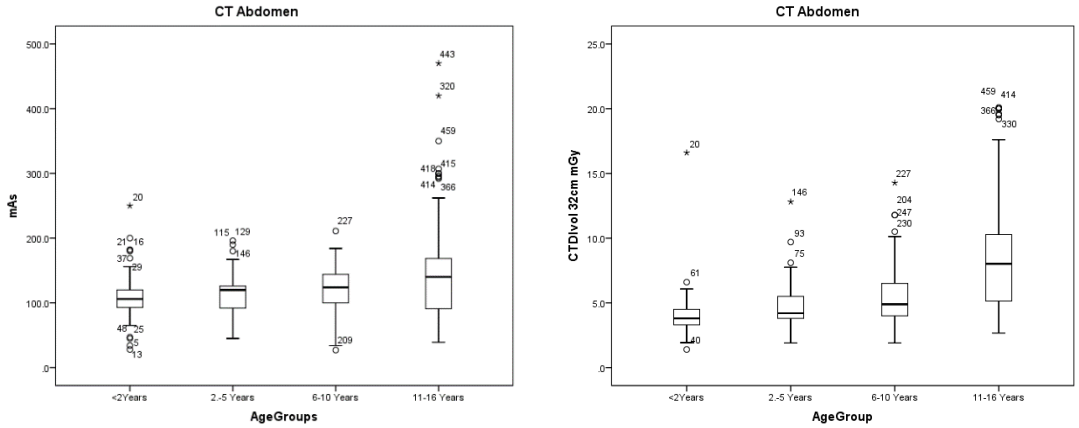

Figure 3.6 Box and whisker plots show variation of the overall CT abdomen mAs and $CTDI_{vol}$ in corresponding to age groups

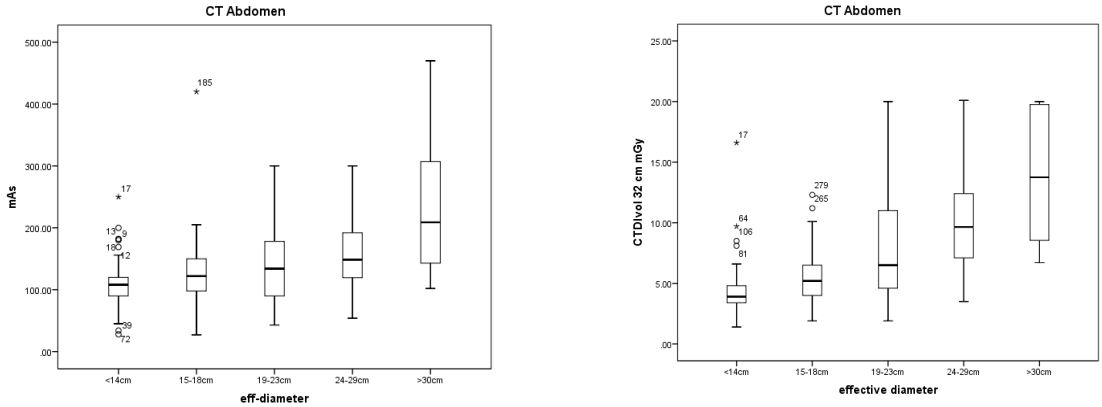

Figure 3.7 Box and whisker show variation of the overall CT abdomen mAs and $CTDI_{vol}$ corresponding size groups

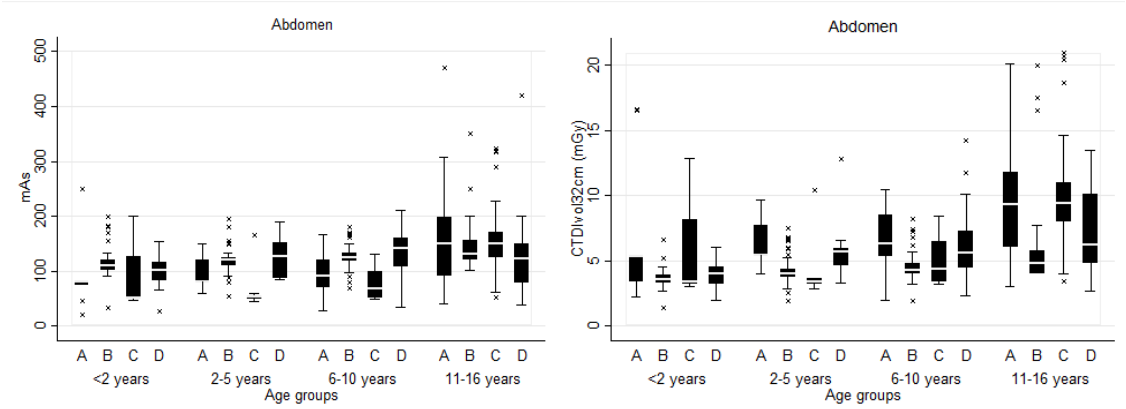

Figure 3.8 Box and whisker plots show variation of the multi-centre CT abdomen mAs and CTD_{Ivol} corresponding to the age groups

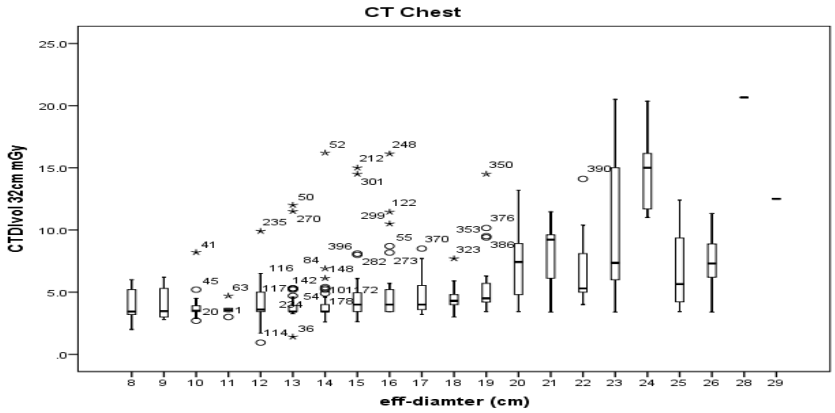

Figure 3.9 Box and whisker show variation of CT chest $CTDI_{vol}$ corresponding to effective diameter

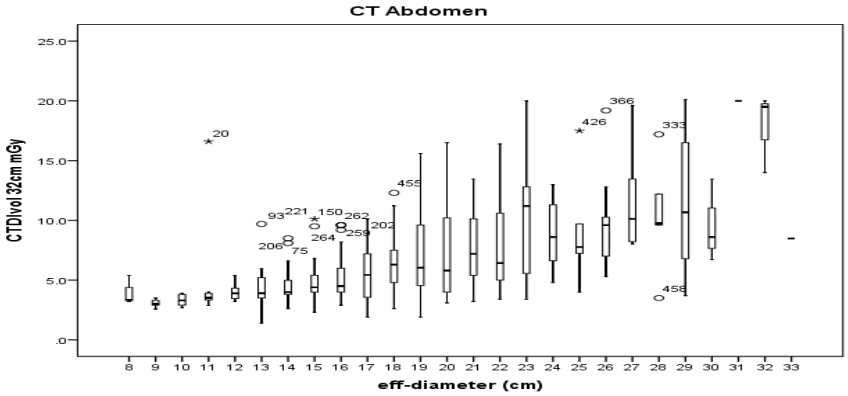

Figure 3.10 Box and whisker show variation of CT abdomen $CTDI_{vol}$ corresponding to effective diameter

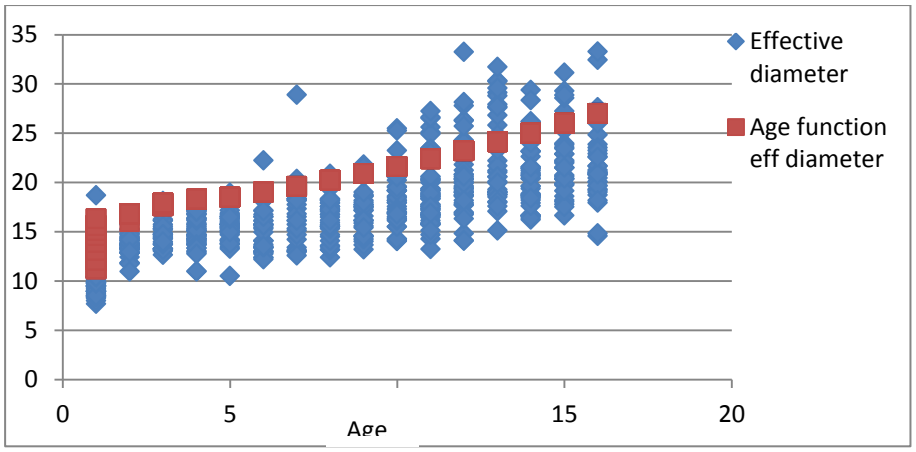

Figure 3.11 Variation of effective diameter (corresponding to age) versus ICRU age function effective diameter, (also corresponding to age)

Table 3.7 Comparison of 3rd quartiles of dose values of the present study with standard DRLs from Switzerland (S), Germany (G), Belgium (B) and Thailand (TH)

Age	**Dose**	**HEAD**					**CHEST**					**ABDOMEN**				
		O	S [8]	G [11]	BE [10]	TH [2]	O	S	G	BE	TH	O	S	G	BE	TH
0-1	$CTDI_{vol}$	25	20	33.6	35	25	8	5	6.9	8.4	4.5	9	7	6.8	7.8	7.7
		12-51	8.3-41	4.8-83	11-60	12-48	2.8-32	0.8-11	1.2-21.1	1.2-29	1.6-9.4	2.8-33	1.4-16	1.3-23	2.8-22	2.8-11.8
	DLP	508	270	393	280	400	251	110	93	76	80	256	130	164	101	220
		104-1322	66-414	48-896	88-480	162-866	64-886	12-198	20-360	11-261	20-210	126-480	29-258	39-705	36-286	56-352
2.5	$CTDI_{vol}$	38	30	49	43	30	8.8	8	8.4	9.3	5.7	10.8	9	8.3	11	9
		13-60	13-41	4.8-83	11-64	10-48	3.2-30	0.8-20	1.7-22.5	2-37	3.2-10.6	3.7-25.6	1.4-16	1-27.2	4-25	3.6-12
	DLP	888	420	611	473	570	351	200	137	111	140	371	300	261	209	275
		19-1402	144-538	60-1186	121-704	212-818	82-534	12-617	30-407	24-444	64-270	114-544	29-650	10-777	76-475	98-428
6-10	$CTDI_{vol}$	50	40	58	49	40	9.8	10	11.9	9	10	13	13	13.7	9.5	14
		13-61	13-50	10.9-113	11-64	17-56	3.2-30	2.1-20	2-25.5	2.9-37	2.8-21.6	3.7-28.5	1.4-14	2.2-22.2	4-25	4.2-28
	DLP	655	560	711	637	610	360	220	257	144	305	547	380	477	238	560
		206-1482	173-621	132-1424	143-832	265-923	86-892	32-352	49-63	46-592	90-552	118-1102	29-627	49-756	100-625	82-1086
11-16	$CTDI_{vol}$	51	60	64.5	50	45	10.5	12	5.9	13	15.6	10.9	16	10.1	13	17
		14.6-56	14-85	10.9-113	11-60	17-45	2.3-20	2.1-26	1.6-26	3.9-29	3.6-19.4	2.7-20.9	1.5-18	2.9-17.5	4-21	6.6-38
	DLP	1196	1000	920	650	800	727	460	166	260	470	542	500	402	403	765
		265-1695	216-148	178-1638	143-780	350-968	71-1246	32-1298	35-416	78-580	96-674	84-1098	90-738	101-694	124-651	262-1952

Key - DRLs: diagnostic reference levels; O: Oman; S: Switzerland; G: Germany; BE: Belgium; TH: Thailand; $CTDI_{vol}$: volume CT dose index; DLP: dose length product

3.3.5 Benchmarking of the dose reading

The dose distributions of $CTDI_{vol}$ and DLP obtained from the four centres, were further quantified to 3rd quartile, to facilitate comparison with figures from national surveys and studies in Table 3.5. The 3rd quartile dose values of the present study were lower than standard values from Germany, Belgium and Thailand, for all age groups. The 11-16 years age group showed $CTDI_{vol}$ values that were lower than all studies despite the application of adult protocols by centres A and B.

In the present research study, the third quartile values of $CTDI_{vol}$ (chest and abdomen examination) were higher than those reported by Switzerland, Germany and Belgium for children below 2 years, but were similar across all the other age groups. The DLP values however, were found to be high and widespread compared to other studies.

3.4 Discussion

The present multi-institutional paediatric CT study has important clinical implications: firstly, it defines the wide range of scanner types using 64 or more MDCT, and secondly, it represents both the acquisition parameters and their corresponding dose readings, thereby giving a direct indication of the influence of acquisition parameters on radiation dose. The data could serve as a platform for the evaluation of CT practices in individual institutions, and further, be used for benchmarking with results from the literature review (Chapter 2), to establish optimal acquisition parameters that will be verified in the pages to follow (Chapter 4). Although the number of institutions covered is small (four), the selected centres are mostly located within the metropolitan areas of the capital city of Oman, and account for the vast majority of paediatric CT examinations in the area. Therefore, the results of the present study would be invaluable as they form representative data of a national standing.

3.4.1 Head CT study results

The image quality and radiation dose during CT examinations are determined by a number of factors, including kV, tube current (mA), scan time (s), pitch, filtration, section thickness and reconstruction algorithms [21-23]. In most instances, kV and mAs are the primary determinants of image quality and radiation dose, when other imaging parameters are constant [19, 23-25].

Tube voltage is highly recommended as one of the scan parameters for determining the optimisation of paediatric CT imaging [19, 23-26]. Optimal tube voltage is usually decided according to patient size, diagnostic task, and type of scanner, so that optimal tradeoff is achieved between image noise, image contrast, artifacts and scan time [19, 22, 27]. Although several studies have discussed the possibility of lowering both kV and tube current, while maintaining, or even improving the diagnostic image quality in paediatric CT scanning [22, 28-31], the present study showed that some centres failed to apply tube voltage lower than 120 kV. In contrast, the pattern of practices in centre D, revealed the awareness of the radiology team about safe CT imaging, and this was reflected in the low $CTDI_{vol}$values observed in all obtained scans.

In centre D, head CT scanning was largely performed using a median 100 kV with a significant reduction in radiation dose of 100%, and preservation of diagnostic value, yielding results that were comparable with the standard 120 kV outcomes seen in the other three centres Fig 3. 12.

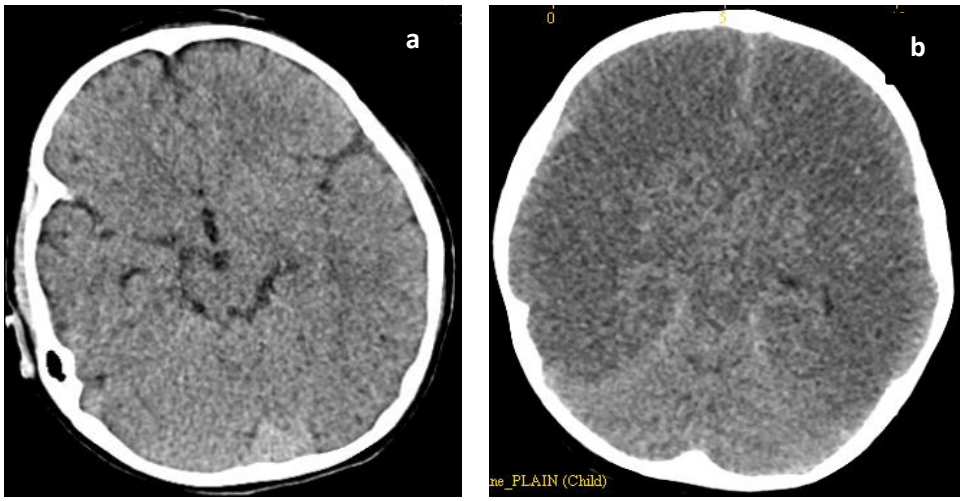

Figure 3.12 Images **a** and **b** for different 2 year-old children. Image **a** acquired by 120 kV, mAs 200, slice thickness 3 cm, $CTDI_{vol}$ 29 mGy (Siemens 64 MDCT); Image **b** used 100 kV, 135 mAs, TCM, slice thickness 3 cm, IR and $CTDI_{vol}$13 mGy (Siemens 128FLAS MDCT).

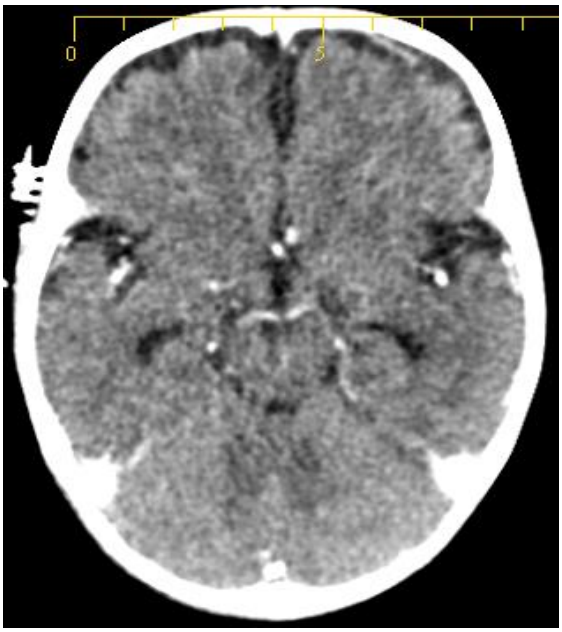

Figure 3.13 Image of CT brain post-contrast, for 1 year child. Acquired by 80 kV, 247 mAs, TCM, $CTDI_{vol}$ 12 mGy (Siemens 128 FLASH MDCT)

During the present study, it was observed that, in patients below 10 years, a 100 kV with TCM technique, was adequate for all head CT scans, performed with both Siemens Healthcare 64 and 128 FLASH MDCT scanners. Furthermore, it was seen that reduction up to 80 kV in some post-contrast head CT studies, was advantageous because low tube voltage was more effective for small children, and also provided a better iodine signal, which improved the conspicuity of hyper- or hypo vascular structures Fig 3.13. More importantly, the implementation of a low tube current brain CT protocol in centre D, substantially reduced the amount of radiation exposure. In contrast, centres equipped with Philips Healthcare 64 MDCT scanners, used 120 kV in all CT brain scans, unlike their counterpart (Siemens scanners). This could be probably due to the characteristics of scanners mentioned earlier in Chapter 2. The next chapter will discuss further, the outcome of the phantom study on the efficacy of scanners supplied by the two manufacturers, and how well they compare when low kV is applied.

Several research studies have reiterated the fact that a decrease in the tube current will reduce radiation dose significantly without affecting the quality of images if the tube current is not optimised prior to the change [22, 31-34]. Scientific literature emphasises the need for selecting mAs according to patient size, and recommends low exposure for small children. The present study however, revealed significant variation in the tube current-time product during the examination of all anatomical areas across all age groups.

Although all centres are equipped with the latest state-of-the-art CT scanners, and have access to pre-programmed paediatric protocols, the practices of applied acquisition parameters in both centres A and B, particularly in head CT studies, indicated the application of some adult protocols, irrespective of age group. Tube current was selected manual, and showed wide variation, up to five-folds, within the range, for the same age group. This was reflected in the wide interquartile span of the $CTDI_{vol}$ corresponding to the applied tube current at 120 kV. For instance, in children below 2 years, the markedly wide range of head $CTDI_{vol}$ indicated improper tailoring of the mAs into this specific age group. On the other hand, much lower median mAs and $CTDI_{vol}$ were observed in centres C and D, for all age groups, clearly indicating the awareness of the radiology team about radiation exposure of children. Both centres performed routine scans by means of the TCM technique,

which led to a significant reduction in radiation dose, without compromising on the diagnostic value of the outcome. Moreover, centre C used 70% - 96% axial scan mode with TCM, and this technique, coupled with tilting the gantry, is believed to extensively reduce radiation dose to the eye lens [31, 35].

Appreciable reduction in radiation dose was observed at centre D, which is equipped with SOMATOM Definition Flash 128, Siemens Healthcare (Germany) scanner. This was achieved by incorporating both tube current and tube voltage modulations; this combination technique achieved a three-fold reduction in the radiation dose, compared to the standard protocols used in other centres. Literature cites several reports on the benefits of (a) lowering tube voltage from 120 kV to 80 kV, and (b) the tube modulation technique, which results in more than 40% increase in contrast to noise ratio (CNR), and effectively reduces radiation dose to more than 70% [23, 26, 30, 34, 36, 37]

Data analysis revealed that centre D was the only institution equipped with a scanner with iterative reconstruction (IR): this instrument has produced image of better quality, for most of the low dose techniques used in head CT scans. For example, in a majority of the head CT examinations where $CTDI_{vol}$ was below 16 mGy, the IR technique was employed for children below 10 years, resulting in substantial reduction of radiation dose, without negatively affecting the diagnostic value Figure 3.13 Image (b).

3.4.2 Chest and abdomen CT studies

Analysis of data elicited from the present research effort, revealed that a median tube voltage of 120 kV was uniformly applied for all chest and abdomen scans, in all centres except centre D. Recent research reports largely advocate the application of 80 kV and 100 kV tube voltages for chest and abdomen CT examinations, particularly in children with weight below 45 kg, because of its high intrinsic contrast [22, 23, 29, 38, 39]. Centre D predominantly used 100 kV tube voltage for chest/abdomen scans in paediatric patients below 10 years, occasionally reducing it to 80 kV in some contrast CT studies. Recent phantom studies suggest the use of low kV for most contrast studies, which would take advantage of the aforementioned effect of attenuation of iodine at lower tube voltages [29, 37, 40]. Figure 3.14

illustrates the clinical effects of low tube voltage on a post-contrast abdomen CT scan – used in centre D without compromising on either diagnostic value or image quality.

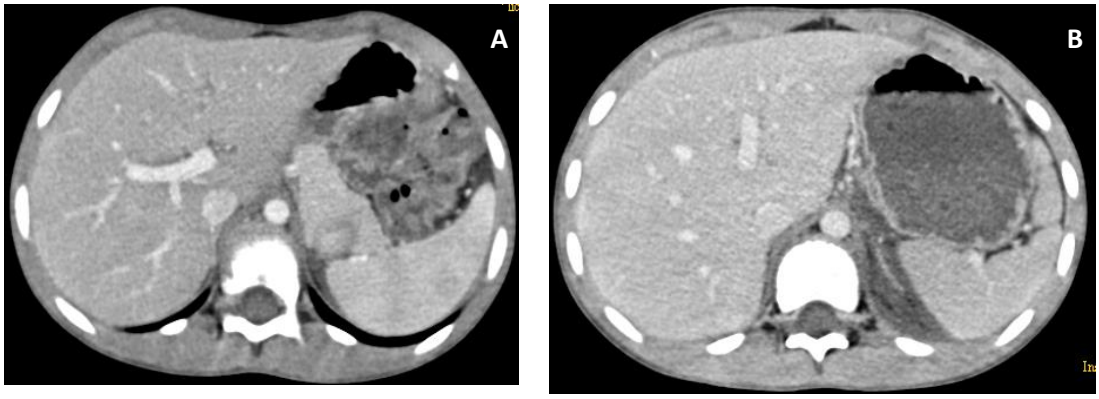

Figure 3.14 Image A and B of post- contrast iodine from separate studies of 11 year-old girls with identical body size (23 cm effective diameter). Image A was obtained at kV, 120, mAs 113 TCM, slice thickness 2 cm, $CTDI_{vol}$ 6.3 mGy; Image B was obtained at kV,100, mAs 120, TCM, slice thickness 2 cm, $CTDI_{vol}$ 4 mGy. Both studies are of diagnostic quality. Although image B is slightly noisier than image A, its CNR is slightly better, and the radiation dose is reduced to half. (Siemens 64 MDCT)

Despite the fact that chest and abdomen paediatric protocols must necessarily be tailored to suit children's body size, data from the present study evidenced an extensive interquartile range of mAs within age groups, with great discrepancy being evident in the 11-16 years age group. This was reflected in the $CTDI_{vol}$, possibly due to the lack of standardisation of protocols among the centres. Furthermore, the wide differences in $CTDI_{vol}$ for the age group 11-16 years, pointed to a lack of standardisation with respect to age categorisation of paediatric patients, thus leading to the use of a mixture of adult and paediatric protocols. Centre A displayed significant high median mAs and $CTDI_{vol}$ for all age groups, in comparison to centre D, which showed a narrow interquartile range, and significantly low median mAs and $CTDI_{vol}$ for children below 10 years. Centre D modified the tube voltage to 80 - 100 kV for children below 11 years, and combined this feature with tube current modulation, to great advantage.

Centre D also used the iterative reconstruction technique in a manner similar to that of head CT examination, with an iterative strength of 3. Siemens scanners utilise the Sinogram Affirmed Iterative Reconstruction technique (SAFIRE), which offers 5

iterative strengths. Research literature [41-44] and clinical data, advocate strengths of 2 and 3 in preference to other strengths, for both chest and abdomen scans.

To ascertain whether the observed variation of acquisition parameters and high dose delivered for each specific age group, was caused by bigger body size of the paediatric patient, effective diameter was extracted to estimate body size. Research results from the present study, pointed to substantial variation of $CTDI_{vol}$ within each body size, indicating improper normalisation of paediatric CT protocols (Fig 3.9 and 3.10).

Adaptation to the patient's body size is an integral part of CT dose optimisation, because children's body size shows variation within the same age group. Various patient size parameters such as body weight [43], effective body diameter, and automatic body diameter [18, 38, 45], have been previously used for CT dose optimisation, but these measurements may be either laborious to extract, or unavailable in a dose database. Therefore, a comparison was made, of the effective diameter computed in the present study, with the ICRU effective diameter age function. Differences were evident between the two methods, with respect to the age context. In general, the effective diameter for children below 11 years in this study, evinced lower variation in body size, compared to the ICRU method. Until the automatic estimation of body size [38, 45] takes shape, the currently available ICRU effective diameter tools can be easily used to normalise the acquisition protocols for routine CT practices.

Evaluation of scanner specific factors was carried out by analysing data from chest examinations, and some abdomen examinations, acquired with application of a standard tube voltage of 120 kV and fixed tube current of 45 mAs. Results obtained were in the range of 3.5-4 mGy (using 32 cm reference CTDI phantom), in both Siemens and Phillips 64 MDCT. It is expected that these results would help to optimise standard CT protocols, and mitigate the issue of scanner specific factors in routine paediatric imaging. Detailed investigation of scanner specifics will be carried out in the next chapter of the phantom study.

3.4.3 Iterative reconstruction

Where image quality is concerned, performance of different IR products particularly in routine paediatric CT examinations is currently a controversial topic among radiologists, since these products are scanner-specific, and many other system parameters can also have a remarkable influence on the reconstruction performance, e.g., level of iteration in relation to the anatomical areas, and detector efficiency. In fact, it was understood from the analysis of the present study's clinical data, that, despite centre D's Radiology department being equipped with the latest 128 Flash Somatom scanner, (which employs the SAFIRE technique), more than 50% of paediartic studies were still reconstructed with FBP.

3.4.4 Reconstruction image slice thickness

Image noise developed mainly as the result of the low dose technique, and this is the most significant factor affecting image quality. Noise is proportionate to the square root of the quantity of the x-ray flax that is responsible for image formation [21, 46-49]. As mentioned earlier, the iterative reconstruction technique has revolutionised the application of the CT low-dose technique, by enabling reduction in image noise. Apart from this, the reconstructed image with a large slice thickness, further reduces image noise, and improves image quality. In the present data analysis, participating centres used median 2 mm thickness for head CT, chest and abdomen scans, including centre D, which displayed awareness about optimisation of paediatric CT imaging.

3.4.5 Pitch value

For the MDCT scanners, the conceptual relationship between pitch and radiation dose is not as straightforward as for single-detector CT scanners. In some scanners such as Siemens and Phillips, the operator must be cautious when using pitch value, particularly with the low dose technique. For example, increasing the pitch value in Siemens and Phillips scanners while using TCM, results in the automatic adjustment of the tube current, and maintenance of the effective mAs and $CTDI_{vol}$ as constant [21, 49]. To some extent, there was no discrepancy observed in pitch value among the selected centres, except for centre D, which used a high pitch factor of 3 in most

of the chest and abdomen routine studies. The majority of helical CT studies in the present study, showed utilisation of pitch values in the range 0.9 - 1.4. The influence of the pitch factor on patient dose and image quality is covered in Chapters 2 and 4.

3.4.6 Scan time

Scanning time (s) is one of the core factors affecting image quality of the paediatric patient population. Most modern MDCT scanners apply tube rotation time intervals of 0.28 - 0.5 seconds [21, 50]. This technique shortens acquisition time, and the need for sedation, and enables the imaging of less cooperative children, thereby facilitating the use of CT in paediatrics [21, 51]. However, shorter rotation time may produce more image noise, caused by a reduction in the number of profiles that are used in image reconstruction [21].

The dataset showed the use of a constant scan time uniformly for all age groups: For example, centre D applied 0.28 s for all CT chest and abdomen examinations, though a scan time of 0.5 s could have been used for abdomen scans, and children above 5 years. Basically shorter exposure time is crucial for small children to minimise the motion artifacts, and further adjustment of scan time is recommended for low dose exposure techniques and for cooperative children.

3.4.7 CTDI: indicator of tube output for the optimisation of CT practice

Many studies by radiation experts and professional organisations, have recommended the use of CTDI and DLP matrices, to facilitate the development of the diagnostic reference level concept, which provides reference values for upper limits of radiation dose for optimum patient protection [1-4, 8-11, 52]. Notwithstanding, understanding and monitoring radiation exposure requires a basic knowledge of how these matrices were derived, as well as how they are influenced by scanner parameters and a patient's body size. $CTDI_{vol}$ values depend heavily on the selected acquisition parameters, such as tube voltage, tube current time product, pitch and beam filtration [16, 53]. Therefore, these dose readings served as a reliable index of tube output, but did not accurately represent the individual patient radiation dose, as they do not take into consideration the actual patient size. In the present study, $CTDI_{vol}$ was extensively used to investigate how paediatric protocols can be

normalised in a clinical environment. The wide variation of $CTDI_{vol}$ of children within the same age group, and across age groups of the study data, revealed improper normalisation of paediatric protocols, and the need for optimisation of paediatric practices. Furthermore, this tool has helped to gain an understanding of the influence of each acquisition parameter on radiation dose, in terms of tube output, in conjunction with the obtained image quality. Results indicated a direct relation between applied parameters and the given $CTDI_{vol}$. To explain further, when the same protocols were used in both 64 MDCT and 128MDCT Flash Siemens, similar CTDI values were obtained. Similarly, when comparing the Siemens 64 MDCT and Philips 64 MDCT, similar protocols evinced close $CTDI_{vol}$ values, particularly in chest and abdomen examinations. The topic of establishment of routine protocols that could be shared between scanners with identical scan modes, will be further investigated in Chapter 4.

Benchmarking of the study's $CTDI_{vol}$ values with other published European DRLs, showed that the former were lower than the cited values in literature, despite the application of adult protocols in some centres across all age groups. Published DRLs show substantial variation of dose, delivered for the same age groups in the same anatomical areas. Using the 3^{rd} quartile values, the study's $CTDI_{vol}$ values for all anatomical areas, fell below those followed in Germany [11] and Belgium [10] (Table 3.7)**.** In addition, results of the study were in corroboration with those obtained from Switzerland [8] and Thailand [2].These findings raised concerns, about the high dose presently being administered in paediatric CT imaging, despite the initiation of optimisation measures more than three decades ago. Results from the present study highlight the need for correlating scanner specifics with attempts to establish standards for a national reference dose, especially if the objective is to pinpoint the actual method for monitoring of CT scanning practices.

It is hoped that the dose value obtained in the present research undertaking, would provide a platform for paediatric protocols by each participating institution. The obtained dose reading would also be used to establish an upper boundary diagnostic reference dose of the devised optimisation protocols.

3.4.8 Body-size to facilitate CT practice

Implementation of child-size CT protocols, and reduction of CT radiation dose have both been recommended by radiation dose experts, and those concerned about paediatric CT imaging [3, 13, 14, 54]. It is regarded as a fundamental part of the optimisation process, because the radiation dose required to obtain the best diagnostic imaging for patients with similar age and body weight, may vary depending on the body habitus. Various body size parameters have been used to normalise paediatric protocols, including body weight or body mass index. Nevertheless, these basic body parameters are not always available in day to day clinical practice. Tube current modulation in the contemporary MDCT scanners, tailored the acquisition parameters based on attenuation of body size. However, this technique solely relied on the scanner specific, as well as the extent of optimisation of paediatric protocols. Some studies have reported that the effective diameter as the function of cross-sectional dimensions is a criterion that is better adapted to body size, than the parameters based on weight and attenuation. However, this kind of normalising protocol, according to body size, is quite complicated on a daily basis.

The recorded values for effective diameter showed that the applied acquisition parameters were not tailored to suit neither the children's age nor to their body size. This was evident from the similarity in median tube current and interquartile values for almost all ages, although there was variation in children's body size, even within the same age group. The obtained results also strengthen the need for intermediate CTDI phantom references between the existing reference 16-cm and 32-cm phantoms, particularly for children above 10 years. These findings are consistent with Brady and Kaufman's study [12] of the Association of Physicists, in Medicine Report 204, titled "Size-Specific Dose Estimates for Paediatric CT Implementation". They recommend an intermediate 24-cm CTDI phantom for patients weighing between 36 and 100 kg. Existing chest and abdomen DRLs for children below 10 years, referred to the 16-cm CTDI phantom, by multiplication of the 32-cm reference $CTDI_{vol}$ values by a factor of two; DRLs for children above 10 years referred to a 32-cm phantom. In the same context, the study's dataset demonstrated a gradual increase in the effective diameter with increase in age; thus, it is unrealistic to have the age of 10 as the cutoff between the 16-cm and 32-cm $CTDI_{vol}$, because it either underestimates or overestimates the delivered radiation dose. Until this issue is

sorted out, paediatric DRLs would not be a reliable means to monitor scanning practices, and be referred to when optimising CT protocols.

3.5 Devising the routine paediatric CT protocols

In this chapter, a retrospective analysis strengthened our perception of how paediatric protocols were tailored in clinical practices. This analysis demonstrated a significant variety of acquisition parameters and dose readings between the four centres. Low dose techniques observed in this chapter, in conjunction with additional findings in Chapter 2, were synthesised to help devise optimised routine paediatric CT protocols (Tables 3.8–3.10). These devised protocols would be warranted when the empirical study in Chapter 4 supported the use of the body size (effective diameter) protocols acquired in this chapter. It is expected that the reference of the 5-year (16 cm effective diameter) anthropomorphic phantom would validate the protocols of body size in the range of 15–19 cm for the effective diameter. Although, the devised protocols of each group of the chest and abdomen are provided with range of mAs and $CTDI_{vol}$ to cover the 5 cm variation in effective diameter, its effect is of little importance.

Notably, the devised protocols categorised children into five groups. Head CT protocols (Table 3.8) are age-based because the primary attenuation comes from the skull, and the process of bone formation in the skull is age dependent. Although the chest and abdomen protocols are body size based, the age and weight details are included along with effective diameter details in the devised protocols (Tables 3.9–3.10). These details have been extracted from the optimisation studies (Chapter 2), which would be used as guidelines for the body size specific protocols as well as the alternative means when the effective diameters are unavailable. Additionally, each group, based on age and body size, is designed to have different acquisition parameters applied, while still providing similar results to fulfil the various diagnostic purposes such as post-contrast studies, which are positively influenced by low tube voltage techniques.

Because the retrospective analysis and phantom study were conducted using 64 MDCT Philips, Siemens 64 and 128 MDCT scanners, the devised protocols will eventually coincide with these scanners. Nevertheless, it is expected that the devised

protocols would not significantly differ across scanners made by different manufacturers.

Table 3.8 Optimised Paediatric Head Protocols Specific to the Age for the 64-Slice Computed Tomography Systems

Age (year)	Acquisition Parameter											DRLs		Reconstruction Parameter	
	kV	Eff-mAs	Time (s)	Pitch	Beam Colli (mm)	FOV (mm)	TCM	Scan Length (mm)	Slice Thick-ness (mm)	Scan Mode	CE	$CTDI_{vol}$ (mGy)	DLP (mGy-cm)	Conv- Ke	Reco- algo
<2 y	100	100-120	0.5	-	1x5.0	Small	ON	Restricted	2-3	Axial	NO	13-14	100-200	SF/B 3	IR-S2-S3
	100	120-130		0.6	64x0.6					Helical	NO	13-15	100-200	SF/B 3	
	100	80-120		0.6	64X0.6					Helical	YES	12-14	100-200	SF/B 3	
2-4	100	100-130	0.5	-	1x5.0	Small	ON		2-3	Axial	NO	14-17	150-250	SF/B 3	IR-S2-S3
	120	60-80		0.6	64x0.6					Helical	NO	14-15	150-250	SF/B 3	
	100	100-150		0.6	64x0.6					Helical	YES	14-16	150-250	SF/B 3	
5-9	120	80-100	1	-	1x5.0	Small	ON		2.5	Axial	NO	15-18	150-300	SF/B 3	IR-S2-S3
	100	150-200		0.6	64x0.6					Helical	NO	15-18	150-300	SF/B 3	
	100	110-180		0.6	64x0.6					Helical	YES	12-14	150-300	SF/B 3	
10-13	120	100-120	1	-	1x5.0	Medium	ON		2.5	Axial	NO	20-23	200-350	SF/B 3	IR-S2-S3
	100	200-250		0.6	64.x0.6					Helical	NO	17-21	200-350	SF/B 3	
	100	180-200		0.6	64x0.6					Helical	YES	16-19	200-350	SF/B 3	
>14Y	120	100-120	1	-	1x5.0	Medium	ON		2.5	Axial	NO	22-27	250-400	SF/B 3	IR-S2-S3
	120	120-150		0.6	64.x0.6					Helical	NO	20-27	250-400	SF/B 3	
	100	180-200		0.6	64x0.6					Helical	YES	17-20	250-400	SF/B 3	

Eff-dia: effective diameter; Eff mAs: effective mAs; FOV: field of view; CE: contrast medium; $CTDI_{vol}$,: volume computed tomography dose index; DLP: dose-length product; DRLs: dose reference levels; kV: kilovoltage; mAs: milliampere seconds; SF: soft tissue; TCM: tube-current modulation; Convo-Ke: convolution kernel; IR: iterative reconstruction; S2&S3: interactives' strength that range in Siemens 1-5.
*Reference mAs for TCM.
Note: Scout-view must be obtained in PA with a tube voltage of 80-100 kV.
Each age group has three different protocols but with similar radiation doses.
Head protocols are specific to age because primary attenuation comes from skull and the process of bone formation in the skull is age dependent.

Table 3.9 Optimised Paediatric Chest Routine Protocols Specific to Age and Body Size (Weight and Effective Diameter) for the 64-Slice Computed Tomography Systems

Age (year)	Body Size		Acquisition Parameter										DRLs		Recon
	Weight (kg)	Eff-dia (cm)	kV	Eff-mAs	Time (s)	Pitch	Beam Colli (mm)	FOV (mm)	TCM	Scan Length (mm)	Slice Thick (mm)	CE	$CTDI_{vol}$ (mGy)	DLP (mGy-cm)	Convo-Ke
Chest															
<2	4-9	<14	100	45-50	0.28	0.6	64x0.6	Small	OFF	Restricted	2-3	No	1.5-3	30-50	I70f/I31f IR-S3
			100	50-80					100		2-3	Yes			
			80	50-100					150		2-3	Yes			
2-5	10-19	15-19	100	45-60	0.5	0.6		Small	OFF		2-3	No	1.5-3	50-70	
			100	50-80					100		2-3	Yes			
			80	50-100					200		2-3	Yes			
6-9	20-29	20-24	120	45-60	0.5	0.6		Medium	OFF		2-3	No	2-3.4	70-100	
			100	60-100					200		2-3	Yes			
			80	70-120					250		2.3	Yes			
10-14	30-39	25-29	120	45-60	0.5	0.9		Medium	130		2-3	No	2.5-4	100-150	
			100	70-150							2-3	Yes			
>15	>40	>30	120	100-150	1	0.9		Medium	150		2-3	NO	3-5	>150	
			100	150-250	1	0.9			200		2-3	YS			

Eff-dia: effective diameter; kV: kilovoltage; Eff mAs: effective mAs; FOV: field of view; CE: contrast medium; $CTDI_{vol}$,: volume computed tomography dose index; DLP: dose-length product; DRLs: dose reference levels; Convo-Ke: convolution kernel; TCM: tube-current modulation; I70f: convolution kernel for lungs; I31f: convolution kernel for mediastinum; IR: iterative reconstruction; S3: interactive's strength that ranges in Siemens 1-5.
*Reference mAs for TCM.

Note: Scout-view must be obtained in PA with a tube voltage of 80-100 kV.
Each size group has three different protocols but with similar radiation doses.
The age and weight provided are the typical figures for each effective diameter range and these are included as guidelines only.

Table 3.10 Optimised Paediatric Chest Routine Protocols Specific to Age and Body Size (Weight and Effective Diameter) for the 64-Slice Computed Tomography Systems

Age (year)	Body Size		Acquisition Parameter										DRLs		Recon
	Weight (kg)	Eff-dia (cm)	kV	Eff-mAs	Time (s)	Pitch	Beam Colli (mm)	FOV (mm)	TCM	Scan Length (mm)	Slice Thick (mm)	CE	$CTDI_{vol}$ (mGy)	DLP (mGy-cm)	Convo-Ke
ABDOMEN															
<2	4-9	<14	100	45-50	0.5	0.6	64x0.6	Small	OFF	Restricted	2-3	No	2.5-3	40-60	I31f IR-S3
			100	50-80					150		2-3	Yes			
			80	50-100					200		2-3	Yes			
2-5	10-19	15-19	100	45-60	0.5	0.6		Small	OFF		2-3	No	2.5-3	50-80	
			100	50-80					150		2-3	Yes			
			80	50-100							2-3	Yes			
6-9	20-29	20-24	120	60-100	1	0.9		Medium	OFF		2-3	No	2.5.4	80-100	
			100	80-150					150		2-3	Yes			
			80	100-180					200		2.3	Yes			
10-14	30-39	25-29	120	60-120	1	0.9		Medium	160		2-3	No	3-5	100-150	
			100	100-150					250		2-3	Yes			
>15	>40	>30	120	150-200	1	0.9		Medium	200		2-3	NO	4-6	>200	
			100	200-250	1	0.9			250		2-3	YS			

Eff-dia: effective diameter; kV: kilovoltage; Eff mAs: effective mAs; FOV: field of view; CE: contrast medium; $CTDI_{vol}$,: volume computed tomography dose index; DLP: dose-length product; DRLs: dose reference levels; Convo-Ke: convolution kernel; TCM: tube-current modulation; 131f: convolution kernel for soft tissue; IR: iterative reconstruction; S3: interactive's strength that ranges in Siemens 1-5.

*Reference mAs for TCM.

Note: Scout-view must be obtained in PA with a tube voltage of 80-100 kV.

Each size group has three different protocols but with similar radiation doses.

The age and weight provided are the typical figures for each effective diameter range and these are included as guidelines only.

3.6 Limitations of the study

The present study has the following limitations.

Firstly, the findings of the study need to be considered in the context of the limitations of the population sampled for some age groups and anatomical areas. The number of chest and abdomen examinations accessed, were limited in the <2 years and 2-5 years age groups, either due to (a) restrictions/justification required to access CT scan records, or (b) availability of alternative paediatric modalities (such as ultrasound), in the participating centres.

Secondly, the data set lacked information about children's weight and height, due to (a) unavailability of these details in the participating centres, and (b) because the study was based on retrospective data analysis. However, extracted data for effective diameter of the chest and abdomen provided a reliable comparison between acquired acquisition parameters and body size of the paediatric patients.

Finally, the study was limited to only two manufacturers; this is due to the fact that these two manufacturers are the most popular in Oman, as well as in the local geographical region. Inclusion of other manufactures, especially those supplying the latest CT scanner models, would have lent more strength to the results.

3.7 Conclusion

Routine paediatric CT scanning protocols in Oman, were found to show wide variations of $CTDI_{vol}$ across all age groups, for the same anatomical areas, indicating improper normalisation of acquisition protocols in children. However, centre D is a beneficiary of advanced technology in the field of CT scanning, and utilises a combination of modulation technique and iterative reconstruction, for most of the examinations. This has helped immensely, by significantly reducing radiation dose, while preserving the quality of diagnostic images.

It is expected that, for all anatomical areas, the obtained low dose techniques (yielding images of optimal quality), would be used to revise the preliminarily

devised optimisation paediatric CT protocols. The next phase of the study consisting of a phantom study would be verifying these protocols (Tables 3.8 - 3.10).

The present study also threw light on the current practices being followed for normalising paediatric chest and abdomen $CTDI_{vol}$ values. These practices were not compliant with the study data, which was based on the effective diameter values, possibly due to underestimation of the dose delivered for children above 10 years. Accordingly, the present retrospective study provides a platform for computing the average effective body size, within an age group of the target paediatric population in Oman. These figures could be used as reference values when implementing the protocols validated in Chapter four.

Furthermore, the data set strengthens the need for an intermediate reference phantom between the 16-cm and 32-cm reference CTDI phantom. Finally, it may be said in conclusion that the study illuminates the current practices in Oman, and provides a platform for implementation of the outcomes of the entire optimisation process, in clinical practices.

3.8 References

1. Fukushima Y, Tsushima Y, Takei H, Taketomi-Takahashi A, et al. 2012. Diagnostic reference level of computed tomography (CT) in Japan. Radiat Prot Dosimetry. 151(1): 51-7.

2. Kritsaneepaiboon S, Trinavarat P, Visrutaratna P. 2012. Survey of pediatric MDCT radiation dose from university hospitals in Thailand: A preliminary for national dose survey. Acta Radiologica 53(7): 820-6.

3. Granata C, Origgi D, Palorini F, Matranga D, et al. 2015. Radiation dose from multidetector CT studies in children: Results from the first Italian nationwide survey. Pediatr Radiol. 45(5): 695-705.

4. Watson DJ, Coakley KS. 2010. Paediatric CT reference doses based on weight and CT dosimetry phantom size: Local experience using a 64-slice CT scanner. Pediatr Radiol. 40(5): 693-703.

5. Lee YW, Yang CC, Mok GS, Wu TH. 2012. Infant cardiac CT angiography with 64-slice and 256-slice CT: Comparison of radiation dose and image quality using a pediatric phantom. PloS One 7(11): e49609.

6. Huda W, Vance A. 2007. Patient radiation doses from adult and pediatric CT. Am J Roentgenol.188(2): 540-6.

7. Vassileva J, Rehani MM, Applegate K, Ahmed NA, et al. 2013. IAEA survey of paediatric computed tomography practice in 40 countries in Asia, Europe, Latin America and Africa: Procedures and protocols. Eur Radiol. 23(3): 623-31.

8. Verdun FR, Gutierrez D, Vader JP, Aroua A, et al. 2008. CT radiation dose in children: A survey to establish age-based diagnostic reference levels in Switzerland. Eur Radiol. 18(9): 1980-6.

9. Santos J, Foley S, Paulo G, McEntee MF, et al. 2014.The establishment of computed tomography diagnostic reference levels in Portugal. Radiat Prot Dosimetry 158(3): 307-17.

10. Buls N, Bosmans H, Mommaert C, Malchair F, et al. CT Paediatric Doses in Belgium: A Multi-centre Study. Belgium: Belgium Federal Agency of Nuclear Control, 2010.

11. Galanski M, Nagel H, Stamm G. Paediatric CT Exposure Practice in the Federal Republic of Germany: Results of a Nationwide Survey in 2005–2006. Hannover: Medizinische Hochschule; 2007.

12. Brady S, Kaufman R. 2012. Investigation of American Association of Physicists in Medicine Report 204 size-specific dose estimates for pediatric CT implementation. Radiology 265: 832-40.

13. Boone JM, Strauss KJ, Cody DD, McCollough CH, et al. Size Specific Dose Estimation (SSDE) in Paediatric and Adult Body CT Examination. American Association of Physicists in Medicine (AAPM) Report NO. 204, 2011.

14. Brink JA, Morin RL. 2012. Size-specific dose estimation for CT: How should it be used and what does it mean? Radiology 265(3): 666–8.

15. Zoetelief J, Dance DR, Drexler G, Jarvinen H, et al. 2005. Patient dosimetry for x rays used in medical imaging. Journal of the ICRU 5(2): i.

16. Goske MJ, Strauss KP, Coombs LP, Mandel KE, et al. 2012. Diagnostic reference ranges for pediatric abdominal CT. Radiology 268(1): 208-18.

17. Brady Z, Ramanauskasr F, Cain M, Franzcrf, et al. 2012. Assessment of paediatric CT dose indicators for the purpose of optimisation. Brit J Radiol. 85: 1488-98.

18. Kleinman PL, Strauss KJ, Zurakowski D, Buckley KS, et al. 2010. Patient size measured on CT images as a function of age at a tertiary care children's hospital. Am J Roentgenol. 194(6): 1611-9.

19. Brisse HJ, Brenot J, Pierrat N, Gaboriaud G, et al. 2009. The relevance of image quality indices for dose optimization in abdominal multi-detector row CT in children:Experimental assessment with pediatric phantoms. Physics Med Biology 54(7): 1871-92.

20. Vardhanabhuti V, Olubaniyi B, Loader R, Riordan RD, et al. 2012. Image quality assessment in torso phantom comparing effects of varying automatic current modulation with filtered back projection, adaptive statistical, and model-based iterative reconstruction techniques in CT. J Med Imaging Radiat Sci. 43(4): 228-38.

21. Nievelstein RA, van Dam IM, van der Molen AJ. 2010. Multidetector CT in children: Current concepts and dose reduction strategies. Pediatr Radiol. 40(8): 1324-44.

22. Dong F, Davros W, Pozzuto J, Reid J. 2012. Optimization of kilovoltage and tube current-exposure time product based on abdominal circumference: An oval phantom study for pediatric abdominal CT. Am J Roentgenol. 199(3): 670-6.

23. Nakaura T, Awai K, Oda S, Funama Y, et al. 2011. Low-kilovoltage, high-tube-current MDCT of liver in thin adults: Pilot study evaluating radiation dose, image quality, and display settings. Am J Roentgenol. 196(6): 1332-8.

24. Papadakis AE, Perisinakis K, Raissaki M, Damilakis J. 2013. Effect of x-ray tube parameters and iodine concentration on image quality and radiation dose in cerebral pediatric and adult CT angiography: A phantom study. Invest Radiol. 48(4): 192-9.

25. Schindera ST, Winklehner A, Alkadhi H, Goetti R, Fischer M, Gnanntc R, et al. 2013. Effect of automatic tube voltage selection on image quality and radiation dose in abdominal CT angiography of various body sizes: A phantom study. Clin Radiol. 68(2): 79-86.

26. Reid J, Gamberoni J, Dong F, Davros W. 2010. Optimization of kVp and mAs for pediatric low-dose simulated abdominal CT: Is it best to base parameter selection on object circumference? Am J Roentgenol.195(4): 1015-20.

27. Al Mahrooqi KMS, Ng CKC, Sun Z. 2015. Pediatric computed tomography dose optimization strategies: A literature review. J Med Imaging Radiat Sci. 46(2): 241-9.

28. Park YJ, Kim YJ, Lee JW, Kim HY, Hong YJ, Lee HJ, et al. 2012. Automatic tube potential selection with tube current modulation (APSCM) in coronary CT angiography: Comparison of image quality and radiation dose with conventional body mass index-based protocol. J Cardiov CT 6(3): 184-90.

29. Hough DM, Fletcher JG, Grant KL, Fidler JL, et al. 2012. Lowering kilovoltage to reduce radiation dose in contrast-enhanced abdominal CT: Initial assessment of a prototype automated kilovoltage selection tool. Am J Roentgenol. 199(5): 1070-7.

30. Morton RP, Reynolds RM, Ramakrishna R, Levitt MR, et al. 2013. Low-dose head computed tomography in children: a single institutional experience in pediatric radiation risk reduction. J Neur Pediat.12(4): 406-10.

31. Rao P, Bekhit E, Ramanauskas F, Kumbla S. 2013.CT head in children. Eur J Radiol. 82(7): 1050-8.

32. Greess H, Lutze J, Nomayr A, Wolf H, Hothorn T, Kalender WA, et al. 2004. Dose reduction in subsecond multislice spiral CT examination of children by online tube current modulation. Eur J Radiol. 14(6): 995-9.

33. Herzog C, Mulvihill DM, Nguyen SA, Savino G, et al. 2008. Pediatric cardiovascular CT angiography: Radiation dose reduction using automatic anatomic tube current modulation. Am J Roentgenol. 190(5): 1232-40.

34. Staniszewska MA, Obrzut M, Rybka K. 2005. Phantom studies for possible dose reduction in CT head procedures. Radiat Prot Dosim. 114(1–3): 326–31. Radiat Prot Dosimtry. 114:326-31.

35. Michel M, Jacob S, Roger G, Pelosse B, Laurier D, et al. 2012. Eye lens radiation exposure and repeated head CT scans: A problem to keep in mind. Eur J Radiol. 81(8): 1896-900.

36. Kim JH, Kim MJ, Kim HY, Lee MJ. 2014.Radiation dose reduction and image quality in pediatric abdominal CT with kVp and mAs modulation and an iterative reconstruction technique. Clin Imaging 38(5): 710-4.

37. Schindera ST, Nelson RC, Mukundan S, Paulson EK, Jaffe TA, Miller CM, et al. 2008. Hypervascular liver tumors: Low tube voltage, high tube current multi-detector row CT for enhanced detection-Phantom study. Radiology 246(1):125-32.

38. Cheng PM, Vachon LA, Duddalwar VA. 2013. Automated pediatric abdominal effective diameter measurements versus age-predicted body size for normalization of CT dose. J Digit Imaging 26(6): 1151-5.

39. Siegel MJ, Hildebolt C, Bradley D. 2013. Effects of automated kilovoltage selection technology on contrast-enhanced pediatric CT and CT angiography. Radiology 268(2): 538-47.

40. Eller A, Wuest W, Scharf M, Brand M, et al. 2013. Attenuation-based automatic kilovolt (kV)-selection in computed tomography of the chest: Effects on radiation exposure and image quality. Eur J Radiol. 82(12): 2386-91.

41. Hwang HJ, Seo JB, Lee HJ, Lee SM, Kim EY, Oh SY, et al. 2013. Low-dose chest computed tomography with sinogram-affirmed iterative reconstruction, iterative reconstruction in image space, and filtered back projection: studies on image quality. J Comput Assist Tomogr. 37(4): 610-7.

42. Lee SH, Kim MJ, Yoon CS, Lee MJ. 2012.Radiation dose reduction with the adaptive statistical iterative reconstruction (ASIR) technique for chest CT in children: An intra-individual comparison. Eur J Radiol. 81(9): e938-43.

43. Singh S, Kalra MK, Moore MA, Shailam R, et al. 2009. Dose reduction and compliance with pediatric CT protocols adapted to patient size, clinical indication, and number of prior studies. Radiology 252(1): 200-8.

44. Chapman T, Swanson JO, Phillips GS, Parisi MT, et al. 2013. Pediatric chest CT radiation dose reduction: Protocol refinement based on noise injection for pulmonary nodule detection accuracy. Clin Imaging 37(2): 334-41.

45. Cheng PM. 2013.Automated estimation of abdominal effective diameter for body size normalization of CT dose. J Digit Imaging 26(3): 406-11.

46. Tack D, Kalra Mk, Gevenois PA. Radiation Dose from Multidetector CT. 2nd ed. New York: Springer Heidelberg; 2012.

47. Sodickson A. 2012. Strategies for reducing radiation exposure in multi-detector row CT. Radiol Clin N Am. 50: 1-14.

48. McCollough CH, Bruesewitz MR, Kofler JM. 2006. CT dose reduction and dose management tools: Overview of available options. Radiographics 26(6): 503-12.

49. McCollough CH, Primak AN, Braun N, Kofler J, et al. 2009. Strategies for reducing radiation dose in CT. Radiol Clni N Am. 47(1): 27-40.

50. Angel E, Yaghmai N, Jude CM, DeMarco JJ, et al. 2009. Dose to radiosensitive organs during routine chest CT: Effects of tube current modulation. Am J Roentgenol. 193(5): 1340-5.

51. Sorantin E, Weissensteiner S, Hasenburger G, Riccabona M. 2013. CT in children-dose protection and general considerations when planning a CT in a child. Eur J Radiol. 82(7): 1043-9.

52. Roch P, Aubert B. 2013.French diagnostic reference levels in diagnostic radiology, computed tomography and nuclear medicine: 2004-2008 review. Radiat Prot Dosimetry 154(1): 52-75.

53. Paterson A, Frush DP. 2007. Dose reduction in paediatric MDCT: General principles. Clin Radiol. 62(6): 507-17.

54. Arch ME, Frush DP. 2008. Pediatric body MDCT: A 5-year follow-up survey of scanning parameters used by pediatric radiologists. Am J Roentgenol. 191(2): 611-7.

Chapter 4

Evaluation of the devised optimal paediatric routine CT scanning protocol

4.1 Introduction

This chapter evaluates selected protocols from the devised optimised protocols based on the outcomes of Chapters 2 and 3 through the use of an anthropomorphic paediatric phantom to confirm the feasibility of the devised protocols. In addition, other relevant scanning parameters not given in the Chapter 3 were also evaluated so as to further refine the protocols.

4.2 Material and methods

4.2.1 CT scanning details

A phantom-based optimisation was carried out using a paediatric anthropomorphic phantom (PBU-70B, Kyoto Kagaku, Japan) representing a five-year-old child (weight = 20 kg; height = 105 cm). This full-body anthropomorphic phantom, with a state of art synthetic skeleton, lungs, liver, mediastinum and kidneys, has a Hounsfield unit (HU) value that corresponds to the human tissue (Figure 4.1).

Initially, three anthropomorphic phantoms of neonate, 5 year and 10 year old reference children size were recommended. However, in this study, only a 5-year-old (16 cm effective diameter) paediatric phantom was used for the following reasons: First, these kinds of state-of-the-art anthropomorphic phantoms are quite expensive and it is impractical to have them for a single study. Second, our retrospective data shows that the 5-year-old phantom could cover a wide range of body size age between 5 and 10 years. Third, the phantom represents the middle age of children with most of the body organs taking their normal shape and contains fairly enough protein matrix and fat that are crucial in image formation. This empirical study evaluated the devised optimised protocols for 5-year-old (16-cm effective diameter) patients presented in Chapter 3. The feasibility of the optimised protocols devised

based on the previous literature review (Chapter 2) and retrospective study (Chapter 3) for other patient types presented in Tables 3.8-3.10 would be warranted when the empirical data in this chapter supported the use of the protocols for 5-year-old patients from Chapter 3.

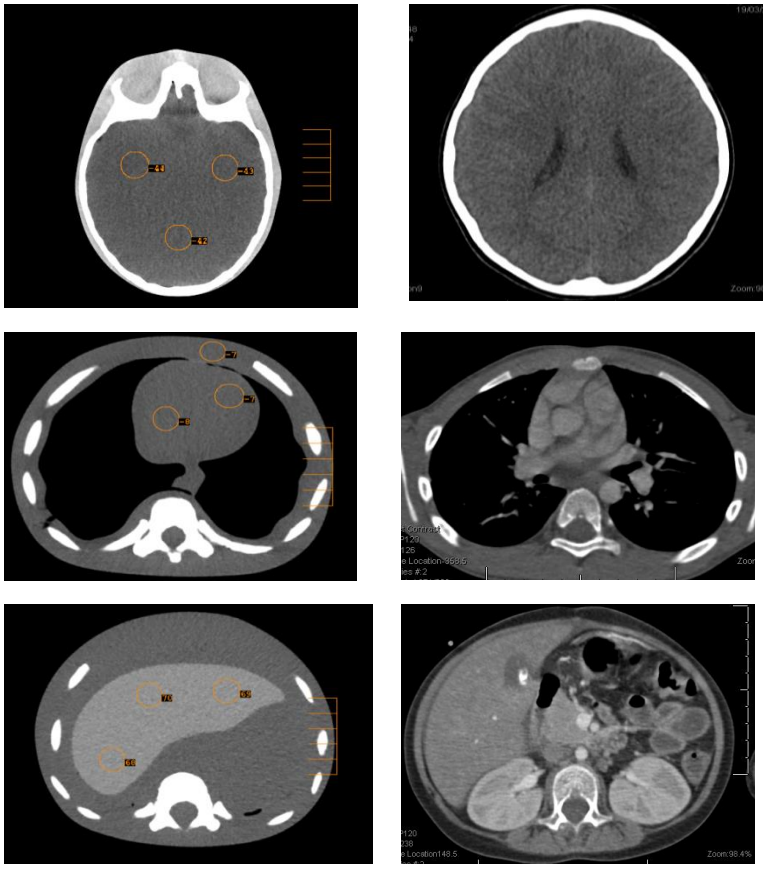

Figure 4.1. Anthropomorphic phantom of brain, chest and abdomen that corresponds to the human tissue. Sample of the reference CT brain 5 years 120 kV 250 mAs $CTDI_{vol}$ 37 mGy, Chest 120 kV, mAs 45 $CTDI_{vol}$ 4.4 mGy and Abdomen 120 kV 85 mAs $CTDI_{vol}$ 5.7 mGy

The whole study used the same CT scanners, as was done in the previous chapter of the retrospective review: three scanners: a 128-MDCT scanner (SOMATOM Definition Flash, Siemens Healthcare Germany); 64-MDCT scanner (SOMATOM Definition AS, Siemens Healthcare Germany) and 64-MDCT scanner (iDose^4 care Brilliance, Phillips Healthcare Netherlands).

All the MDCT scanners used in this study were subject to a regular and ongoing quality assurance program handled by in house medical physicist. Nevertheless, a test was conducted for each CT scanner by rescanning the phantom with the same parameters, and the dose reading, image noise measured and overall subjective image quality score determined by a radiologist were compared. No discrepancies were found.

The phantom was scanned with the devised protocols for 5-year-old (16-cm effective diameter) patients by the following CT scanners: Siemens SA 64-MDCT brain (n=15), chest (n=4) and abdomen (n=4); Phillips Brilliance 64 MDCT brain (n=8), chest (n=4), abdomen (n=3) and Siemens Flash 128-MDCT brain (n=15), chest (n=8) and abdomen (n=4). n is the number of protocols. More reduction in both tube voltage and tube current from the devised protocols obtained in Chapter 3 were manipulated to enforce further optimisation of the recommended protocols. Other factors such as axial versus helical, spiral pitch factors, scan field of view (S_FOV), scan time, tube current modulation (TCM) and gantry off-centre were assessed in each anatomical area. Also, the scanner specific performance was assessed whether the devised protocols could interchange between Philips and Siemens 64-MDCT scanners. Tube current in terms of mAs was manipulated in steps, while other parameters were kept constant. Similarly, the tube voltage setting (80-120 kV) was acquired. The tube current modulation was applied based on the specific manufacturers and compared with the scans obtained by the manual setting. Each acquired protocols were reconstructed with different reconstruction slice thicknesses, filtered back projection (FBP) and iterative reconstruction (IR) techniques. To maximise and guarantee the effectiveness of the optimisation protocols, practices such as off-centre of patients within the gantry were tested. The phantom was off-centred both above and below the patient plane. The image noise and $CTDI_{vol}$ were assessed to determine the influence of patient's isocentre to the image quality and patient radiation dose. Finally, a total of 81 (Tables 4.5-4.10) series were obtained and 65 (Tables 4.5-4.9) series were further assessed subjectively and objectively.

A reference protocol of each anatomical area was obtained to compare the image quality, radiation dose and the acquisition parameters with the devised protocols. The reference protocols were derived from those standard protocols used by the participated centres in the retrospective analysis. The image quality obtained by the

reference protocols was characterised with less image noise, no artefacts and excellent image quality. A radiologist assessed the image quality for each area to determine the reference protocols for phantom scanning. Images were presented to the observer in random order. Table 4.1 lists these reference protocols as designed by the radiologist.

Table 4.1 Reference protocols used in brain, chest and abdomen CT scans

P	kV	mAs	Time	ST	Pitch	$CTDI_{vol}$	DLP	TCM	RA	SM
					Brain					
1.1	120	300	1	3		54	832	ON	IR	Axial
1.2	120	300	1	3		54	832	ON	FBP	Axial
					Chest					
2.1	120	120	0.75	2	0.6	8	201	ON	IR	Helical
2.2	120	120	0.75	2	0.6	8	201	ON	FBP	Helical
					Abdomen					
3.1	120	150	0.5	2	0.6	7.8	170	ON	IR	Helical
3.2	120	150	0.5	2	0.6	7.8	170	ON	FBP	Helical

P: protocol, ST: slice thickness, SM-scanning mode, TCM: tube current modulation, $CTDI_{vol}$, volume CT dose index, DLP: dose length product, TCM: tube current modulation, RA: Reconstruction algorithm, IR: iterative reconstruction, FBP: filter back projection

4.2.2 Qualitative assessment of image quality

Two radiologists, with more than ten years of experience in CT imaging have independently reviewed the images to determine the image quality in terms of image noise, artefacts, visualisation of structures and image quality confidence. These image quality criteria were modified from previous studies [1-5] and the European Guidelines on Quality Criteria for Computerised Tomography [6].

Subjective assessment of image quality was graded for anatomical structures including cerebrum, cerebellum and skull base for brain CT; thoracic wall, thoracic aorta, vena cava, heart and lung parenchyma for chest CT; and diaphragm, liver, spleen, pancreas, kidneys, abdominal aorta, common iliac arteries and abdominal wall for abdomen CT on a 4-point Likert scale as follows: (1) Image noise: 1 = less noise, 2 = average noise, 3 = above average noise and 4 = significant noise; (2) Beam hardening and streak artefacts: 1 = no artefacts, 2 = moderate artefacts, 3 =

pronounced artefacts interfering with image details but with acceptable quality, and 4 = unacceptable artefacts obscuring image details and not diagnostic; (3) Visibility of structures: 1 = excellent, 2 = good, 3 = acceptable and 4 = unacceptable; and (4) Overall image quality confidence: 1 = highly acceptable, 2 = acceptable, 3 = probably acceptable and 4 = unacceptable.

The radiologists were informed of the series of studies that needed to be reviewed, but unaware of acquisition parameters. The agreement of two radiologists was assessed using inter-rater agreement weighted by Kappa coefficient statistic [2].

4.2.3 Quantitative assessment of image quality

Objective (quantitative) image quality analysis was performed using Analyze Direct V 12.0 software (Analyze Direct, Inc., Lexana, KS, USA).

Image noise was assessed by measuring the mean standard deviation (SD) of the Hounsfield unit (HU) of specific regions of interest (ROIs). Since noise is the SD of the pixel HU of the selected ROIs, changing the pixel number within ROIs could affect the subsequent SD value, hence a constant size and location for ROIs, approximately 2cm² (5270 pixels) was used for all of the measurements [2, 7].

The locations of ROIs were adjusted in conjunction with other phantom studies [7-10]. For abdomen, five ROIs were localised in the middle and periphery of the liver. The rationale for selecting liver is that it is a significant organ that is prone to many diseases and is homogenous in nature. For the chest, 6 ROIs were localised at the apex (two at anterior muscles and four at the posterior muscles) and three ROIs at the base of the heart, by the left and right ventricles, as they are the most homogenous large muscles in the mediastinum. For the brain, three ROIs were localised in the base of the skull brain tissue and 5 ROIs were above the superior orbital margin brain tissues. The placement of these ROIs was consistent in all images of each examination. Finally, the window level and window width of the soft tissue, lung and bone were adjusted, which were consistent with the clinical use for viewing abdominal and chest CT.

4.2.4 Radiation dose assessment

The radiation dose which was described as the volume CT dose index ($CTDI_{vol}$) to quantify the radiation output from a CT examination consists of multiple contiguous CT scans [11-15]. The output $CTDI_{vol}$ and dose length product (DLP) obtained in this phantom study in conjunction with findings in Chapters 2 and 3 were further used to quantify the upper limit of each devised protocols for each specific age and body size groups.

4.2.5 Statistical analysis

Data were entered into SPSS 22.0 for statistical analysis. Continuous variables were presented as mean ± standard deviation, while categorical variables were shown in percentage of frequency. Subjective image analysis was assessed using inter-rater agreement weight kappa (k) coefficients, percentage of agreement and 95% confidence intervals (CI). Interpretation of inter-observer agreement levels was classified based on the k values scaled as following: poor=0-0.2; fair=0.21-0.4; moderate=0.41-0.6; good=0.61-0.8; and excellent=0.81-1.0 [2]. A *p* value less than 0.05 is considered statistically significant.

4.3 Results

A total of 81 CT scan series were acquired from an anthropomorphic phantom involving the application of devised paediatric acquisition parameters consisting of brain (*n*=38), chest (*n*=16) and abdomen (*n*=11) (Tables 4.5-4.9). In addition, a series of scans (n=16) were acquired to assess the influence of acquisition parameters on both the image quality and radiation dose.

Inter observer reliability was assessed using Cohen's kappa (k) weighting statistics as shown in (Tables 4.2-4.4): with good agreement in image noise; moderate agreement in artefacts; poor agreement in visualisation of structures and good agreement in overall image quality.

4.3.1 Brain CT protocols

Of these protocols, 49% (40/81) scan series were for brain scans. Tables 4.5 and 4.6 summarise the acquisition parameters, dose readings, objective image quality assessment in terms of noise (SD) and the subjective image quality evaluation among the two CT manufacturers. Results showed that the series scan 4 obtained with 120 kV and 150 mAs using 64-MDCT Siemens scanner produced substantial reduction of $CTDI_{vol}$, which leads to 50% reduction compared to the reference protocol, while still achieving diagnostic image quality. Further, the series scan 5 with 80 mAs yielded 72% reduction in $CTDI_{vol}$ while preserving the image quality (Table 4.5, series scan5) and (Figure 4.2). In contrast, the same protocol used in the series scan 4 was scanned with Phillips 64-MDCT (series-2), and results showed reduction of 63% in $CTDI_{vol}$ but leading to degradation of image quality by increasing 2 folds of SD in both brain tissues at the base of skull. The 120 kV was found to be an ideal tube voltage for all the brain protocols with tube current ranging from 80 mAs to 150 mAs, and the overall $CTDI_{vol}$ dose output ranging between 14 mGy and 22 mGy $CTDI_{vol}$ Figure. 4.2.

Furthermore, in comparison with the reference protocol, a tube voltage of 100 kV and tube current of 250 and 150 mAs demonstrated 61% and 69% dose reduction and optimal image quality, respectively as shown in Table 4.5 (series scans 6&8) and (Figure 4.3). Similarly, the use of TCM was shown to result in extensive lower radiation dose while image quality was still preserved (Table 4.5 series scans 3, 6 &7). However, the series scan 11 led to degraded image quality by using 100 kV and TCM technique with low reference mAs.

In general, the image quality obtained by 100 kV with corresponding $CTDI_{vol}$ and mean pixel SD values ranged 13-22 mGy and 2.5-5 SD, respectively were found to be acceptable based on subjective assessment, except for the images acquired by Phillips Healthcare 64-MDCT. The results obtained by Siemens were consistent with clinical acquisition protocols obtained from retrospective data analysis (centre D) as shown in Chapter 3 (Figure 4.4).

Table 4.6 lists the various scan series with same protocols but different reconstruction algorithms. The use of IR technique shows improvement in both objective and subjective image quality compared to the FBP reconstruction.

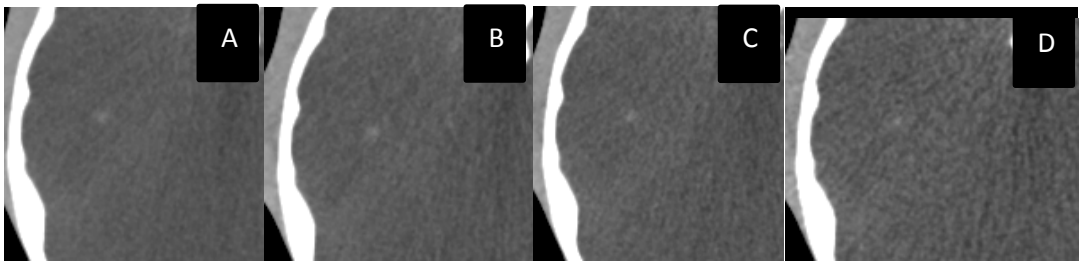

Figure 4.2 Images A-D obtained with fixed 120 kV, slice thickness 3mm, IR SAFIRE/3 and various eff-mAs as following: image A 300 eff-mAs , $CTDI_{vol}$ 54 mGy; image B 200 eff-mAs $CTDI_{vol}$ 37 mGy; image C 150 eff-mAs, $CTDI_{vol}$ 27 mGy and image D 80 eff-mAs, $CTDI_{vol}$ 14 mGy. Note: 73% reduction of the tube current in image D resulted in almost 4 folds decreasing dose without degrading the image quality.

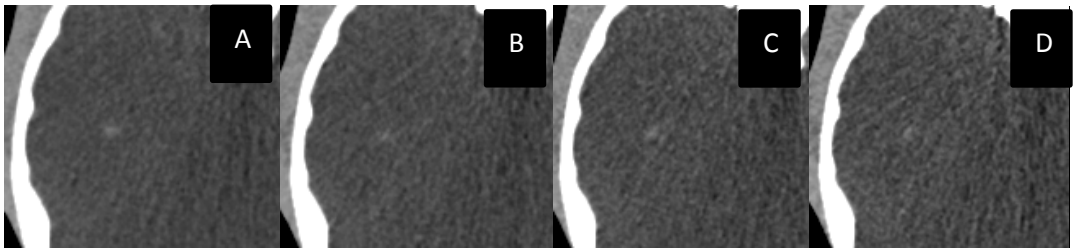

Figure 4.3 Images A-D obtained with fixed 100kV, slice thickness 3, IR SAFIRE/3 and various tube current as following: image A 200 eff-mAs, $CTDI_{vol}$ 22mGy; image B 150 eff-mAs, $CTDI_{vol}$ 16 mGy; image C 100 eff-mAs, $CTDI_{vol}$ 11 mGy and image D 80 eff-mAs, $CTDI_{vol}$ 9 mGy. Images A-C demonstrate substantial reduction of radiation dose, yet preserve the visualisation of small structures. However, image D demonstrates degrading of image details of the brain tissues and the focal hyper-dense area of the bone

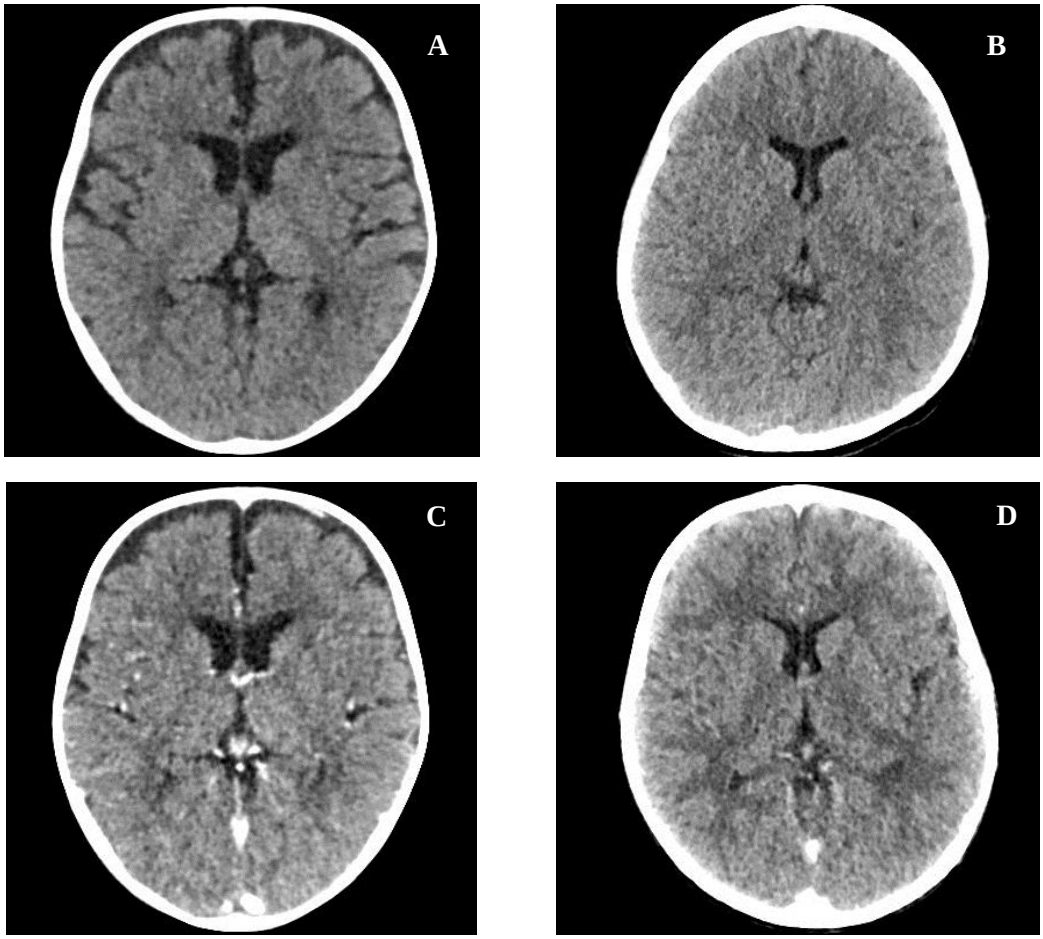

Figure 4.4 Images A&B for 5 year old child pre-contrast brain obtained by 100kV, 260 mAs TCM, $CTDI_{vol}$ 16 mGy, slice thickness 3mm and reconstructed by IR J30S/3 whereas image C&D post-contrast acquired by 80kV, 260mAs TCM, $CTDI_{vol}$ 13mGy, slice thickness 3 mm and IR J30s/3 (Siemens Healthcare 64 MDCT). Brain tissues, ventricles are clearly visualised in plain images. Also, the 80kV post-contrast images demonstrate optimum image quality

Table 4.2 Cohen's kappa for CT brain scans

Characteristic	Observed kappa (k)	P value	Interpretation
Image noise	0.651	0.002	Good
Artifacts	0.545	0.004	Moderate
Visualisation of the structures	0.105	0.212	Poor
Overall image quality confidence	0.651	0.023	Good

Table 4.3 Cohen's kappa for CT chest scans

Characteristic	Observed kappa (k)	P value	Interpretation
Image noise	0.651	0.001	Good
Artifacts	0.545	0.004	Moderate
Visualisation of the structures	0.167	0.111	Poor
Overall image quality confidence	0.621	0.000	Good

Table 4.4 Cohen's kappa for CT abdomen scans

Characteristic	Observed kappa (k)	P value	Interpretation
Image noise	0.651	0.001	Good
Artifacts	0.545	0.004	Moderate
Visualisation of the structures	0.167	0.111	Poor
Overall image quality confidence	0.621	0.000	Good

Table 4.5 Image quality assessment for CT brain scans– Part 1

	Acquisition parameters						Dose reading		Objectives image analysis (noise SD)		Subjective image analysis							
P	kV	mAs	ST (mm)	T *(s)*	Pitch	TCM	$CTDI_{vol}$ mGy	DLP mGy cm			Noise		Artefacts		Structures		Image Quality		Scanner
							%*	%*	BS	BT	R1	R2	R1	R2	R1	R2	R1	R2	
RP	120	300	3	1	Ax	OFF	54	832	3	2	1	1	1	1	3	2	2	2	Siemens 64
1	120	250	3	0.75	0.6	OFF	33(39)	620(25)	4(25)	3(33)	2	2	2	2	3	2	3	2	IR/Phillips 64
2	120	150	2.5	0.75	Ax	OFF	20(63)	250(70)	6(50)	5(60)	3	3	3	3	3	3	3	3	IR/Phillips 64
3	120	136	3	1	0.8	201	22(59)	346(58)	4(25)	3(33)	1	2	1	2	3	2	2	2	IR/Siemens 64
4	120	150	3	1	Ax	OFF	27(50)	418(50)	4(25)	3(33)	1	2	1	2	2	1	1	1	IR/Siemens 64
5	120	80	3	1	Ax	OFF	15(72)	221(73)	5(40)	4(46)	1	1	1	2	3	2	2	2	IR/Siemens 64
6	100	250	3	0.75	0.4	ON	21(61)	343(57)	4(25)	3(33)	2	2	2	2	3	2	3	2	IR/Phillips 64
7	100	132	3	1	0.8	201	13(76)	204(76)	5(40)	4(46)	2	2	2	2	3	2	2	2	IR/Siemens 64
8	100	150	3	1	Ax	OFF	17(69)	253(70)	5(40)	4(46)	2	2	2	2	3	2	2	2	IR/Siemens 64
9	100	120	3	1	Ax	OFF	13(76)	176(79)	5(40)	5(60)	2	2	2	2	3	2	2	2	IR/Siemens 128
10	100	100	3	1	Ax	OFF	11(80)	168(80)	6(50)	5(60)	2	2	2	2	3	2	2	3	IR/Siemens 64
11	100	100	3	1	Ax	ON	7(87)	109(87)	8(63)	7(60)	3	2	3	3	3	2	3	3	IR/Siemens 64
12	100	100	3	1	Ax	OFF	11(79)	147(82)	7(57)	6(60)	2	2	2	2	3	2	2	2	IR/Siemens 128

P: protocol, ST: slice thickness, TCM: tube current modulation, $CTDI_{vol}$, volume CT dose index, DLP: dose length product, SD: standard deviation of noise, BS: base of the skull, BT: brain tissue, %* reduction in percentage in corresponding to the reference protocol values, RP: reference protocol, R1: reader 1, R2: reader 2, Ax: axial mode, IR: iterative reconstruction.

Note:

Numbers in parentheses are percentages in compared to the reference protocols, and the percentages were rounded

All presented series obtained with iterative reconstruction and from three different scanners. For the same protocols, DLP might not be the same because of the variation of scanner designs.

Table 4.6 Image quality assessment for CT brain scans– Part 2

	Acquisition parameters						Dose reading		Objective image analysis (noise SD)		Subjective image analysis								
P	kV	mAs	ST mm	T (s)	Pitch	TCM	$CTDI_{Vol}$ mGy	DLP mGy cm			Noise		Artefacts		Structures		Image quality		Scanner
							%*	%*	BS	BT	R1	R2	R1	R2	R1	R2	R1	R2	
RP	120	300	3	1	Ax	OFF	54	832	3	2	1	1	1	1	2	2	1	1	IR/Siemens
13	120	200	3	1	Ax	OFF	37(32)	338(59)	5(40)	4(50)	2	2	3	2	3	2	2	2	FB/Siemens
14	120	200	3	1	Ax	OFF	37(37)	338(59)	4(25)	3(33)	1	1	3	2	3	2	2	1	IR/Siemens
15	120	150	3	1	Ax	OFF	27(50)	418(50)	7(57)	5(60)	2	2	3	2	3	3	3	2	FB/Siemens
16	120	150	3	1	Ax	OFF	27(50)	418(50)	5(40)	3(33)	2	1	2	2	3	2	2	2	IR/Siemens
17	120	250	3	0.75	0.6	OFF	33(39)	620(26)	8(62)	4(25)	2	3	2	3	3	3	3	3	FB/Phillips
18	120	250	3	0.75	0.6	OFF	33(39)	620(26)	5(40)	3(33)	1	2	2	2	2	2	2	2	IR/ Phillips
19	100	150	3	1	Ax	OFF	17(69)	253(70)	7(57)	6(60)	3	3	3	3	3	3	3	3	FB/Siemens
20	100	150	3	1	Ax	OFF	17(69)	253(70)	5(40)	4(25)	2	2	2	2	3	2	2	2	IR/Siemens
21	100	100	3	1	Ax	OFF	11(80)	168(80)	7(57)	6(67)	3	2	2	2	3	2	3	2	FB/Siemens
22	100	100	3	1	Ax	OFF	11(80)	168(80)	6(50)	5(60)	2	2	2	2	3	3	3	2	IR/Siemens
23	100	250	3	0.75	0.6	OFF	20(63)	343(59	6(50)	5(60)	2	3	3	3	3	3	3	3	FB/ Phillips
24	100	250	3	0.75	0.6	OFF	20(63)	343(59)	5(57)	4(50)	2	2	2	3	3	3	2	3	IR/ Phillips

P: protocol, ST: slice thickness, TCM: tube current modulation, $CTDI_{vol}$, volume CT dose index, DLP: dose length product, SD: standard deviation of noise, Bas: base of the skull, Bra: brain tissue, %* reduction in percentage in corresponding to the reference protocol values, RP: reference protocol, R1: reader 1, R2: reader 2, Ax: axial mode.
Note: numbers in parentheses are percentages, and the percentages were rounded

4.3.2 Chest CT protocols

Table 4.7 demonstrates 9 scan series obtained with the devised acquisition protocols corresponding to the $CTDI_{vol}$ and image quality analysis. The scan series acquired with 120 kV with effective mAs of 45 and 32 were found to substantially decrease $CTDI_{vol}$ by 56% and 68% respectively, while diagnostic image quality was preserved. Further, the use of 100 kV with TCM (scan series 3, 5 & 6) led to reduction in CT dose, yet maintaining image quality as following: series scan 3, 81%; series scan 4, 72%. Likewise, the protocols using 80 kV with TCM resulted in decreasing $CTDI_{vol}$ up to 81%, still producing acceptable image quality (Table 4.7 scan series 8 & 9).

It should be noted that scan series 5 and 6 showed similar findings of both $CTDI_{vol}$ and image quality obtained from the same protocol in both Philips and Siemens 64 MDCT scanners. Thus, this indicates the possible interchange protocols between manufacturers despite using different scan mode.

In summary, $CTDI_{vol}$ and DLP of the devised protocols were significantly lower than those of reference protocols, yet generating similar image quality. The radiation dose ranged 1.3 to 2.2 mGy (measured with 32 cm reference CTDI phantom) when images were acquired with tube voltage of 80 kV and 100 kV resulting in higher image noise at the lungs apex, while the noise index was preserved at the base of the heart.

4.3.3 Abdomen CT protocols

Abdomen scanning protocols were to some extent similar to the chest. In general, images acquired with the protocol of 100 kV with the radiation exposure ranging between 2 and 3 mGy (measured with 32 cm reference CTDI phantom) was acceptable according to objective and subjective assessment of image quality. Use of tube current modulation and iterative reconstruction was found to lower the exposure dose while preserving the image quality.

Table 4.7 Image quality assessment for CT chest scans

P	Acquisition parameters						Dose readings		Objective image analysis (noise SD)		Subjective image analysis								Scanner
	kV	mAs	ST mm	T (s)	pitch	TCM	$CTDI_{vol}$ mGy	DLP mGy cm			Noise		Artefacts		Structures		Image quality		
							%*	%*	App	Hat	R1	R2	R1	R2	R1	R2	R1	R2	
RP	120	121	2	0.7	0.7	ON	7.8	201	6	4	2	2	2	2	2	2	2	2	Phillips 64
1	120	45	2	0.5	0.6	OFF	3.4(56)	78(61)	8	5	2	2	3	2	2	2	3	2	Siemens 64
2	120	32	2	0.5	0.6	125	2.5(68)	57(71)	9	6	2	2	2	2	2	3	2	3	Siemens 64
3	100	97	1	0.28	0.6	100	1.5(81)	31(85)	12	8	2	2	2	2	3	2	2	2	Siemens 128
4	100	60	2	0.5	1.2	OFF	2.7(65)	60(70)	8	5	2	2	2	2	2	2	2	2	Siemens 64
5	100	56	2	0.75	0.7	ON	2.2(72)	60(70)	9	7	2	2	2	2	2	2	2	2	Phillips 64
6	100	49	2	0.5	0.6	200	2(74)	67(67)	9	6	2	2	2	2	3	2	2	2	Siemens 64
7	100	31	1	0.5	0.6	125	1.4(82)	31(72)	11	9	3	2	2	2	3	3	2	3	Siemens 64
8	80	102	1	0.28	3	202	1.6(80)	40(80)	11	7	2	2	2	2	2	2	2	2	Siemens 128
9	80	95	1	0.28	0.6	182	1.5(81)	30(85)	10	7	2	2	2	2	3	2	2	2	Siemens 128

P: protocol, ST: slice thickness, TCM: tube current modulation, $CTDI_{vol}$, volume CT dose index, DLP: dose length product, SD: standard deviation of noise,%* reduction in percentage in corresponding to the reference protocol values App: lungs apex, Hat: heart , R1: reader 1, R2: reader 2, RP: reference protocol
Note: numbers in parentheses are percentages, and the percentages were rounded

Table 4.8 Image quality assessment for CT Abdomen scans – Part 1

P	Acquisition parameters						Dose readings		Object image analysis		Subjective image analysis								Scanner
	kV	mAs	ST mm	T (s)	Pitch	TCM	$CTDI_{vol}$ mGy	DLP mGy cm			Noise		Artefacts		Structures		Image quality		
							%*	%*	Liv	Pel	R1	R2	R1	R2	R1	R2	R1	R2	
RP	120	121	2	0.7	0.7	ON	7	218	6	4	2	2	2	2	2	2	2	2	Phillips 64
1	80	83	3	0.5	0.6	449	1.5(81)	41(81)	9	6	3	2	3	2	3	2	3	2	Siemens 128
2	100	70	2	0.8	0.6	OFF	2.3(71)	80(63)	10	8	2	2	2	2	2	2	2	2	Phillips 64
3	100	49	2	0.5	0.6	250	2(74)	67(69)	9	8	2	2	2	2	3	2	2	2	Siemens 64
4	120	52	2	0.5	0.6	250	4(49)	122(44)	7	6	2	2	2	2	3	3	2	2	Siemens 64

P: protocol, ST: slice thickness, TCM: tube current modulation, $CTDI_{vol}$, volume CT dose index, DLP: dose length product, SD: standard deviation of noise, Liv: liver tissue, Pel: pelvis, *reference protocol, R1: reader 1, R2: reader 2, RP: reference protocol

Note:

numbers in parentheses are percentages in compared to the reference protocols, and the percentages were rounded

all presented series obtained with iterative reconstruction

Table 4.9 Image quality assessment for CT abdomen scans– part 2

P	Acquisition parameters						Dose readings		Object image analysis		Subjective image analysis								Scanner
	kV	mAs	ST mm	T (s)	Pitch	TCM	$CTDI_{vol}$ mGy	DLP mGy cm			Noise		Artefacts		Structures		Image quality		
							%*	%*	Liv	Pel	R1	R2	R1	R2	R1	R2	R1	R2	
RP	120	121	2	0.7	0.7	ON	7	218	6	4	2	2	2	2	2	2	2	2	Phillips 64
1	80	82	2	0.5	1.3	449	1.4	40	14	14	3	3	2	2	2	2	2	3	Siemens 128
2	80	83	2	0.5	1.3	449	1.4	40	11	10	2	2	2	2	2	2	2	2	Siemens 128
3	100	60	2	0.75	0.9	OFF	2.3	80	14	11	3	3	2	2	2	2	3	3	Phillips 64
4	100	60	2	0.75	0.6	OFF	2.3	80	10	9	2	2	2	2	2	2	2	2	Phillips 64

P: protocol, ST: slice thickness, TCM: tube current modulation, $CTDI_{vol}$, volume CT dose index, DLP: dose length product, SD: standard deviation of noise, Liv: liver tissue, Pel: pelvis, *reference protocol, R1: reader 1, R2: reader 2, RP: reference protocol

Note:

numbers in parentheses are percentages in compared to the reference protocols, and the percentages were rounded

4.3.4 Effect of pitch factor on image quality assessment

In regard to the influence of the spiral pitch values on both image quality and radiation dose, different pitch values of the two manufacturers produced different effects regarding the $CTDI_{vol}$ and DLP Table 4.10. Acquisition parameters with use of TCM obtained from the Siemens scanners showed increased $CTDI_{vol}$ and DLP (Table 4.10 scan series 4, 10 & 12) when high pitch values were used; whereas the Phillips scanner demonstrated increasing $CTDI_{vol}$ while DLP was decreased (Table 4.10 scan series 8). When the fixed tube current acquisition protocols were used, images acquired with the Siemens scanner showed a constant $CTDI_{vol}$ and slightly increasing DLP regardless of the pitch values (scan series 15-16). In contrast, images acquired with the Philips scanner resulted in increasing $CTDI_{vol}$ and decreasing DLP with use of high pitch values (scan series 1-2). Image noise was decreased in TCM protocols with use of high pitch value, whereas it was increased in high pitch values when fixed tube current protocols were used. On other hand, images obtained with the Siemens scanner were shown to increase SD by increasing pitch value and vice versa for the Philips scanner. Figure 4.5 shows the effect of high pitch factor with fixed tube current on the image quality. It is noted that the high pitch factor with fixed tube current deteriorates the image quality in terms of image noise and artefacts (Figure 4.5 Images A & B)

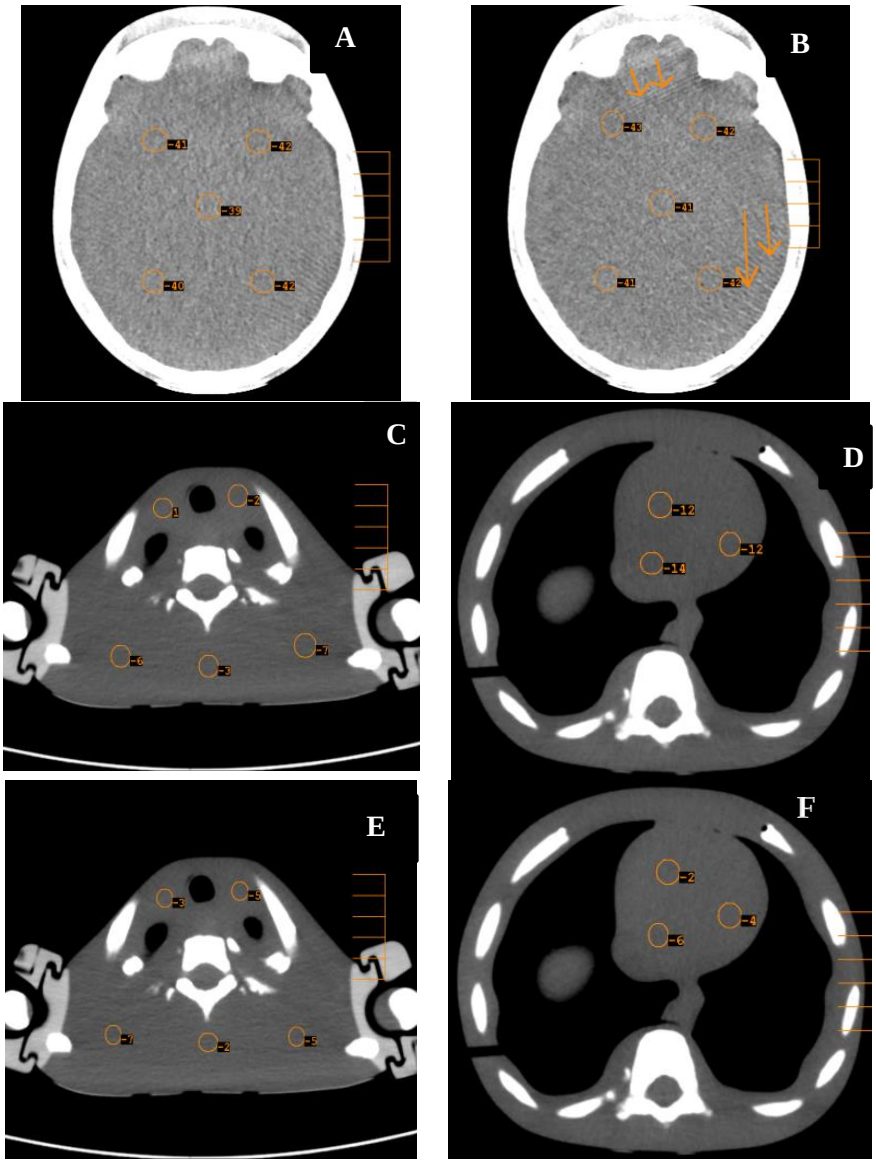

Figure 4.5 Image A 120 kV, 250 mAs P 0.579, time 0.5, Exp time 0.864 $CTDI_{vol}$ 32.3 mGy versus Image B acquired with the same protocols and pitch value 1.224 Exp time 0.613 resulted in high slightly high image noise, artefacts and $CTDI_{vol}$ 33.6 mGy.
Images C-F acquired with the same acquisition parameters except for the pitch values. Images C&D obtained with 0.6 pitch value whereas images D&F with 1.3 pitch value. Images D&F showed increasing of image noise particularly at lung apex areas. Note: increasing in streak artefacts with high pitch in image B (arrows).

Table 4.10 Influence of the spiral pitch factors on the image quality and radiation exposure ($CTDI_{vol}$)

P	kV	mAs	ST	S time	Ex time	Pitch	TCM	$CTDI_{vol}$	DLP	Scanner Specific
					Brain					
1	120	250	3	0.5	0.864	0.579	OFF	32	620	Phillips 64
2	120	250	3	0.75	0.613	1.224	OFF	34	601	Phillips 64
3	100	66	3	1	-	0.8	ON	6.54	102	Siemens 64
4	100	67	3	1	-	1.3	ON	6.76	109	Siemens 64
					Chest					
5	120	121	2	0.5	0.745	0.671	ON	7.8	202	Phillips 64
6	120	121	2	0.5	1.329	0.376	ON	7.9	217	Phillips 64
7	100	60	2	0.75	1.118	0.671	ON	2.2	60	Phillips 64
8	100	56	2	0.75	0.552	1.359	ON	2.3	56	Phillips 64
9	80	60	2	0.5	-	1.2	ON	1.17	26	Siemens 128
10	80	63	2	0.5	-	1.5	ON	1.23	28	Siemens128
11	80	94	1	0.28	-	0.6	ON	1.5	30	Siemens128
12	80	102	1	0.28	-	3	ON	1.61	40	Siemens128
					Abdomen					
13	100	60	2	0.5	-	0.6	OFF	2.7	60	Siemens 64
14	100	60	2	0.5	-	1.2	OFF	2.7	59	Siemens 64
15	80	60	2	0.5	-	0.6	OFF	0.94	21	Siemens 128
16	80	60	2	1	-	1.3	OFF	0.94	20	Siemens 128

ST: slice thickness, S time: scan time, Ex time: exposer time, $CTDI_{vol}$: volume CT dose index, DLP: dose length product

4.3.5 Scan time

Also, scan time showed fluctuation in resultant radiation dose and image quality; the shorter exposure time have slightly increased image noise and radiation exposure. Consequently, 0.75s-1s scan time is ideal for cooperative children.

4.3.6 Iterative reconstruction

In addition, iterative reconstruction was noted to significantly maintain image quality using low dose devised protocols (Tables 4.6 & 4.9). Image noise was found to be reduced to 50% with IR compared to FBP reconstruction technique. The effectiveness of the IR technique was significantly apparent in the brain and abdomen scans compared to the chest imaging. In low dose protocol of brain scans, beam hardening artefacts and mottled noise were suppressed using the Siemens IR sinogram-affirmed iterative reconstruction (SAFIRE) strength (3) technique Fig 4.7. Nevertheless, Figure 4.8 shows the drawback of exaggeration of the IR strength in very low dose protocols.

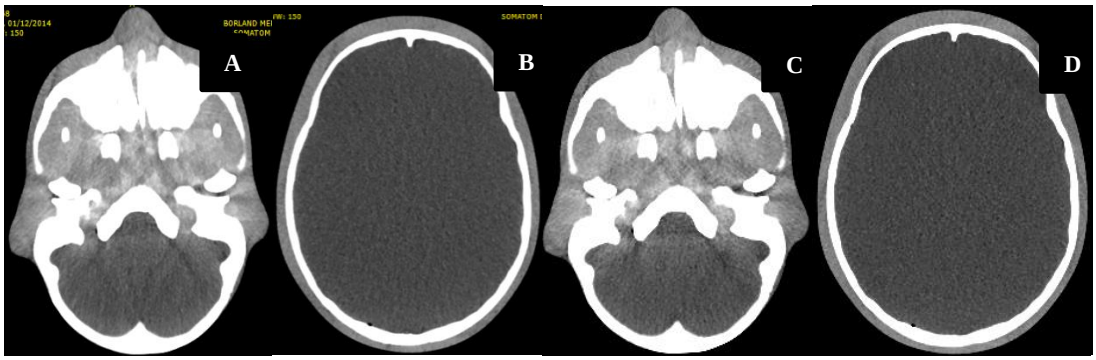

Figure 4.6 Images A&B obtained with 100kV, 308 reference Care dose TCM, Slice thickness 3mm, S-FOV 200mm and SD at the base of skull and brain tissue 5.3 and 3.5 respectively, whereas images C&D acquired with same parameters with S-FOV 300mm and SD at the base of the skull and soft tissue 6 and 4 respectively. Note: image noise increases with larger S-FOV.

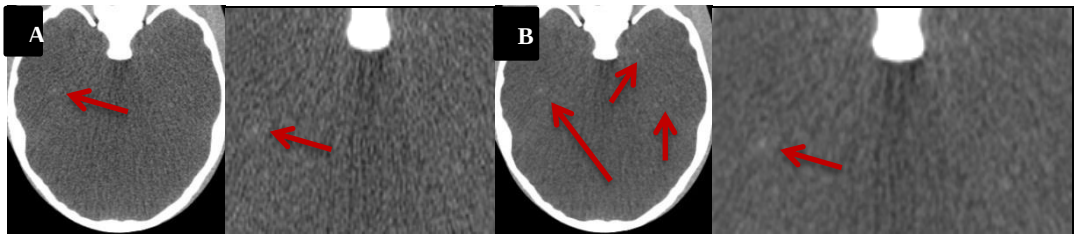

Figure 4.7 Low dose brain protocols obtained with 120 kV, 80 eff-mAs, slice thickness 3mm and $CTDI_{vol}$ 14 mGy. Image A reconstructed with SAFIRE strength 3, whereas image B constructed with filtered back projection (FBP). The image noises around the brain tissue are markedly decreased on IR image comparison with FBP. The fine structures (arrows) are clearly visible on the IR image, whereas on the FBP are unclear due to artefacts and quantum mottle.

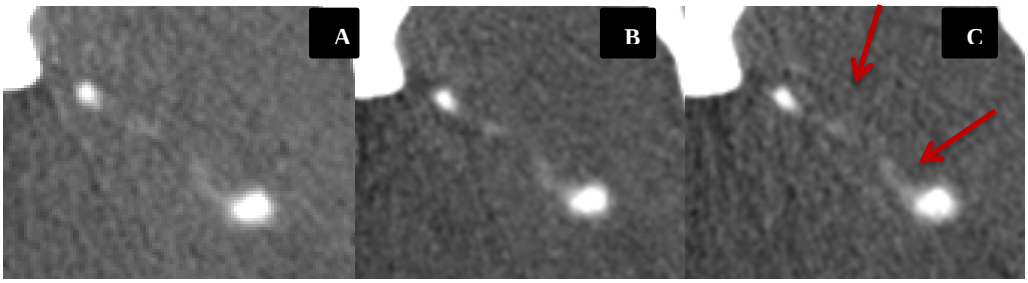

Figure 4.8 Images obtained with phantom show different exposure factor with iterative reconstruction as following. Image A obtained with 120 kV, 100 mAs, slice thickness, $CTDI_{vol}$ 16 mGy and SAFIRE-IR/3. Image B acquired with 100 kV, 150 mAs, $CTDI_{vol}$ 15 mGy and SAFIRE-IR/3 whereas image C acquired with 100 kV, 100 mAs, $CTDI_{vol}$ 12 mGy and SAFIRE IR/3. Image C illustrates changes in the brain tissue and corresponding to bone details compared to images A&B.

4.4 Discussion

Optimizing CT scan protocols essentially require knowledge of factors that influence the distribution of dose within patients and image quality during the diagnostic procedures. Paediatric CT protocols in particular are made up of a complex combination of many adjustable factors that must be tailored to the wide band of children body size. The approach used in this study is to validate the recommended optimisation protocols of CT brain, chest and abdomen based on the subjective perception of the radiologist's interpretation regarding the diagnostic image quality. This phantom study also provides insight into reproduction of clinical acquisition protocols where a broad variety of factors would have negatively influenced on the

image quality and radiation dose. In the following sections, discussion will be focused on these three individual scanning regions, brain, chest and abdomen.

4.4.1 Brain scanning protocols

Review of literature and the retrospective data analysis showed that the high dose of radiation was delivered in most of the brain studies as well as adult protocols were used in paediatrics CT imaging. Also, brain tissues are characterised with low subject contrast that would require precise adjustment of the acquisition parameters. Hence out of 81 scan series, 49% was dedicated to brain protocols.

The tube voltage is regarded as a core element in brain studies and if used wisely, it would reduce the radiation dose significantly, yet preserving diagnostic images. Children's body are characterised with lower fat, low bone density and smaller attenuation than adults, which naturally result in lower image noise [16]. Our phantom test showed a greater reduction of low dose of the devised protocols while image quality is maintained in Siemens's scanners. A standard tube voltage of 120 kV at tube current range between 80-150 effective mAs produce same image quality as that of reference protocol, yet noticeably decreasing $CTDI_{vol}$ up to 72%. The tube current value of 80 effective mAs was accepted for the given phantom size in Siemens 64 and 128 MDCT scanners Figure 4.2 (C). Furthermore, low tube voltage value of 100 kV with tube current-time product values about 100-250 effective mAs, and the $CTDI_{vol}$ of about 13-21 mGy was acceptable in most of the devised low dose protocols. Regardless of the application of the TCM or fixed tube current techniques, the obtained images with $CTDI_{vol}$ values about 13-17 mGy was subjectively acceptable in all protocols Figure 4.3.

On the other hand, 100 kV protocols obtained by the 64-MDCT Phillips scanner demonstrated an increase in image noise and artefacts. The phantom study reveals that brain protocols with tube dose output less than 27 mGy in this scanner were above average noise, with artefacts interfering with image quality, although the overall image quality was acceptable based on assessments.

The inconsistency of tube output between the scanners was within expectation due to the scanner specific parameters, particularly the tube geometry and detector

efficiency. Thus, findings would explain the reason that the high dose was observed in CT brain data in Chapter three acquired with the 64-MDCT Phillips scanner using 120 kV, the tube current-time product values about 250-400 effective mAs, resulting in the tube output "CTDI" about 20-60 mGy.

Among all of the brain protocols, axial acquisition brain protocols with TCM versus helical protocols showed significant reduction in $CTDI_{vol}$ and DLP Fig 4.9. Further reduction in radiation dose was achieved by tilting the gantry that reduces eye lens dose by as much as 87% [17]. In cooperative children particularly above 5 years old, employing the sequential protocol instead of helical would substantially lower the radiation dose, without compromising the diagnostic information. This technique also avoids the over-scanning dose that is usually a phenomenon observed only in helical scanning [18].

Overall, the phantom study indicates the feasibility of low brain CT techniques at 100 kV coupled with optimum tube current or TCM technique, proper slice thickness and wise application of the IR technique. The dose values reported in this study are low compared to those from phantom studies and clinical audits reported earlier [19-21]. In addition, the devised optimisation protocols showed average radiation dose reduction up to 70% compared to the reference protocols and the obtained data of the retrospective analysis. Although the use of 100kV for Phillips 64-MDCT scanner might not be able to obtain images with high quality (in terms of noise and artefacts), an acceptable image quality could still be expected based on the findings of the phantom.

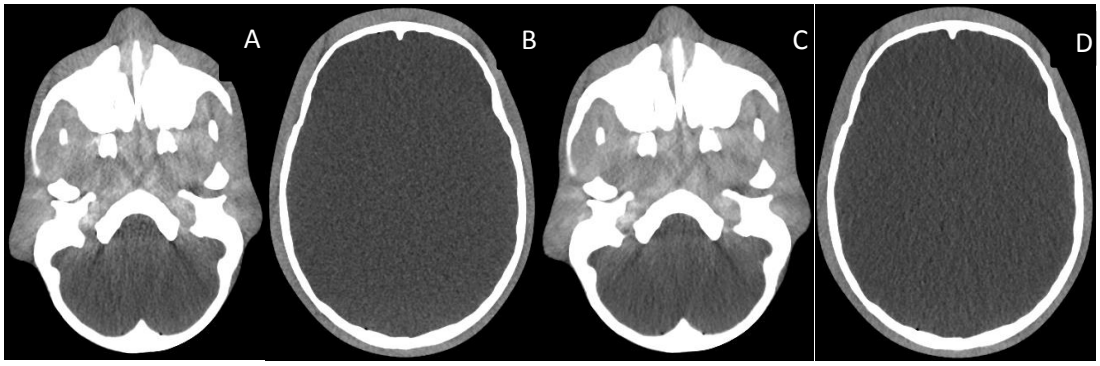

Figure 4.9 images A & B obtained with helical mode 100 kV, 201 mAs, slice thickness 3mm, TCM, iterative reconstruction strength 3, $CTDI_{vol}$ 20mGy, DLP 293 mGy cm. Images C & D acquired with axial mode 100kV, 127 mAs, slice thickness 3, TCM, IR/s3, $CTDI_{vol}$ 16 mGy and DLP 232 mGy cm. Axial mode showed 21 % reduction on dose without compromising the image quality

4.4.2 Chest scanning protocols

For the chest and abdomen protocols, the first approach towards the optimisation of paediatric practices was to strictly minimise the area of the scan as the radiation dose is directly proportional to the scan length [17], followed by the application of low dose techniques. Our phantom results for chest have validated the utilisation of low tube voltage technique with application of the tube current modulation as well as the iterative reconstruction techniques. The protocols obtained with tube voltage of 100 kV, the tube current of about 45-100 effective mAs with resultant $CTDI_{vol}$ values about 1.5-2.7 mGy were acceptable based on subjective assessment of image quality. In addition, subjective assessment of image quality using the 80 kV protocol was also verified, though this kind of low voltage technique is suitable for post-contrast studies. This study suggests that 100 kV could be used in all non-contrast chest studies without degrading image quality, and further reduction of tube voltage to 80 kV would be useful for follow-up and contrast studies. Also, it is expected that the protocols could be used for the wide age ranges (5-10 years). Overall chest radiation doses extracted in the study are quite lower compared to the literatures [4, 22, 23] and could verify some recommendations from scientific studies that encourage the applications of the low dose technique.

4.4.3 Abdomen scanning protocols

Abdomen protocols were to some extent similar to those of chest. Our results suggest that diagnostic-quality images obtained with 80 kV and 100 kV with TCM and the iterative reconstruction techniques were acceptable. Also, 120 kV with tube current less than 50 effective mAs showed the same image quality. Both techniques delivered dose range between 1.5 and 3 mGy (measured by 32-cm diameter CTDI phantom).

In children, decreasing the tube voltage from 140 kV to 120 kV and from 120 kV to 80 kV has shown to reduce organ dose by 40% and 65% respectively [24, 25]. Accordingly, the devised optimisation protocols for the brain, chest and abdomen were consistent with application of the low tube voltage. All validated devised protocols were predominated with 100 kV, yet 80 kV and 120 kV were assessed as well. Currently, studies on CT focus on a combination of the low voltage with TCM

technique mainly highlighted post-contrast and cardiovascular studies that have shown to significantly reduce radiation dose, yet in routine protocols particularly paediatric non-contrast examinations are not fully explored. Thus study is developed to investigate different aspects related to the paediatric routine CT protocols, in particular scanner-specific factors.

Unlike the brain studies, chest and abdomen phantom testing showed consensus between the two manufacturers in terms of the interchangeable performance of the protocols between the manufacturers. It is expected that the convergence of chest and abdomen CT protocols corresponding to image quality and radiation dose would lead to narrow the gap of how protocols applied between the manufacturers. Therefore, understanding the scanner specific factors in terms of how the interlinked factors react during the acquisition process is crucial and thus, the medical imaging technologist must be equipped with strong knowledge of the influence of each acquisition parameters on both image quality and patient's radiation dose.

4.4.4 Other technical considerations

In general, the devised optimisation paediatric CT protocols that have been tested in this study heavily relied on the application of both low tube voltage and tube current modulation using the IR technique. It was important to assess the influence of TCM technique on both image quality and radiation dose due to the fact that it is the most important parameter that has close relationship with other factors such as tube voltage, pitch value, slice thickness, scan time and patient's position in the gantry. Consequently, a rigorous method has been used to approach the employment of the tube current modulation in the devised optimisation protocols. The influences of each parameter were initially investigated in the Chapter 2, the literature review, then in the data analysis from Chapter 3 from the clinical practice and finally the current phantom study.

4.4.4.1 Spiral pitch factor

Although the devised protocols were subjectively and objectively acceptable, their applications may negatively influence the radiation dose and the diagnostic value, if

the operator lacks the basic knowledge of the CT principle. Application of the pitch value in each manufactures may influence differently on other factors such as the TCM. The study has shed some light on the influence of this factor in the two participated manufacturers and thus, results are of paramount importance in determining the pitch value and its relation with both image quality and radiation exposure. Increasing pitch value while using the TCM that relies on the effective mAs for a reference patient size demonstrated slightly increasing effective mAs in both Philips and Siemens scanners. For example, changing pitch from 0.6 to 1.2 values in Siemens 128-MDCT Flash with TCM technique slightly increased effective mAs and thus increased both $CTDI_{vol}$ and DLP by 6% and 13% respectively. The image quality in both scanners was preserved with slightly increased image noise as encountered while using high pitch.

On other hand, increasing pitch value with fixed tube current was noticed to be affected differently in both manufacturers. For instance, changing pitch from 0.6 to 1.2 in Philips scanner with fixed tube current manifested 6% increase in $CTDI_{vol}$ while 4% decrease in DLP. There was 44% increase in image noise in the base of the skull and 33% reduction in noise for the brain tissue above the superior orbital margin. Siemens's scanner showed the same $CTDI_{vol}$ regardless of the pitch value, yet increasing image noise with high pitch. It is noticed that image noise increased with high pitch, particularly in thick slice thickness that required more radiation exposure. Also, DLP values were lower with high pitch value in both manufacturers. It is worth mentioning that $CTDI_{vol}$ is used to monitor the influence of the pitch value to the tube output rather than patient's radiation dose

Indirectly, pitch factor could increase radiation dose in small children with short scan length in what so called over-scanning or over-range doses [18, 26, 27]. Over-scanning is a phenomenon inherent in helical scan mode when an extra rotations outside the planned length is required for image reconstruction [18, 27]. Pitch factor and detector collimation are the most important factors to determine the over-scanning dose. Pitch value larger than one and larger detector collimation such as 64-MDCT compared to the 16-MDCT have shown increasing over-scanning dose [18, 28, 29]. Despite the fact that the advanced technology has limited the effect of the over-scanning dose particularly with latest scanners beyond the 64 MDCT, caution must be taken when scanning short length with fast scanning. Therefore, pitch factor

must be kept less than one or if possible using axial scan modes in small infants as the scan length is usually shorter. Since the influence of the pitch among the manufacturers is quite complex, thus understanding scanner specific factors is crucial during the optimisation process specifically for those factors interlinked to each other such as scan time, scan collimation and pitch. Our results suggest using the pitch factor between 0.5-1 in most of the optimised routine paediatric protocols.

4.4.4.2 Iterative reconstruction technique

Iterative reconstruction technique has substantially improved image quality in terms of the visualisation of the structures and suppresses the image artefacts and mottled noise devised protocols with Siemens scanners using the SAFIRE technique with the strength (3) was sufficient for all anatomical areas. The strength of the iteration technique was inherited from the paediatric phantom and clinical studies [30-32]. The same strength used with Philips iDose4 showed the same results. Since the study focused on the optimisation of routine CT protocols considering a wide range of the factors, selected iterative strength was based on the recommendation of the previous studies that have justified using the medium strength in most of the studies particular in paediatric patients. Despite the significant improvement in image noise with IR compared to the FBP, radiologist's perceptions were fair with both techniques.

4.4.4.3 Patient gantry off-centre

Low dose optimisation protocols with phantom off-centred downwards from the gantry pivot for chest area demonstrated increasing image noise posteriorly while decreasing anteriorly. In general, $CTDI_{vol}$ was slightly lowered from the corresponding centred protocols. Both reduction on $CTDI_{vol}$ and an increase in image noise posteriorly is due to the impact of the bowtie filters, which could compromise the diagnostic information at the lung apex and base of the skull in CT brain. The influence of off-centre could have less impact on image quality compared to the patient radiation dose as most of the sensitive organs are located anteriorly, thus increasing the organ dose.

4.4.4.4 Scan field of view

Also the influence of the bowtie filters in children has been investigated by using various S-FOV that increases the image noise with large size field of view. The scan field of view is variable among the children. Any attempt to modify the main factors of children or young adult protocols to suit infants and small children would result in using large S-FOV that would have negative impact on the image noise and patient's radiation dose.

4.5 Validation of the optimised routine protocols

This chapter further evaluates the feasibility of the optimised protocols obtained in Chapter 3. The empirical phantom study validates the optimised head protocols for 5-year old patients. Based on the findings in both Chapters 2 and 3, the validated protocols would cover the age range of 5–9 years (Table 3.8). In addition, the age variation in the group was addressed with a range of mAs and $CTDI_{vol}$. For the chest and abdomen protocols, this phantom study validated protocols of body size at a range of 15–19 cm effective diameter (Tables 3.9–3.10). The devised protocols of the chest and abdomen were provided with range of mAs and $CTDI_{vol}$ to cover the 5 cm variation in effective diameter. Consequently, the effective diameter parameters obtained in Chapter 3 and the validated protocols in this chapter were considered pivotal for estimating the rest of the optimised paediatric protocols. Eventually, the wide range of acquisition and reconstruction factors as well as the current clinical practices of paediatric CT discussed in this chapter and previous chapters provided a solid framework for the optimisation process.

4.6 Study limitations

This study has some limitations that should be discussed. A major limitation is due to the use of a single phantom to validate the devised protocols. It was recommended to have three phantoms to cover a wide range of children's body sizes. Because of the high cost of this kind of phantom, it was decided to use a median sized phantom to only evaluate the devised optimised protocols for 5-year-old (16-cm effective diameter) patients presented in Chapter 3 empirically. However, the feasibility of the optimised protocols devised based on the previous literature review (Chapter 2) and retrospective study (Chapter 3) for other patient types presented in Tables 3.8-3.10 would be warranted when the empirical data in this chapter supported the use of the protocols for 5-year-old patients from Chapter 3. Although the phantom's window level and window width of the brain soft tissue was consistent with the clinical use for viewing the brain tissue, the phantom lacks the brain structure such as ventricles and the distinction between grey and white matter that would help the radiologists to assess the visualisation of the structures. As a result, a poor agreement was observed during subjective analysis of the visualisation of the small structures. Only noise was quantitatively assessed in the objective image quality assessment. However, the use of subjective assessment could address this limitation to some extent.

It was recommended to have two subspecialty paediatric radiologists with minimum 5 years of experience to assess the image quality subjectively. Images of paediatric patients compared to the adult counterparts naturally containing slightly high noise. Paediatric radiologists have adapted with this kind of image compared to the radiologists who deal with adult imaging. Since the subjective analysis solely relies on the image noise, it is expected greater agreement between the subspecialty paediatric radiologists would be obtained. Further analysis of image quality by paediatric radiologists is recommended to ensure acquisition of more practical results from their clinical perspective.

4.7 Conclusions

In summary, our results represent one of the comprehensive optimisations of the routine paediatric CT protocols of brain, chest and abdomen examinations. The approach used in the validation of the devised optimisation paediatric CT routine protocols is objectively and subjectively assessed. Objectively by quantifying the image noise side to side with given acquisition parameters and $CTDI_{vol}$ values. Subjective perceptions of the radiologists regarding the image quality were assessed. Low dose protocols using low tube voltage, TCM technique and the application of iterative reconstruction were the main elements tested to determine the effectiveness of the optimisation practices. Further factors such as pitch value, slice thickness, scan time and the influence of the bowtie filter were assessed to maximise the effectiveness of the devised protocols, yet without compromising the diagnostic information. Scanner specific factors were also investigated between the two manufacturers and the results were expected to improve the knowledge about scanner specific performance when manipulating the acquisition parameters. Also, development of a diagnostic reference level concept in terms of the standard measures CTDI and DLP has facilitated the optimisation process by having reference values for upper limit of radiation dose. These measures would make it easier for future optimisation process to carry out low dose CT studies. Finally, a number of further approaches are required to make sure that devised protocols would effectively optimise the paediatric routine protocols for children of all age groups and body sizes.

4.8 References

1. Zarb F, McEntee MF, Rainford L. 2015. A multi-phased study of optimisation methodologies and radiation dose savings for head CT examinations. Radiat Prot Dosimetry 163(4): 480-90.

2. Vardhanabhuti V, Olubaniyi B, Loader R, Riordan RD, et al. 2012. Image quality assessment in torso phantom comparing effects of varying automatic current modulation with filtered back projection, adaptive statistical, and model-based iterative reconstruction techniques in CT. J Med Imaging Radiat Sci. 43(4): 228-38.

3. Ledenius K, Stalhammar F, Wiklund LM, Fredriksson C, et al. 2010. Evaluation of image-enhanced paediatric computed tomography brain examinations. Radiat Prot Dosimetry 139(1-3): 287-92.

4. Chapman T, Swanson JO, Phillips GS, Parisi MT, et al. 2013. Pediatric chest CT radiation dose reduction: Protocol refinement based on noise injection for pulmonary nodule detection accuracy. Clin Imaging 37(2): 334-41.

5. Zarb F, McEntee MF. 2013. CT radiation dose and image quality optimization using a porcine model. Radio Techno. 85(2): 127-136.

6. Bongartz G, Golding SJ, Juri H, Leonardi M, et al. European guidelines on quality criteria for computed tomography. Brussels, Belgium: European Commission: European Commission; 2000.

7. Brisse HJ, Brenot J, Pierrat N, Gaboriaud G, et al. 2009. The relevance of image quality indices for dose optimization in abdominal multi-detector row CT in children: Experimental assessment with pediatric phantoms. Phys Med Biol. 54(7): 1871-92.

8. Johnston JH, Podberesky DJ, Yoshizumi TT, Angel E, et al. 2013. Comparison of radiation dose estimates, image noise, and scan duration in pediatric body imaging for volumetric and helical modes on 320-detector CT and helical mode on 64-detector CT. Pediatr Radiol. 43(9): 1117-27.

9. Lee YW, Yang CC, Mok GS, Wu TH. 2012. Infant cardiac CT angiography with 64-slice and 256-slice CT: Comparison of radiation dose and image quality using a pediatric phantom. PLoS One 7(11): e49609.

10. Santos J, Batista MD, Foley S, Paulo G, McEntee MF, Rainford L. 2014. Paediatric CT optimisation utilising Catphan(R) 600 and age-specific anthropomorphic phantoms. Radiat Prot Dosimetry 162(4): 586-96.

11. MacDougall RD, Strauss KJ, Lee EY. 2013. Managing radiation dose from thoracic multidetector computed tomography in pediatric patients: Background, current issues, and recommendations. Radiol Clin North Am. 51(4): 743-60.

12. Thomas KE, Wang B. 2008. Age-specific effective doses for pediatric MSCT examinations at a large children's hospital using DLP conversion coefficients: A simple estimation method. Pediatr Radiol. 38(6): 645-56.

13. Brady Z, Ramanauskasr F, Cain M, Franzcrf, et al. 2012. Assessment of paediatric CT dose indicators for the purpose of optimisation. Brit J Radiol. 85: 1488-1498.

14. Hayton A, Wallace A, Marks P, Edmonds K, et al. 2013. Australian diagnostic reference levels for multi detector computed tomography. Australas Phys Eng Sci Med. 36(1): 19-26.

15. Fukushima Y, Tsushima Y, Takei H, Taketomi-Takahashi A, et al. 2012. Diagnostic reference level of computed tomography (CT) in Japan. Radiat Prot Dosimetry 151(1): 51-7.

16. Rao P, Bekhit E, Ramanauskas F, Kumbla S. 2013. CT head in children. Eur J Radiol. 82(7): 1050-8.

17. Trattner S, Pearson GD, Chin C, Cody DD, et al. 2014. Standardization and optimization of CT protocols to achieve low dose. J Am Coll Radiol. 11(3): 271-8.

18. Schilham A, van der Molen AJ, Prokop M, de Jong HW. 2010. Overranging at multisection CT: An underestimated source of excess radiation exposure. Radiographics 30(4): 1057-67.

19. Wong ST, Yiu G, Poon YM, Yuen MK, et al. 2012. Reducing radiation exposure from computed tomography of the brain in children-Report of a practical approach. Child Nerv Syst. 28(5): 681-9.

20. Galanski M, Nagel H, Stamm G. Paediatric CT Exposure Practice in the Federal Republic of Germany: Results of a Nationwide Survey in 2005–2006. Hannover: Medizinische Hochschule; 2007.

21. Kritsaneepaiboon S, Trinavarat P, Visrutaratna P. 2012. Survey of pediatric MDCT radiation dose from university hospitals in Thailand: A preliminary for national dose survey. Acta Radiol. 53(7): 820-6.

22. Eller A, Wuest W, Scharf M, Brand M, et al. 2013. Attenuation-based automatic kilovolt (kV)-selection in computed tomography of the chest: Effects on radiation exposure and image quality. Eur J Radiol. 82(12): 2386-91.

23. Granata C, Origgi D, Palorini F, Matranga D, et al. 2015. Radiation dose from multidetector CT studies in children: Results from the first Italian nationwide survey. Pediatr Radiol. 45(5): 695-705.

24. Reid J, Gamberoni J, Dong F, Davros W. 2010. Optimization of kVp and mAs for pediatric low-dose simulated abdominal CT: Is it best to base parameter selection on object circumference? Am J Roentgenol. 195(4): 1015-20.

25. Paterson A, Frush DP, Donnelly LF. 2001. Helical CT of the body: Are settings adjusted for pediatric patients? Am J Roentgenol. 176(2): 297-301.

26. Nicholson R, Fetherston S. 2002. Primary radiation outside the imaged volume of a multislice helical CT scan. Brit J Radiol. 75: 518-522.

27. van der Molen AJ, Geleijns J. 2007. Overranging in multisection CT: quantification and relative contribution to dose-Comparison of four 16-section CT scanners. Radiology 242(1): 208-16.

28. Tsalafoutas IA. 2011. The impact of overscan on patient dose with first generation multislice CT scanners. Phys Med. 27(2): 69-74.

29. Irwan R, de Vries HB, Sijens PE. 2008. The impact of scan length on the exposure levels in 16- and 64-row multidetector computed tomography: A phantom study. Acad Radiol. 15(9): 1142-7.

30. Hwang HJ, Seo JB, Lee HJ, Lee SM, Kim EY, Oh SY, et al. 2013. Low-dose chest computed tomography with sinogram-affirmed iterative reconstruction, iterative reconstruction in image space, and filtered back projection: studies on image quality. J Comput Assist Tomogr. 37(4): 610-7.

31. Lee Y, Jin KN, Lee NK. 2012. Low-dose computed tomography of the chest using iterative reconstruction versus filtered back projection: comparison of image quality. J Comput Assist Tomogr. 36(5): 512-7.

32. Froemming AT, Kawashima A, Takahashi N, Hartman RP, Nathan MA, Carter RE, et al. 2013. Individualized kV selection and tube current reduction in excretory phase computed tomography urography: Potential for radiation dose reduction and the contribution of iterative reconstruction to image quality. J Comput Assist Tomogr. 37(4): 551-9.

Chapter 5

Conclusions

5.1 Introduction

This chapter shows how the main findings and discussions from chapters 2-4 have contributed to meeting the aim and objectives of the study. The important components of the refined, devised routine paediatric CT scanning protocols are then highlighted. These can be applied to wider contexts so as to illustrate the contribution of the current study. This leads to claims for study advancements. Reflections on study limitations are also provided so as to suggest directions for further study.

5.2 Achievement of aim and objectives of the study

The aim of this study was to optimise routine paediatric CT scanning protocols in relation to image quality and radiation dose. A literature review was first conducted to identify and discuss a wider range of factors that affect the radiation dose and image quality of routine paediatric CT examinations. The range of factors includes patient body size in terms of age, weight and effective diameter; radiosensitivity; tube voltage and current, automatic tube current modulation; iterative reconstruction; scanogram/scout-view; pitch; scan collimation; over scanning; over beaming; and use of bowtie shaping filters (objective 1). A retrospective study of the routine paediatric CT scanning protocols employed in four leading tertiary hospitals in the Sultanate of Oman was then undertaken to investigate and determine the effects of the identified factors on radiation dose and image quality employed in clinical (practical) environments. Although the focus of this retrospective study was only the relationship between the identified factors and radiation dose, the consideration of image quality was embedded as all the collected cases met the minimum requirements for diagnosis. The outcomes of the literature review and retrospective study were then used to devise the optimum routine paediatric CT scanning protocols that could be readily applied to the clinical environments (objective 2). Some of the devised protocols were also evaluated with the use of a paediatric

anthropomorphic phantom, leading to further validation (objective 3). Collectively, the aim of this study has been achieved.

It is expected that the outcome of this study could help to narrow the gaps and provide a better understanding of paediatric CT practices.

5.3 Study significance and implications

It is believed that the findings of this study will profoundly contribute to optimising routine paediatric CT practices. Unlike many other strategies of optimisation, this study provides a comprehensive review of all factors that influence radiation dose and image quality, including children's body characteristics. Further, the retrospective study has strengthened how the acquisition parameters could be applied to clinical practices. Consequently, it interlinks a comprehensive knowledge of each factor of the CT image formations and how they are applied to clinical practices.

The refined, optimised protocols pinpointed the practices to the 64-MDCT and above that are widely applied in clinical practices, thus narrowing the gaps between the acquisition parameters and radiation dose for specific age or body size groups of children.

In order to ensure that the devised protocols would be carried out in a dose optimisation fashion, the following recommendations should be observed:

- Children's body characteristics are the key element of the optimisation. To guarantee the effectiveness of the given protocols, the institution must establish the age groups for the head and body size for the trunk. Body size is a robust means by which to facilitate the acquisition parameters of the trunk, and it is fundamental for the optimisation [1-3]. In our study, effective diameters from the image were used to design the devised protocols. However, this method is difficult in daily practices. Nevertheless, for the current practices, the ICRU age function effective diameter method accounted as a useful means that could be used to categorise children's body sizes [3].

- Special consideration must be given to the interlinked acquisition factors, such as pitch spiral factor, scan time, detector scan width and modulation technique. For instance, our results showed that high pitch in Siemens and Philips increases the image noise with a fixed tube current and increases the dose with TCM. To safeguard the application of the devised protocols, low pitch is recommended when scanning infants with 64-MDCT helical modes as a short scan length, wide beam collimation and high pitch factors result in increasing the over-scanning dose [5, 7, 8]. This is important in clinical practices as both image noise and radiation dose are a drawback CT imaging.

- A large discrepancy is observed in the radiation dose and dose readings of the head CT between the two CT scanners (Philips and Siemens 64-MDCT) in both retrospective data collection and the phantom study. The Philips 64-MDCT demonstrated a significantly high radiation dose across all age groups. The phantom study showed a significant degradation in image quality in Phillips protocols corresponding to less than 27 mGy $CTDI_{vol}$ compared to the Siemens 64-MDCT, which showed adequate image quality with $CTDI_{vol}$ ranging between 14 and 22 mGy. Thus, one has to consider the specific scanner when using the devised protocols.

- A high level of caution must be given to the $CTDI_{vol}$ and DLP range in the devised optimised protocols of the chest and abdomen when comparing them with the literature as they related to the 32 cm $CTDI_{vol}$ phantom. In the literature, the given dose for children below 10 years of age is usually normalised to the 16 cm CTDI phantom. Yet, most scanners display the trunk $CTDI_{vol}$ which related to the 32 cm CTDI phantom. It is expected that the given range of $CTDI_{vol}$ for each protocol will provide an easy reference for both the radiologist and technologist during routine clinical practices.

- It is highly recommended that the application of TCM in the devised protocols; however, automatic dose control must be used only if it is designed to moderate dose adaptation and the way in which the reference

mAs are already optimised. In addition, the patient-gantry centre and scan field of view are crucial to maximise the effectiveness of the TCM.

- It is encouraged that the radiological community and manufacturers continue to promote the application of the iterative reconstruction technique in paediatric CT. Literature and clinical data revealed the reluctance of some radiologists in the use of this reconstruction method [4, 6]. It is believed that proper implementation of this method will have a potential decrease of CT dose while preserving the diagnostic value.

- Approaching the optimisation of paediatric CT protocols requires a stringent ongoing process. Thus, the radiology team, and especially the medical technologist, must be equipped with strong knowledge of the latest advances in CT technology and be familiar with the influence of each acquisition and reconstruction parameter to the image quality and radiation dose.

5.4 Study limitations

This study encountered a few limitations that are worthwhile for discussion. First, the dataset lacked the children's weight and height due to the unavailability of these details among the participating centres since this is a retrospective data analysis. However, the extracted effective diameter of the chest and abdomen provides a reliable comparison between the acquired acquisition parameters and the children's body size. Second, only the scanners from 2 manufacturers were covered due to the fact that these two manufacturers are the most popular in clinical practices. By including other manufacturers, in particular, the latest CT models would strength the results. One should keep in mind that the devised optimised protocols provide just a starting point prior to clinical implementation and that acquisition parameters vary among the manufacturers, but this may not significantly differ among the same scanner modes. Third, the study was initially designed to test three different sizes of anthropomorphic phantoms representing three age groups to validate the devised protocols. However, due to the high cost of the phantoms, one size of a five-year reference phantom was used. Nonetheless, the phantom study results indicate the

appropriateness of the optimised protocols devised in Chapter 3 for the 5-year-old patients, the feasibility of the other optimised protocols provided in Tables 3.8-3.10 would be warranted to some extent. Fourth, subjective and objective image quality were assessed, and the head phantom demonstrated homogenous brain tissue that affects the analysis of the visualisation of the structures. Nevertheless, the phantom shows equivalent window width and window level to the human tissue. Finally, the image quality on the anthropomorphic phantom, rather than human tissue was evaluated. Nevertheless, enforcement of the devised optimisation protocols in clinical practices would have to be gradual.

5.5. Future study direction

This study has improved the understanding of the influence of acquisition parameters and other technical aspects on the image quality and the radiation dose of patients as well as of how paediatric acquisition protocols are tailored in the clinical environment. The study findings shed light on how low-dose protocols are used in conjunction with the application of advanced CT scanning techniques that ensure a decreasing radiation dose while maintaining the diagnostic image quality. However, further studies are suggested with the following recommendations:

- A prospective study is necessary to implement the optimised imaging protocols for routine paediatric CT imaging in the clinical centres with the aim of improving current clinical practice, therefore, achieving the goal of minimising radiation dose to paediatric patients.

- Further research is required to investigate the over-scanning dose in infants and small children for scanners of >64-MDCT and the efficiency of the adopted dynamic filters needs to be validated.

- Manipulating the pitch factor with a fixed tube current in the Philips scanner demonstrated increased $CTDI_{vol}$ and dose length product (DLP) compared to the Siemens scanner. Thus, further studies are needed to investigate how each scanner responds to the selection of a high pitch factor.

- This study shows that chest and abdomen CT protocols can be used interchangeably between the two manufacturers (Philips and Siemens). Further research is suggested to investigate whether routine protocols could be used for the same scan modes of various manufacturers to narrow the current diversion of the acquisition parameters and their corresponding dose.

5.6 Conclusions

In summary, the study results represent one of the first comprehensive optimisation processes that are systematically approached via three main objectives. It is expected that the findings, recommendations, limitation and future direction would help to shape and strengthen the knowledge towards the optimisation of routine paediatric CT practices. It suggests that the use of TCM, IR and ICRU effective diameter proves to be far superior in optimisation.

5.7 References

1. Cheng PM. 2013. Automated estimation of abdominal effective diameter for body size normalization of CT dose. J Digit Imaging 26(3): 406-11.

2. Cheng PM, Vachon LA, Duddalwar VA. 2013. Automated pediatric abdominal effective diameter measurements versus age-predicted body size for normalization of CT dose. J Digit Imaging 26(6): 1151-5.

3. Granata C, Origgi D, Palorini F, Matranga D, et al. 2015. Radiation dose from multidetector CT studies in children: Results from the first Italian nationwide survey. Pediatr Radiol. 45(5): 695-705.

4. Mieville FA, Berteloot L, Grandjean A, Ayestaran P, et al. 2013. Model-based iterative reconstruction in pediatric chest CT: Assessment of image quality in a prospective study of children with cystic fibrosis. Pediatr Radiol. 43(5): 558-67.

5. Schilham A, van der Molen AJ, Prokop M, de Jong HW. 2010. Overranging at multisection CT: An underestimated source of excess radiation exposure. Radiographics 30(4): 1057-67.

6. Smith EA, Dillman JR, Goodsitt MM, Christodoulou EG, Keshavarzi N, Strouse PJ. 2014. Model-based iterative reconstruction: effect on patient radiation dose and image quality in pediatric body CT. Radiology 270(2): 526-34.

7. Tsalafoutas IA. 2011. The impact of overscan on patient dose with first generation multislice CT scanners. Physica Medica 27(2): 69-74.

8. van der Molen AJ, Geleijns J. 2007. Overranging in multisection CT: quantification and relative contribution to dose-Comparison of four 16-section CT scanners. Radiology 242(1): 208-16.

Appendix 1 Ethical approval from Curtin University

Curtin University

Memorandum

To	Khalid Al Mahrooqi, Department of Imaging and Applied Physics
From	Mun Yin Cheong, Form C Ethics Co-ordinator Faculty of Science and Engineering
Subject	Protocol Approval **SCI-08-14**
Date	5 March 2014
Copy	Zhonghua Sun, Department of Imaging and Applied Physics Curtise K.C. Ng, Department of Imaging and Applied Physics

Office of Research and Development

Human Research Ethics Committee

Telephone 9266 2784
Facsimile 9266 3793
Email hrec@curtin.edu.au

Thank you for your "Form C Application for Approval of Research with Low Risk (Ethical Requirements)" for the project titled *"The Optimization of Paediatric Routine CT Scanning Protocol"*. On behalf of the Human Research Ethics Committee, I am authorised to inform you that the project is approved.

Approval of this project is for a period of 4 years **4th March 2014** to **3rd March 2018**.

Your approval has the following conditions:

(i) Annual progress reports on the project must be submitted to the Ethics Office.

(ii) It is your responsibility, as the researcher, to meet the conditions outlined above and to retain the necessary records demonstrating that these have been completed.

The approval number for your project is **SCI-08-14**. Please quote this number in any future correspondence. If at any time during the approval term changes/amendments occur, or if a serious or unexpected adverse event occurs, please advise me immediately.

Regards,

Mun Yin

MUN YIN CHEONG
Form C Ethics Co-ordinator
Faculty of Science and Engineering

Please Note: The following standard statement must be included in the information sheet to participants:
This study has been approved under Curtin University's process for lower-risk Studies (Approval Number xxxx). This process complies with the National Statement on Ethical Conduct in Human Research (Chapter 5.1.7 and Chapters 5.1.18-5.1.21). For further information on this study contact the researchers named above or the Curtin University Human Research Ethics Committee. c/- Office of Research and Development, Curtin University, GPO Box U1987, Perth 6845 or by telephoning 9266 9223 or by emailing hrec@curtin.edu.au.

Appendix 2 Ethical approval from Armed Forces Medical Service Sultanate of Oman

بسم الله الرحمن الرحيم

SULTANATE OF OMAN
MINISTRY OF DEFENCE
ROYAL ARMY OF OMAN
Headquarters
The Armed Forces Medical Services
P.O. Box 721 Seeb
Postal Code 111
Fax : (00968) 24331951

سلطنة عمان
وزارة الدفاع
الجيش السلطاني العماني
قيادة
الخدمات الطبية للقوات المسلحة
ص.ب : ٧٢١ السيب
الرمز البريدي : ١١١
فاكس : ٢٤٣٣١٩٥١ (٠٠٩٦٨)

Tel : 0096824331727

MOD/FMS/RC/01/2014

8 Dhul Qa'ada 1435 AH
3 Sep 2014

Mr Khalid Mohammed Salim AL-Mahrooqi

THE OPTIMIZATION OF PAEDIATRIC ROUTINE CT SCANNING PROTOCOLS

1. We are pleased to inform you that your research proposal has been approved by the research committee.

2. If the protocol of this study is changed in any way, you must inform the Research Committee and seek reapproval.

3. Thank you

Lt. Col. (Dr)
Rashid AL-Saidi
Chairman
Research Committee

Copy to:-

The Researcher
RC Co-Ordinator

Appendix 3: Ethical Approval from Ministry of Health Sultanate of Oman

Sultanate of Oman
Ministry of Health
Directorate General of Planning

سلطنة عمان
وزارة الصحة
المديرية العامة للتخطيط

Ref. : MH/DGP/R&S/PROPOSAL_ APPROVED/10/2014 ..... الرقم :

Date. : 25.05.2014 ..... التاريخ :

..... الموافق :

Mr. Khalid Mohammed Al Mahrooqi
Principal Investigator

Study Title: **"The Optimization of Routine Paediatric CT Protocols"**

After compliments

We are pleased to inform you that your research proposal **"The Optimization of Routine Paediatric CT Protocols"** has been approved by Research and Ethical Review and Approve Committee, Ministry of Health.

Regards,

Dr. Ahmed Mohamed Al Qasmi
Director General of Planning,
Chairman, Research and Ethical Review and Approve Committee
Ministry of Health, Sultanate of Oman.

Cc
Day file

P.O. Box : 393, Postal Code : 100, Muscat, Tel. : 24601161, Fax : 24696533 ص.ب : ٣٩٣ ، الرمز البريدي : ١٠٠ ، مسقط ، هاتف : ٢٤٦٠١١٦١ ، فاكس : ٢٤٦٩٦٥٣٣